
DELIVERABLE

D25.2 Updated databases of seismicity, faults, and strain rates for ESHM20

Work package	WP25 Updating and extending the European Seismic Hazard Model (JRA 3)
Lead	INGV
Authors	Basili R., Carafa M.M.C., Kastelic V., Maesano F.E., Tiberti M.M., Rovida A., Antonucci A., INGV; Weatherill G., Lammers S., GFZ; Danciu L., ETH.
Reviewers	
Approval	Management Board
Status	Final
Dissemination level	Public
Delivery deadline	30.04.2018
Submission date	31.10.2018
Intranet path	DOCUMENTS/DELIVERABLES



Table of Contents

Summary	7
1 Introduction	9
2 Seismicity.....	10
2.1 EMEC.....	10
2.1.1 Motivation	10
2.1.2 New Seismic Data Sources in the Euro-Mediterranean Area	10
2.1.3 Compilation Procedures of the EMEC 2018	11
2.1.4 Current Status & Statistics.....	12
2.2 SHEEC 1000 - 1899	24
2.2.1 Updates of the input macroseismic datasets	26
2.2.2 Updates of the input regional catalogues	28
3 Faults.....	38
3.1 Summary of fault data published after the end of project SHARE.....	38
3.2 Description of the fault source data model.....	48
4 Strain rates	57
4.1 Summary of strain rate data published after the end of project SHARE	57
5 Conclusive remarks	62
6 References.....	63
Contact.....	70

Figure 1: Comparison of Mw estimates from the GEOFON network against those of the RCMT (left), with the <i>normalised</i> residuals shown with respect to magnitude (top right) and time and magnitude (bottom right).....	11
Figure 2: Geographical polygons and identifiers used in the compilation of the EMEC catalogue	12
Figure 3: The EMEC catalogue as of October 2018 with new events added since the Grünthal & Wahlström (2012) catalogue shown in red, and the contents of the previous EMEC in white.....	13
Figure 4: Density of earthquakes in the 2012 EMEC catalogue (Grünthal & Wahlström, 2012): pre-1900 (left) and post-1900 (right).....	14
Figure 5: Density of earthquakes in new 2018 EMEC catalogue: pre-1900 (left) and post-1900 (right).....	14
Figure 6: Relative increase in number of events from 2012 EMEC to new version for pre-1900 (left) and post-1900 (right) (white cells indicate no change).....	14
Figure 7: Workflow followed in the compilation of SHEEC 1000-1899 (from Stucchi et al., 2013).	25
Figure 8: Location differences ≥ 10 km between SHEEC 1000-1899 and CPTI15. The area of validity of CPTI15 is also shown.	29
Figure 9: Comparison of the Mw values in SHEEC 1000-1899 and CPTI15.....	30
Figure 10: Comparison of the Mw values from MDPs in SHEEC 1000-1899 and CPTI15, according to the APD (left) and WAP (right) calibrations.	31
Figure 11: Comparison of the Mw values from the same MDP distributions in SHEEC 1000-1899 and CPTI15, according to the APD (left) and WAP (right) calibrations.	31
Figure 12: Comparison of the epicentral intensity to Mw empirical relations for the APD and WAP calibrations, with the new CPTI15 one.	32
Figure 13: Comparison of the Mw values in CPTI04 and CPTI15 for the earthquakes that consider CPTI04 as a reference catalogue.	32
Figure 14: Comparison of SHEEC 1000-1899 “default” Mw and of its two components, from macroseismic data (MMw) and from the regional catalogue CPTI04 (CMw), with the Mw of CPTI15..	33
Figure 15: Location differences ≥ 10 km between SHEEC 1000-1899 and FCAT-17.....	34
Figure 16: Magnitude comparison of FCAT-17 and SHEEC 1000-1899 for all the magnitudes (left), and for Mw calculated with Boxer in SHEEC (right).....	35
Figure 17: Magnitude comparison of FPEC V:1.1 and FCAT-17 and SHEEC 1000-1899.....	35
Figure 18: Depth comparison of FPEC V:1.1 and FCAT-17 and SHEEC 1000-1899.	36
Figure 19: Comparison of SHEEC 1000-1899 “default” Mw and of its two components, from macroseismic data (MMw) and from the regional catalogue FPEC V.1.1 (CMw), with the Mw of FCAT-17.	36
Figure 20: Generalized scheme representing a crustal seismogenic fault (left) and a subduction (right).	38
Figure 21: Map view of the EDSF crustal faults covering the Euro-Mediterranean region (Basili et al., 2013).	40
Figure 22: Map view of selected fault datasets that are freely available online: (upper left) composite seismogenic sources (CSS) in the Lower Rhine Graben (Vanneste et al., 2013); (lower left) Quaternary Active Faults Database of Iberia v.3 covering the Iberia region (Garcia-Mayordomo et al., 2012); (upper right) Database of Individual Seismogenic Sources (DISS v.3.2.1) covering the central Mediterranean region (DISS Working Group, 2018); (lower right) Greek Database of Seismogenic Sources (GreDaSS v.2.0.0) covering the Aegean region (Caputo and Pavlides, 2013).	41
Figure 23: (Top) Map of active faults in Anatolia (Emre et al., 2013, 2018). (Middle) Map of faults included in EDSF 2013 but not in the Turkish Hazard Project database (left) and map of faults included in the MTA Active Fault Database, but not in EDSF 2013. (Bottom) Map of the fault source model used in the Turkey Hazard Project (Demircioğlu et al., 2018).	42
Figure 24: Map of collated fault datasets (see Table 4) compared with EDSF. Datasets that still needs to be evaluated, such as those of Turkey, Gulf of Cadiz, Romania, and France are not shown.....	43
Figure 25: Map view of the EDSF subduction zones in the eastern Mediterranean region (Basili et al., 2013).	45

Figure 26: Slab model of the Calabrian Arc (Maesano et al., 2017)..... 46

Figure 27: Slab 2 models (Hayes et al., 2018)..... 46

Figure 28: Comparison of the slab geometry between Slab 2 (Hayes, 2018) and the models for the Hellenic Arc from EDSF (Basili et al., 2013) and Cyprus Arc updated by the TSUMAPS-NEAM Team (2017) from EDSF and the Calabrian Arc from Maesano et al., 2017). 47

Figure 29: Example of a map of Mediterranean subduction zones generated using the SUBMAP 4.2 tools (Heuret & Lallemand, 2005). 48

Figure 30: Comparison of relations by Leonard (2014; LE14) for interplate (INT) and stable continental regions (SCR) in predicting moment magnitude (M_w) from either rupture length (L ; top) or width (W ; bottom) in the case of dip-slip (DS; left) and strike-slip (SS; right) faulting earthquakes. Same-color dotted lines are obtained with the one standard deviation of coefficient a , while b is fixed (see Table 6). 51

Figure 31: Comparison of relations by Strasser et al. (2010; ST10) for interface (INF) and intraslab (INS) in predicting moment magnitude (M_w) from either rupture length (L ; left) or width (W ; right) in the case of dip-slip (reverse only) faulting earthquakes. Same-color dotted lines are obtained with the one standard deviation of coefficient a and b . (see Table 7)..... 51

Figure 32: Comparison of relations by Leonard (2014; LE14) and those by Strasser et al. (2010; ST10) for dip-slip faulting earthquakes in different tectonic settings, interplate (INT), stable continental regions (SCR), subduction interface (INF), and subduction intraslab (INS) in predicting moment magnitude (M_w) from either rupture length (L ; left) or width (W ; right) in the case of dip-slip (reverse only) faulting earthquakes..... 52

Figure 33: Comparison of relations by Leonard (2014; LE14) and Strasser et al. (2010; ST10) in predicting moment magnitude (M_w) from either rupture length (L ; top) or width (W ; bottom) in the case of dip-slip (DS; left) and strike-slip (SS; right) faulting earthquakes with other common relations such as those by Wells and Coppersmith (1994; WC94) and Blaser et al. (2010; BL10). 52

Figure 34: Scalar strain rates and orientations of conjugate microfaults from Carafa et al. (2015). 57

Figure 35: (a) Long-term horizontal velocity field. (b) Predicted long-term fault heave rates. (c) Scalar strain rates and orientation of conjugate microfaults, with area proportional to strain rates. From Neres et al. (2016). 58

Figure 36: Contours of the second invariant of the strain rate tensor from Kreemer et al. (2014)..... 59

Figure 37: Strain map from the EPOS-GNSS Data and Products portal (<https://gnssproducts.epos.ubi.pt/>). 59

Figure 38: GEAR1 (Bird et al., 2015) preferred hybrid forecasts for threshold magnitude $m \geq 5.767+$, both with and without overlay of test earthquakes. (a) Preferred hybrid forecast H for years 2005+ compared with 1694 shallow test earthquakes from the Global Centroid Moment Tensor (CMT) catalog years 2005–2012. (b) Global earthquake activity rate model 1 (GEAR1) forecast for years 2014 and after. . 60

Summary

This deliverable is a contribution to WP25 - JRA3 "Updating and extending the European Seismic Hazard Model". This WP is subdivided into five tasks that deal with different aspects of the making and usage of a continent-scale seismic hazard map. Task 25.2 concerns the update and extension of the seismogenic source model. This document illustrates the work done in updating relevant datasets of the seismogenic source model compiled during the EU-FP7 Project SHARE. This includes the collection of the most recent information on instrumental earthquake catalogues with data of the past 8 years, on historical earthquakes based on macroseismic data, on seismogenic faults based on geologic and tectonic data, and on deformation rates constrained by geodetic (GPS) data. All datasets presented here were put together with the aim of providing the basis for re-computating all hazard input parameters and covering the entire area of ESHM20. This document has five chapters and a list of contextual references. The first chapter is an introduction to the background and scopes of the work being done, and the last chapter summarizes the results and presents the remaining challenges with the use of the collected data for ESHM20.

Chapter 2 deals with the databases of seismicity. It is splitted into two subchapters. The first deals with the instrumental catalog post-1900. Importantly, this part of the catalog contains the data of the years 2006-2014 that were not included in the European-Mediterranean Earthquake Catalogue released in 2012 as a product of SHARE. The compilation and homogenisation of the EMEC catalogue are done on a region-by-region basis across Europe and the Mediterranean, considering local data sources and a set of hierarchies. The second deals with the historical seismicity of the period between 1000 to 1899. It relies upon the homogenous assessment of locations and moment magnitude, achieved through the processing of macroseismic intensity data with the same procedure throughout Europe. The main source in this case is represented by AHEAD (also available through SERA VA3), two regional update catalogues, one for Italy and the other for France, and 14 single studies providing data for about 150 earthquakes.

Chapter 3 deals with the database of seismogenic faults. It describes the updated information about seismogenic faults that appeared in the literature since the completion of the European Database of Seismogenic Faults (EDSF 2013) in the Euro-Mediterranean region (also available through SERA VA3). Only the compilations covering significantly large regions are considered, most of which were taken from publicly accessible online databases, but also voluntarily contributed by groups of scientists. Two main categories of seismogenic faults are considered: 1) crustal faults; and 2) subduction zones. For each category, we present a first evaluation of the level of changes with respect to EDSF. A schema of the relevant parameters to formulate magnitude-frequency distributions from these fault data is given.

Chapter 4 deals with the estimates of crustal deformation based on GPS data. Here the starting point is the outcomes of SHARE WP3 and in its preliminary version (Deliverable D3.5). Since then several deformation models have been published. However, they vary in geographical extent, temporal scope, type of output, accessibility and reusability, and data formats. We foresee to use these models to validate the outcomes of the ESHM20 seismicity rates obtained from the earthquake catalog and the seismogenic faults. Decisions must be made on how to extract seismicity rates at the temporal scale and units of interest from the deformation models and devise the testing strategy.

All the datasets describe here, including relevant publications, will be shared within the WP working group in a private repository (dropbox). In the long term, the derived data products and elaborations will be distributed through EFEHR and EPOS services, as well as the SERA VAs where applicable.

1 Introduction

In the last decade, there has been an increasing concern toward multi-hazard assessment as a tool for disaster risk reduction (e.g. Hyogo Framework 2005-2015, Sendai Framework 2015-2030, GAR15; <https://www.unisdr.org/>). Although the multi-hazard definition refers to a large variety of natural and human-induced processes, a significant role in disaster risk reduction is played by ground-shaking hazard that, among all disastrous effects generated by earthquakes, is responsible for the largest level of damage (Bird and Bommer, 2004). Probabilistic seismic hazard assessment (PSHA) is thus a critical element for establishing priorities for intervention, risk cost-benefit analysis of earthquake mitigation measures, and for ensuring uniform level of defense against threats posed by earthquakes anywhere, and without the limitations posed by political boundaries.

At European level, the reference PSHA is provided by the 2013 European Seismic Hazard Model (ESHM13; Woessner et al., 2015), which resulted from a community-based probabilistic seismic hazard assessment supported by the EU-FP7 project “Seismic Hazard Harmonization in Europe” (SHARE, 2009-2013), whose input data and results are made available through the European Facilities for Earthquake Hazard and Risk (EFEHR; <http://www.efehr.org/>).

Since the seminal work by Cornell (1968), the approach to risk based on PSHA combines all the available information on earthquake processes (source, path, and target site) into a complete model, considering also the uncertainty in knowledge and the variability of data and processes (e.g. Budnitz et al., 1997).

The goal of the SERA WP25 - JRA3 is to update and extend the previous ESHM13. This effort is timely because Europe is in the process of revising the European building code EN 1998-1: Eurocode 8: Design of structures for earthquake resistance. ESHM13 was an important milestone for PSHA across Europe, however, since the model was constructed there have been several advancements in the available data and in our understanding of the process that generates ground motions. WP25-JRA3 is structured in five tasks spanning all aspects of seismic hazard, from the definition of the engineering output requirements for natural and anthropogenic earthquake hazard, to the seismogenic source model, ground-motion predictive equations, hazard computation, and finally to the interface with the Eurocode 8 and risk modelling.

Within this large scope, this deliverable is a contribution to Task 25.2, concerned with the update and extension of the seismogenic source model. This document illustrates the work done in updating relevant datasets of the seismogenic source model compiled during the EU-FP7 Project SHARE. This includes the collection of the most recent information on instrumental earthquake catalogues with data of the past 8 years, on historical earthquakes based on macroseismic data, on seismogenic faults based on geologic and tectonic data, and on deformation rates constrained by geodetic (GPS) data. All datasets presented here were put together with the aim of providing the basis for re-computating all hazard input parameters and covering the entire area of ESHM20.

The research activities illustrated below benefit not only from the legacy of the SHARE and other sibling projects, but also from the on-going efforts of the EPOS service development. In turn, all the data products and elaborations derived from this effort will be distributed through EFEHR and EPOS services, as well as the SERA VAs as applicable.

2 Seismicity

2.1 EMEC

2.1.1 Motivation

One of key datasets used in the compilation of the ESHM2013 (Wössner *et al.*, 2015) was the Share European Earthquake Catalogue (SHEEC), comprising a homogenised historical earthquake database from the period 1000 Common Era (CE) to 1899 CE (Stucchi *et al.* 2013), and archive of instrumental seismicity data for the period 1900 CE to 2006 CE that incorporates the European-Mediterranean Earthquake Catalogue (EMEC) (Grünthal & Wahlström, 2012) with subsequent adaptations described in Grünthal *et al.* (2013). Recognising the ongoing need to update and maintain a magnitude-homogeneous earthquake catalogue for Europe and the surrounding regions, the compilation of an updated European-Mediterranean Earthquake Catalogue (EMEC) of is undertaken within this project.

Following the approach adopted by Grünthal & Wahlström (2012), described in further detail in Grünthal *et al.* (2009a), the EMEC catalogue integrates local sources of data on a region-by-region basis to construct a harmonised catalogue, selecting preferred sources by hierarchy and applying established empirical models to permit the conversion of magnitudes from the heterogeneous locally-reported scales to a common *proxy* magnitude scale equivalent to moment magnitude M_w (Grünthal *et al.*, 2009b). The importance of local data sources within this process is a key motivation for regular updating of the EMEC catalogue. Not only is there a need to integrate recent earthquakes into the earthquake catalogue, the emergence of new recording networks, combined with efforts in the European seismological community for updating and homogenising catalogues undertaken at national scales, results in a continuously evolving process of investigation and recalibration of events recorded in previous bulletins.

2.1.2 New Seismic Data Sources in the Euro-Mediterranean Area

Since the compilation of the EMEC catalogue of Grünthal & Wahström (2012), which took the end of 2006 as the cut-off time, several significant data sources have become available, whose integration into the homogenised EMEC catalogue is crucial. At a regional level the emergence of the moment tensor bulletin of the GEOFON network (<https://geofon.gfz-potsdam.de/>). Initially established by GeoForschungsZentrum (GFZ) in 1993, GEOFON now operates more than 80 recording stations worldwide, concentrated primarily around the Euro-Mediterranean region. The seismic bulletin of GEOFON has reached maturity such that it can be recognised as a leading source of information for seismic data. Since 2011, this bulletin has also been reporting seismic moment tensors routinely for moderate to large magnitude earthquakes, with more than 3000 reported worldwide for magnitudes greater than M_w 3.0 between 2011 and 2014.

Similar databases with regional and global scope contributing new data in the 2006 – 2014 time period are the International Seismological Centre (ISC), the Regional Centroid Moment Tensor database of the INGV (RCMT, Pondrelli *et al.*, 2006 – updated 2017), the Global Centroid Moment Tensor Database (Ekström *et al.*, 2012). For those databases reporting moment tensors directly provide information in either in real time, or with a delay on the order of only few months. In addition, a global archive of seismic events is compiled by the International Seismological Centre (ISC), whose Reviewed Bulletin spans the global, typically providing earthquake location and magnitude estimates (mostly in body- or surface-wave magnitudes) and with a delay of approximately two years behind real-time.

The RCMT catalogue is of particular relevance as this was one of two moment tensor catalogues forming a backbone around which the previous EMEC catalogue was constructed, the other being the Swiss Moment Tensor Solutions (SMTS). As such, moment magnitude estimates from the RCMT could be considered as the effective reference scale to which the harmonised proxy magnitude is directly equivalent. The introduction of the GEOFON moment tensor database in the new version of EMEC provides a third “backbone” dataset, and one that supplants RCMT within the selection hierarchies. A comparison of MW estimates from events reported in both scales is shown in Figure 1, which demonstrates that the two estimates scale equivalently, albeit with GEOFON values suggesting a slight offset of approximately 0.1 magnitudes compared to RCMT.

At a national scale several significant catalogues have been compiled since the end of the time period covered within EMEC, often for application to seismic hazard analysis within their respective countries. Notable amongst these is the Catalogo Parametrico dei Terremoti Italiani (CPTI 2015) (Rovida *et al.*, 2015), the Earthquake Catalogue of Switzerland (ECOS-09, Fäh *et al.*, 2011) and the Papazachos *et al.* (2009) catalogue of earthquakes from Greece. A comprehensive list of data sources both at European and national scales, as well their compilation hierarchies used in the new EMEC construction, can be found in Table 1 and Table 2.

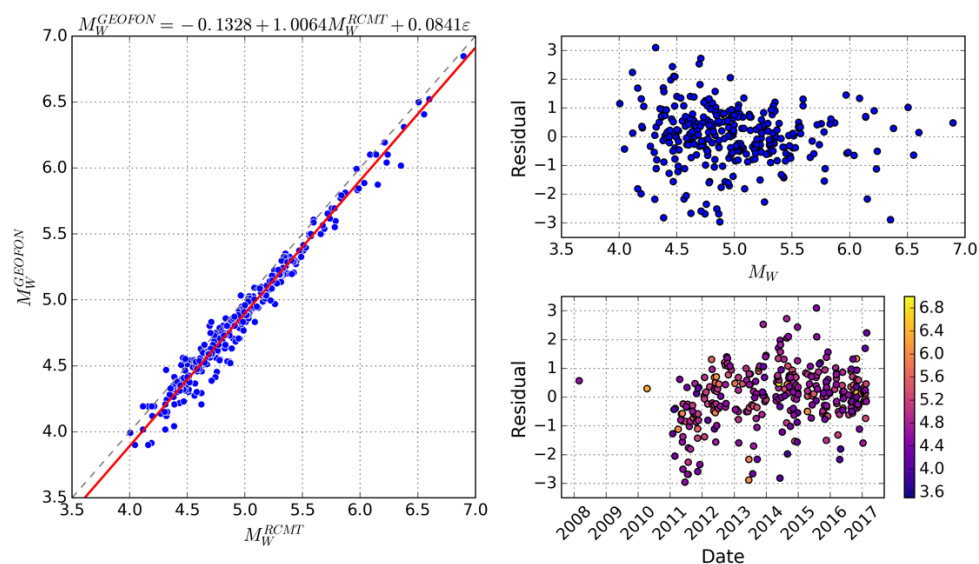


Figure 1: Comparison of M_W estimates from the GEOFON network against those of the RCMT (left), with the *normalised* residuals shown with respect to magnitude (top right) and time and magnitude (bottom right).

2.1.3 Compilation Procedures of the EMEC 2018

The compilation and homogenisation of the EMEC catalogue is done on a region-by-region basis across Europe and the Mediterranean. The region is divided into a set of geographical polygons, as shown in Figure 2, with local data sources and selection hierarchies applied polygon-by-polygon. The polygons broadly follow national borders, which facilitates the application of hierarchies that select national catalogues preferentially within their political boundaries. Some regions have been extended offshore in order to encompass additional seismicity reported by their networks. Further details on the definition of the polygons can be found within Grünthal *et al.* (2009a) and Grünthal & Wahlström (2012).

For the selection of the preferred parameterisation of an earthquake in each region, a general strategy is followed for the development of the hierarchies, with some revisions possible depending on the specific information available within a polygon. The highest preference is given to moment magnitudes obtained directly from earthquakes for which special investigations have been conducted. These may take the form of investigations of specific events, seismic sequences or sub-regions, within which

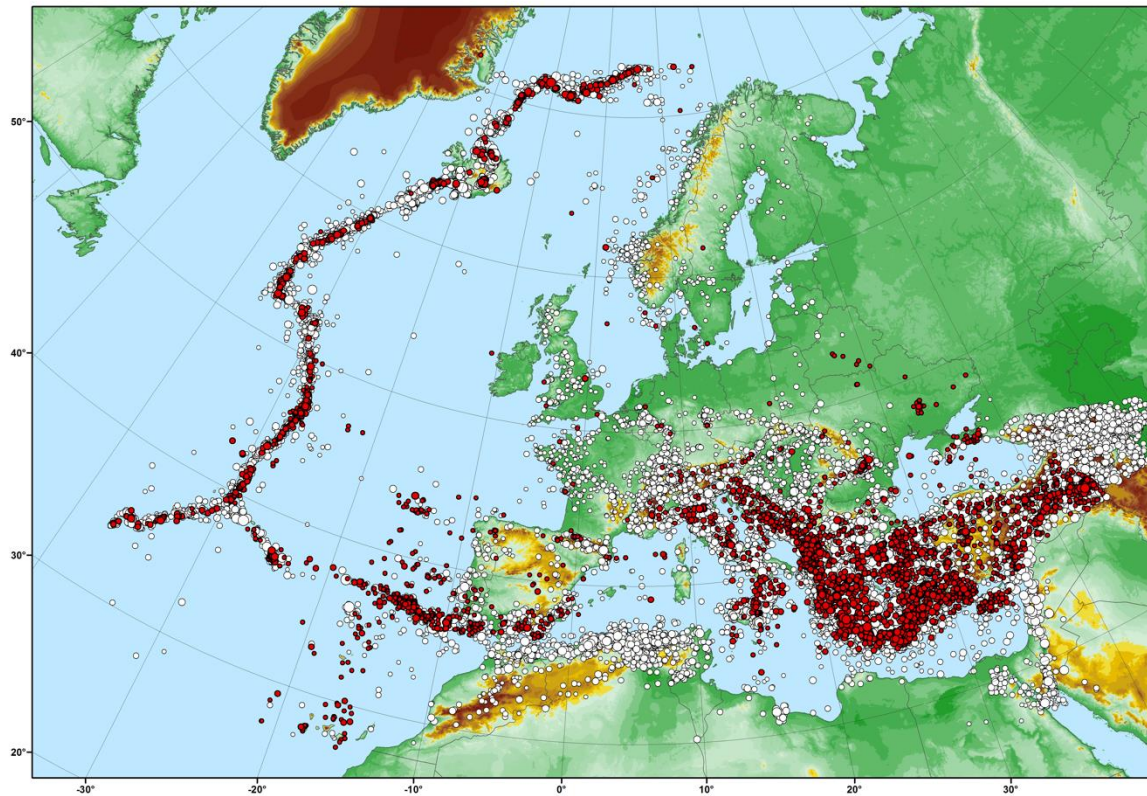


Figure 3: The EMEC catalogue as of October 2018 with new events added since the Grünthal & Wahlström (2012) catalogue shown in red, and the contents of the previous EMEC in white.

The updated EMEC catalogue consists of the following attributes, and is distributed in the form of a delimited text file¹:

eventID: A unique identifier for each event in the database

year, month, day, hour, minute, second: The date and time of the event in Coordinated Universal Time (UTC)

latitude, longitude: The geographical location of the event in decimal degrees

depth: The hypocentral depth of the event in kilometres (km)

Mw: The harmonised *proxy* moment magnitude

originalMag: The magnitude value in the scale reported in the original source

originalMagType: The magnitude scale *origMag*

reference: The source reference code for the event

polygon: The polygon code for the event

¹ Note that the attribute names and format may be revised in subsequent versions of the catalogue, albeit the core attributes themselves should be present.

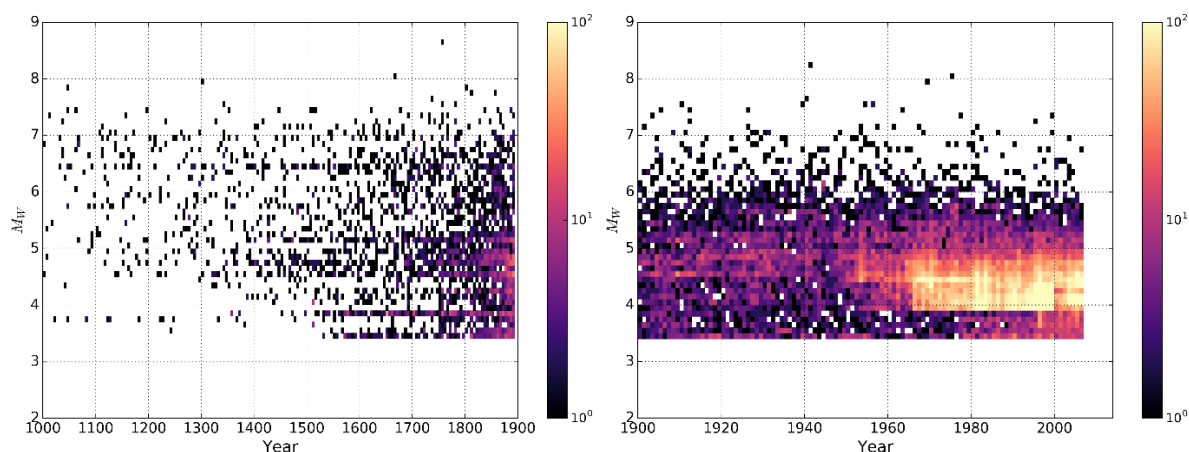


Figure 4: Density of earthquakes in the 2012 EMEC catalogue (Grünthal & Wahlström, 2012): pre-1900 (left) and post-1900 (right)

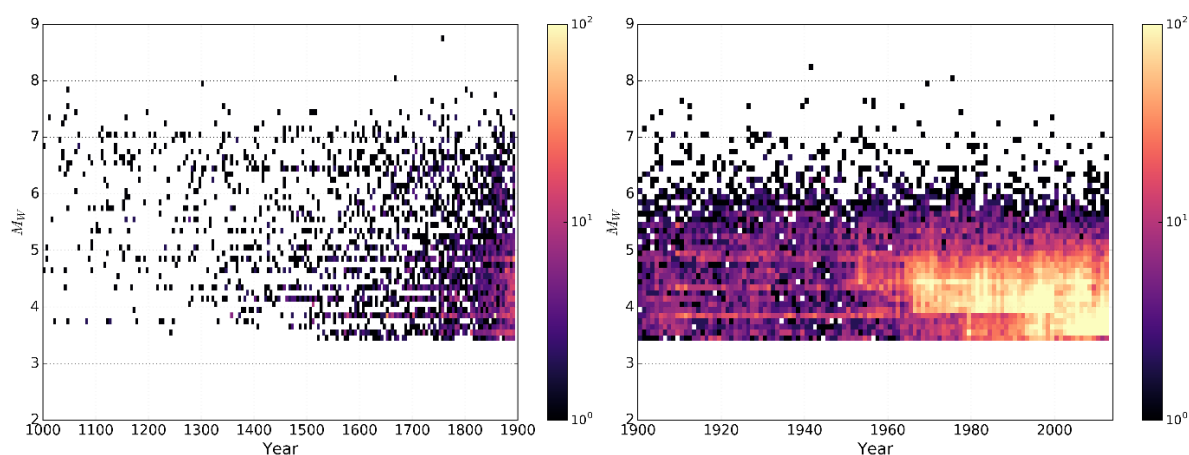


Figure 5: Density of earthquakes in new 2018 EMEC catalogue: pre-1900 (left) and post-1900 (right)

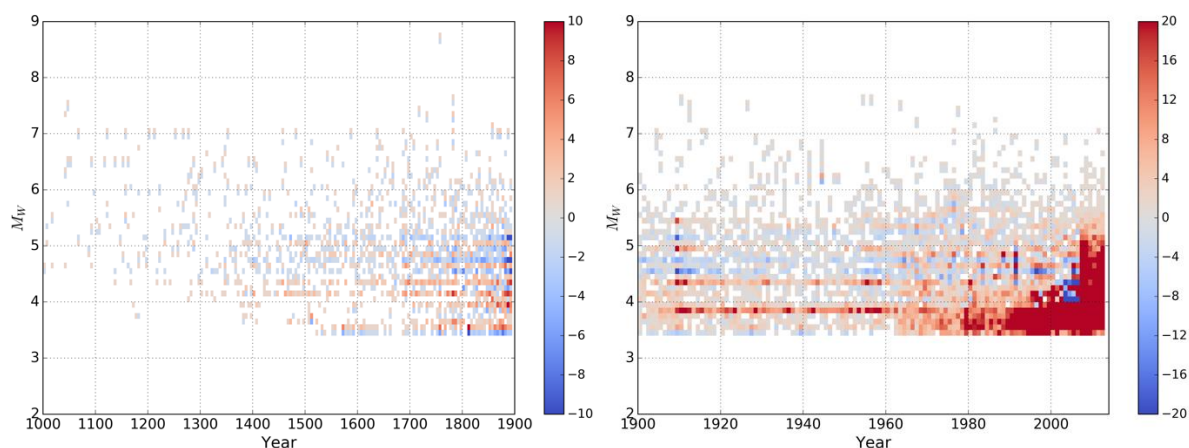


Figure 6: Relative increase in number of events from 2012 EMEC to new version for pre-1900 (left) and post-1900 (right) (white cells indicate no change).

A comparative change in the number of events between the original 2012 EMEC catalogue (Grünthal & Wahlström, 2012) and the present EMEC is shown in Figure 4, Figure 5, and Figure 6. Naturally we see the biggest increase in events in the most recent years (post-2006), though it is relevant to note in the difference maps shown in Figure 6 evidence of changes in the magnitude calibration. This is demonstrated by the blue-shaded grid cells, reflecting the redistribution of events to different magnitude bins. Of additional note is a change in the threshold magnitude adopted in the catalogue. In

the previous EMEC different threshold magnitudes of M_w 4.0 and M_w 3.5 had been adopted in the northern and southern European areas respectively, the demarcating latitude being 44°N. In the updated version a threshold of M_w 3.5 has been adopted uniformly throughout Europe, adding an additional 7,700 events in the 1000 CE to 2006 CE period.

Forthcoming Developments

The EMEC catalogue as it is presented here has been made available on limited release to project partners in order to solicit feedback and presented to the broader scientific community at the 2018 European Geosciences Union meeting in Vienna, Austria. In the forthcoming months a process of feedback and revision is underway, both from SERA project partners and through forthcoming workshops involving the broader European seismological community. From this process a period of further revision is anticipated before a final release of the catalogue, and submission of a journal publication (currently under preparation) in early 2019.

Data Sources and Hierarchies applied in the Compilation of the EMEC Catalogue are listed in the following Table 1 and Table 2.

Table 1: Data sources and hierarchies used in the compilation of the new EMEC catalogue, with references given in Table 2

Polygon (with respect to Figure #)	Time Range	Priority
A	1000 - 1993 1994 - 1995 1996 - 2008 2009 - 2014	ZAMG09L, ZAMG, Ley15, HHM, ECOS-09 ZAMG09L, ZAMG, GRF, ECOS-09 ZAMG09L, GRF, ECOS-09 ZAMG
AL	1000 - 1968 1969 - 1999 2000 - 2006 2007 - 2014	Sul, Pap RKB10, Sul, Pap RKB10, Pap09, Gla TIR
AOC	1000 - 1998 1999 - 2014	NFO, ISC ISC
AOI	1000 - 1990 1991 - 2006 2007 - 2014	IMO, ISC, NEIC, FEN09/FEN11 IMO07, ISC, FEN09/FEN11 ISC, FEN16
BG	1000 - 1904 1905 - 1990 1991 - 09/1998 10/1998 - 1999 2000 - 2006 2007 - 2008 2009 - 2014	Gleva, Onc, She, Pap, Gla Onc, She, Pap, Gla Onc, Pap, Gla INFP, Pap, Gla INFP, Pap09, Gla INFP, Gla, SOF SOF
BIH	1000 - 2004 2005 - 2006 2007 - 2009 2010 - 2014	HHM, Gla Gla Gla, BEO, PDG, LIU BEO, PDG, LIU
BL	1000 - 2014	ORB, ORB07, ORB10
BY	1000 - 1983 1984 - 2006	Bob, ISC ISC

CAU	1000 -1997	God
	1998 - 2014	ISC
CH	1000 - 2006	ECOS-09
	2007 - 2014	SED_2016
CRO	1000 - 2004	HHM
	2005 - 2006	Gla
	2007 - 2009	Gla, BEO, PDG, LIU
	2010 - 2014	BEO, PDG, LIU
CY	1000 - 1499	GC, GD, FA
	1500 - 1889	GD, FA
	1890 - 1895	AA, GD, FA
	1896 - 1899	Pou, PP, AA, GD, FA
	1900 - 1963	Pou, PP, AA, AFS, KOERI, GD
	1964 - 1990	Pou, PP, AA, AFS, KOERI
	1991 - 1997	Pou, PP, AFS, KOERI
	1998 - 2005	Pou, AFS, KOERI
	2006	Pou, AFS
	2007 - 2014	CGSD
CZ	1000 - 1984	CAS, GLM, Gru ¹⁾
	1985 - 1991	GFU; Gru91 ¹⁾
	1992 - 1993	GFU
	1994 - 2014	GFU, GRF
D	1000 - 1984	Gru
	1985 - 1991	Gru91
	1992 - 1993	Ley15
	1994 - 2014	GRF
DZ	1000 - 1799	Pel, HPP10, Ham, IGN
	1800 - 2004	HPP10, Ham, IGN
	2005	SMM, HPP10, Ham, IGN
	2006 - 2008	SMM, HPP10, Ham, IGN
	2009 - 2014	IGN
E	1000 - 1799	IGC1, Pel, IGN, MzS, SisF10 ²⁾
	1800 - 1899	IGC1, IGN, MzS, SisF10 ²⁾
	1900 - 1960	IGC1, IGN, SisF10 ²⁾
	1961	IGC1, IGN, CNP, SisF10 ²⁾
	1962 - 1995	IGC1, IGN, CNP, SisF10 ²⁾
	1996 - 2000	IGC2, IGN, CNP, SisF10 ²⁾
	2001 - 2002	IGC2, IGN, SisF10 ²⁾
	2003 - 2004	IGC2, IGN, SisF10 ²⁾
	2005 - 2006	SMM, IGN, SisF10 ²⁾
	2007 - 2014	IGN
F	1000 - 1961	SisF10, Ley15, ECOS-09 ³⁾
	1962 - 1981	LDG, SisF10, Ley15
	1982 - 1993	LDG, SisF10, Ley15
	1994 - 2004	LDG, SisF10

	2005 - 2006 2007 2008 - 2014	LDG11, SisF10 LDG, SisF10 LDG
FEN	1000 - 1984 1985 - 1988 1989 - 2006 2007 - 2014	WG, Nik, Bob, FEN09 Nik, Bob, FEN09 FEN09 FEN11/FEN16
GR	1000 - 1968 1969 - 1999 2000 - 2005 2006 - 2009 2010 - 2014	Pap RKB10, Pap RKB10, Pap09 RKB10, RKB11, Pap09 DGA16
H	1000 - 1986 1987 - 1994 1995 - 1999 2000 - 2005 2006 - 2014	Zsi Zsi94 Zsi99 Tot Georisk
I	1000 - 2014 08/2001 - 2006	CPTI15 CPTI15, INGV
LWE	1000 - 1899 1900 - 1963 1964 - 1976 1977 - 1990 1991 - 1992 1993 - 2014	AMA AMA, Amb94, Amb84 AMA, Amb94, Amb84, ISC AMA, Amb94, ISC AMA, ISC ISC
MA	1000 - 1799 1800 - 1960 1961 - 2000 2001 - 2004 2005 2006 2007 2008 - 2014	Pel, Ham, IGN Ham, IGN Ham, IGN, CNP Ham, IGN SMM, Ham, IGN SMM, Ham, IGN SMM, IGN IGN
MD	1000 - 1977 1978 - 1995 10/1998 - 2014	KU, KSh, Onc KU, Onc INFP
MK	1000 - 1968 1969 - 1990 1991 - 1999 2000 - 2004 2005 - 2006 2007 - 2009 2010 - 2014	Pap, HHM, She, Gla RKB10, Pap, HHM, She, Gla RKB10, Pap, HHM, Gla RKB10, Pap09, HHM, Gla RKB10, Pap09, Gla Pap09, SKO SKO
NL	1000 - 06/1906 07/1906 - 2014	Hou KNMI

P	1000 - 1799	PeI, IGN
	1800 - 1960	IGN
	1961 - 2000	CNP, IGN
	2001 - 2004	IGN
	2005 - 2010	SMM, IGN
	2011 - 2014	IGN
PL	1000 - 1482	Pag, Gru ¹⁾
	1483 - 1984	GLM, Gru ¹⁾
	1985 - 1993	GLM
	1994 - 1995	GLM, GRF
	1996 - 2014	GRF
RO	1000 - 1986	Onc, Zsi
	1987 - 1994	Onc, Zsi94
	1995 - 09/1998	Onc, Zsi99
	10/1998 - 1999	INFP, Zsi99
	2000 - 2005	INFP, Tot
	2006 - 2014	INFP, Georisk
SK	1000 - 1994	Lab
	1995 - 1999	Zsi99
	2000 - 2005	Tot
	2006 - 2014	Georisk
SLO	1000 - 2004	Ziv18, ZivS, HHM
	2005 - 2008	Gla, Ziv18
	2009 - 2014	Ziv18, LJU
SEM	1000 - 1499	Amb09, Amb06, SDM, KKP, GC, FA, AMA
	1500 - 1895	Amb06, SDM, KKP, FA, AMA
	1896 - 1899	Pou, PP, SDM, KKP, FA, AMA
	1900 - 1963	Pou, PP, KKP, AMA, AFS, KOERI
	1964 - 1992	Pou, PP, KKP, AMA, AFS, KOERI, ISC
	1993 - 1997	Pou, PP, KKP, AFS, KOERI, ISC
	1998 - 2005	Pou, AFS, KOERI, ISC
	2006	Pou, AFS, ISC
	2007 - 2008	Pou, ISC
2009 - 2014	GII, ISC	
TN	1000 - 2005	HPP10, Ham, IGN
	2006 - 2008	HPP10, ISC
	2009 - 2014	ISC
TR lon. ≤ 30.5°E	1000 - 1899	Amb02, Pap
	1900 - 1963	Amb02, KOERI, Pap
	1964 - 1968	Amb02, KOERI, Pap, Lep13
	1969 - 1999	Amb02, KOERI, RKB10, Pap, Lep13
	2000 - 2005	KOERI, RKB10, Pap09, Lep13
	2006 - 2008	KaI, KOERI, Pap09, Lep13
	2009 - 2010	KOERI, Pap10, Lep13
	2011 - 2014	KOERI

TR lon. > 30.5°E	1000 - 1499	Amb09, SDM, KKP, GC, TR-GSHAP, God, KU
	1500 - 1895	SDM, KKP, TR-GSHAP, God, KU
	1896 - 1899	Pou, PP, SDM, KKP, TR-GSHAP, God, KU
	1900 - 1963	KOERI, Pou, PP, KKP, God, KU
	1964 - 1995	KOERI, Pou, PP, KKP, God, KU, Lep13
	1996 - 1997	KOERI, Pou, PP, KKP, God, Lep13
	1998 - 1999	KOERI, Pou, Lep13
	2000 - 2005	KOERI, Pou, Lep13
	2006 - 2008	Kal, KOERI, Pou, Lep13
	2009 - 2014	KOERI, Lep13
UA	1000 - 1899	KU, KSh, Zsi, Onc
	1900 - 1977	KU, KSh, Zsi, Onc, KOERI
	1978 - 1986	KU, Zsi, Onc, KOERI
	1987 - 1994	KU, Onc, KOERI
	1995	KU, Onc, KOERI
	1996 -09/1998	Onc, KOERI
	10/1998 - 2005	INFP, KOERI
	2006 - 2014	INFP
UK	1000 - 1961	MS, Mus, SisF10
	1962 - 1993	MS, Mus, LDG
	1994 - 2004	MS, LDG
	2005 - 2014	MS
YU	1000 - 09/1998	Onc, HHM, Gla
	10/1998 - 2004	INFP, HHM, Gla
	2005 - 2006	INFP, Gla
	2006 - 2009	INFP, Gla, BEO, PDG
	2009 - 2014	INFP, BEO, PDG

- 1) Part of polygon inside the area 49.6°N–54.8°N, 9.5°E–15.5°E (with first priority)
- 2) An LDG, LDG11, or SisF10 entry in the polygon E (Spain) enters EMEC only if there is a corresponding IGC1, IGC2 or IG10 entry in the polygon F (France)
- 3) Selected events

Table 2. References for data sources used in the compilation of EMEC (Table 1)

AA	Ambraseys, NN, Adams RD (1993) Seismicity of the Cyprus region. Terra Nova 5:85-94 Ambraseys NN, Adams RD (1993) Seismicity of the Cyprus region. Terra Nova 5(1): 85-94; DOI: 10.1111/j.1365-3121.1993.tb00229.x
AFS	Abdallah A-QA, Feldman L, Shapira A (2004) The Unified Earthquake Catalogue of the region. Geophysical Institute of Israel (http://seis.gii.co.il/heb/hazards/docs/Catalog-rprt.pdf)
AFS	Abdallah A-QA, Feldman L, Shapira A (2004) The Unified Earthquake Catalogue of the region. Geophysical Institute of Israel (http://seis.gii.co.il/heb/hazards/docs/Catalog-rprt.pdf)
AMA	Ambraseys NN, Melville CP, Adams RD (1994) The Seismicity of Egypt, Arabia and the Red Sea. Cambridge University Press, 181 pp
Amb02	Ambraseys NN (2002) The seismic activity of the Marmara Sea region over the last 2000 years. Bull Seism Soc Am 92(1): 1-18

Amb06	Ambraseys NN (2006) Comparison of frequency of occurrence of earthquakes with slip rates from long-term seismicity data: the cases of Gulf of Corinth, Sea of Marmara and Dead Sea Fault Zone. <i>Geophys J Int</i> 165(2): 516–526; doi:10.1111/j.1365-246X.2006.02858.x
Amb09	Ambraseys NN (2009) Earthquakes in the Mediterranean and Middle East, a multidisciplinary study of seismicity up to 1900. Cambridge University Press, 968 pp
Amb94	Ambraseys NN (1994) Material for the investigation of the seismicity of Libya. <i>Libyan Studies</i> 25: 7-22
BEO	Seismological Survey of Serbia
BGS	British Geological Survey
Bob	Boborikin AM, Gareckij RG, Emeljanow AP, Cildvee ChCh, Cuvejedis PI (1993) Sowremennoye sostoyaniye seismitsheskich nablyudenyh i ich obobshtshenyh. In: Semletryasseniya Belarussi I Pribaltiki, Minsk, Belorussia, pp 29-40
CAS	Schenkova Z, Schenk V, Kárník V (1981) Seismic Hazard Estimate for a Low Seismicity Region - Example of Bohemia, <i>PAGEOPH</i> 119: 1077 - 1092
CGSD	Bulletins of Geological Survey Department, Cyprus
CNP	Carrilho FJR, Nunes JAC, Pena JOA (2004) Catálogo Sísmico de Portugal Continental e Região Adjacente para o Período 1970-2000. Ministério da Ciência, Inovação e Ensino Superior, Instituto de Meteorologia, Divisão de Sismologia, 221 955/05, 227 pp /+ Data file since 1961/
CPTI15	Rovida A, Locati M, Camassi R, Lolli B, Gasperini P (eds.), 2016. CPTI15, the 2015 version of the Parametric Catalogue of Italian Earthquakes. Istituto Nazionale di Geofisica e Vulcanologia. doi:http://doi.org/10.6092/INGV.IT-CPTI15
DGA16	EARTHQUAKE CATALOGUE - SEISMOLOGICAL STATION - DEP. OF GEOPHYSICS - ARISTOTLE UNIVERSITY OF THESSALONIKI
Diehl14	Diehl T, Deichmann N, Clinton J, Kästli P, Cauzzi C, Kraft T, Behr Y, Edwards B, Guilhem A, Korgner E, Hobiger M, Haslinger F, Fäh D, Wiemer S (2014) Earthquakes in Switzerland and surrounding regions during 2014. <i>Swiss J Geosci</i> (2015) 108:425–443 DOI 10.1007/s00015-015-0204-1
ECOS-09	Fäh D, Giardini D, Kästli P, Deichmann N, Gisler M, Schwarz-Zanetti G, Alvarez-Rubio S, Sellami S, Edwards B, Allmann B, Bethmann F, Wössner J, Gassner-Stamm G, Fritsche S, Eberhard D (2011) ECOS-09 Earthquake Catalogue of Switzerland Release 2011. Report
FA	Feldman L, Amrat, A-Q (2007) Data file of historical earthquakes. GII Israel and NRA Jordan
FEN09	FENCAT (2009) Data file of earthquakes in northern Europe. Institute of Seismology, University of Helsinki, Helsinki, Finland (www.seismo.helsinki.fi/english/bulletins/catalog_northeurope.html)
FEN16	FENCAT (2016) Data file of earthquakes in northern Europe. Institute of Seismology, University of Helsinki, Helsinki, Finland (http://www.seismo.helsinki.fi/english/bulletins/catalog_northeurope.html) (Suche: http://www.seismo.helsinki.fi/EQ-search/query).
GC	Guidoboni E, Comastri A (2005) Catalogue of earthquakes and tsunamis in the Mediterranean area from the 11th to the 15th century. <i>Inst Naz Geofis Vulc</i> , 1037 pp
GD	Galanopoulos AG, Delibasis ND (1965) Seismic activity in the Cyprus area. <i>Praktika, Academy of Athens</i> 40:386-405
Georisk	Georisk Data file of Hungarian earthquakes. GeoRisk Ltd, Budapest, Hungary /for 2006 and on/ (www.georisk.hu)

GFU	Zedník J (2005) Catalogs of regional seismic events - Czech Regional Seismological Network. Geophysical Institute, Czech Academy of Sciences, Prague, The Czech Republic
GII	Seismological Bulletin, Earthquakes in and around Israel. The Geophysical Institute of Israel, http://www.seis.gii.co.il
Gla	Glavatović B (2009) MSO BALKAN Catalogue. Montenegro Seismological Observatory, Podgorica, Montenegro, Data file
Gleva	Glavcheva R (2004) State-of-the-art of historical earthquake investigation in Bulgaria. Ann Geophys 47(2-3): 705-721: doi: 10.4401/ag-3332
GLM	Guterch B, Lewandowska-Marciniak H (2002) Seismicity and seismic hazard in Poland. Folia Quaternaria 73: 85-99
God	Godzikovskaya AA (2001) Data Base "The catalogue of the Caucasus earthquakes $M \geq 4$ ($k \geq 11$) from ancient times to 2000". World Data Center for Solid Earth Physics, Geophysical Center, Russian Academy of Sciences, Moscow, Russia (zeus.wdcb.ru/wdcb/sep/caucasus/welcomen.html)
GRF	Seismological Central Observatory Gräfenberg (SZGRF) bulletins, Erlangen, Germany (http://www.szgrf.bgr.de/bulletins.html)
Gru	Grünthal G (1988) Erdbebenkatalog des Territoriums der Deutschen Demokratischen Republik und der angrenzenden Gebiete von 823 bis 1984. Akademie der Wissenschaften der DDR, Zentralinstitut für Physik der Erde 99, 38 pp + Appendix, 139 pp
Gru91	Grünthal G (1991) Data file continuing the earthquake catalogue by Grünthal (1988) for the years 1985-1991.
Ham	Hamdache M, Peláez JA, Talbi A, López Casado C (2010) A unified catalog of main earthquakes for Northern Algeria from 856 to 2008. Seismol Res Letters 81(5): 732-739 / + Data file also for smaller events
HCMTS	The Harvard Centroid Moment Tensor Catalog (http://www.globalcmt.org/)
HHM	Herak M, Herak D, Markušić S (1996) Revision of the earthquake catalogue and seismicity of Croatia, 1908-1992. Terra Nova 8(1): 86-94; DOI: 10.1111/j.1365-3121.1996.tb00728.x / + Data file until 2004
Hou	Houtgast G (1995) Aardbevingen in Nederland. Koninklijk Nederlands Meteorologisch Instituut, De Bilt, The Netherlands 179, 166 pp
HPP10	Harbi A, Peresan A, Panza G (2010) Seismicity of Eastern Algeria: a revised and extended earthquake catalogue. Nat Hazards 54(3): 725-747; DOI 10.1007/s11069-009-9497-6
IGC1	IGC (2009a) Atles sísmic de Catalunya. Institut Geològic de Catalunya
IGN	Earthquakes Catalogue of Iberian, 2005, instituto Geografico Nacional, Espania
IMO	IMO (2007a) Data file of large Icelandic earthquakes up to 1990. Icelandic Meteorological Office, Reykjavik, Iceland (http://hraun.vedur.is/ja/ymislegt/storskjalf.html)
IMO07	IMO (2007b) Data file of Icelandic earthquakes with $ML \geq 3$ from 1991 on. Icelandic Meteorological Office, Reykjavik, Iceland (http://hraun.vedur.is/cgi-bin/sellib)
INGV	INGV - Istituto Nazionale di Geofisica e Vulcanologia, http://cnt.rm.ingv.it
INFP	INFP (2009) Data file of Romanian earthquakes. National Institute for Earth Physics, Bucharest, Romania (www-old.infp.ro/catal.php)
ISC	ISC bulletins International Seismological Centre (previously International Seismological Summary) bulletins. Newbury (previously Edinburgh), United Kingdom (http://www.isc.ac.uk/iscbulletin/)

Kal	Kalafat D, Kekovali K, Günes Y, Yilmazer M, Kara M, Deniz P, Berberoğlu M (2009) A catalogue of source parameters of moderate and strong earthquakes for Turkey and its surrounding area (1938-2008). Boğaziçç Üniversitesi Report, Istanbul, Turkey
KKP	Khair K, Karakaisis GF, Papadimitriou EE (2000) Seismic zonation of the Dead Sea Transform Fault area. <i>Annali di Geofisica</i> 43(1): 61-79
KNMI	KNMI (2009) Data file of Dutch earthquakes. Het Koninklijk Nederlands Meteorologisch Instituut, De Bilt, The Netherlands http://www.knmi.nl/kennis-en-datacentrum/dataset/aardbevingscatalogus)
KOERI	Kalafat D, Güneş Y, Kara M, Deniz P, Kekovali K, Sadi Kuleli H, Gülen L, Yilmazer M, Özel NM (2010) A revised and extended earthquake catalogue for Turkey since 1900 ($M \geq 4.0$). Kandilli Observatory, Istanbul, Turkey (http://www.koeri.boun.edu.tr/sismo/2/earthquake-catalog/)
KSh	Kondorskaya NW, Shebalin NW (1982) New Catalogue of strong earthquakes in the USSR from ancient times through 1977. World Data Center A for Seismology, Report SE-31, Boulder, Colorado, USA, 608 pp
KU	Kondorskaya NV, Ulomov VI (1999) Special earthquake catalogue of Northern Eurasia from ancient times through 1995 (SECNE). Joint Institute of Physics of the Earth (JIPE), Russian Academy of Sciences, Moscow, Russia.
Lab	Labak P (1998) Data file of Slovak earthquakes. Geophysical Institute, Slovak Academy of Sciences, Bratislava, Slovakia
LDG	Laboratoire de Détection et de Géophysique, France http://www-dase.cea.fr/evenement/syntheses_resultat.php?n=1&type_bulletin=tele&lang=fr
Lep13	Leptokaropoulos K M, Karakostas V G, Papadimitriou E E, Adamaki A K, Tan O, and Inan (2013) A Homogeneous Earthquake Catalog for Western Turkey and Magnitude of Completeness Determination. <i>Bulletin of the Seismological Society of America</i> , Vol. 103, No. 5, pp. 2739-2751, October 2013, doi: 10.1785/0120120174
Ley15	Leydecker G (2011) Erdbebenkatalog für die Bundesrepublik Deutschland mit Randgebieten für die Jahre 800-2008. <i>Geol Jb E59</i> , 198 S., aktualisierte Version Sept. 28, 2015
LJU	Slovenian Environment Agency, Seismology Office
MS	Musson RMW, Sargeant SL (2007) Eurocode 8 seismic hazard zoning maps for the UK. British Geological Survey, Technical Report CR/07/125, 70 pp
Mus	Musson R (1994) Earthquake catalogue of Great Britain and surroundings. British Geological Survey, Technical Report WL/94/04, Edinburgh, 99 pp
MzS	Martínez Solares JM (2003), Historical seismicity of the Iberian Peninsula, <i>Física de la Tierra</i> 15: 13-28
NEIC	NEIC bulletins US National Earthquake Information Center bulletins 1917-1999. US Geological Survey, World Data Center A for Seismology, Boulder, Colorado, USA (http://neic.usgs.gov/neis/epic)
NFO	Nunes JC, Forjaz VH, Oliveira CS (2004) Catálogo Sísmico da Região dos Açores. Versão 1.0 (1850-1998). Universidade dos Açores (Ed.). Ponta Delgada. Edição CD-ROM. ISBN: 972-8612-17-6
Nik	Nikonov AA (1992) Distribution of maximum observed tremors and zones of possible occurrence of earthquakes in Estonia. <i>Izvestiya, Earth Physics</i> 28(5): 430-434
Onc	Oncescu MC, Marza VI, Rizescu M, Popa M (1999) The Romanian earthquake catalogue between 984-1997. In: Wenzel F, Lungu D, Novak O (eds) <i>Vrancea Earthquakes: Tectonics, Hazard and Risk Mitigation</i> . Contributions from the First International Workshop on

	Vrančea Earthquakes, Bucharest, Romania, November 1-4, 1997, 43-47; doi: 10.1007/978-94-011-4748-4_4 / + Data file until September 1998
ORB	ORB (2007) Data files of Belgian earthquakes. Observatoire Royale du Belgique, Brussels, Belgium (http://seismologie.oma.be/index.php?)
ORB07	ORB (2007) Data files of Belgian earthquakes. Observatoire Royale du Belgique, Brussels, Belgium (http://seismologie.oma.be/index.php?)
ORB10	ORB, Observatoire Royale du Belgique, Brussels, Belgium (http://seismologie.oma.be/index.php?)
Pag	Pagaczewski J (1972) Catalogue of earthquakes in Poland in 1000-1970 years. Institute of Geophysics, Polish Academy of Sciences, Warsaw, Poland, Volume 51, 61 pp
Pap	Papazachos BC, Comninakis PE, Karakaisis GF, Karakostas BG, Papaioannou ChA, Papazachos CB, Scordilis EM (2003) A catalogue of earthquakes in Greece and surrounding area for the period 550BC - 1999. In: Lee WHK, Kanamori H, Jennings PC, Kisslinger C (eds) International Handbook of Earthquake and Engineering Seismology, IASPEI, Part B, CD #3, Academic Press
Pap09	Papazachos BC, Comninakis PE, Scordilis EM, Karakaisis GF, Papazachos CB (2009) A catalogue of earthquakes in Greece and surrounding area for the period 1901-2008 Publication of the Geophysics Laboratory, University of Thessaloniki http://geophysics.geo.auth.gr/the_seisnet/WEBSITE_2005/station_index_en.html
Pap10	Papazachos BC, Comninakis PE, Scordilis EM, Karakaisis GF, Papazachos CB (2010) A catalogue of earthquakes in Greece and surrounding area for the period 1901-2010 Publication of the Geophysics Laboratory, University of Thessaloniki http://geophysics.geo.auth.gr/ss/CATALOGS/seiscat.dat ; doi:10.7914/SN/HT
PDG	Seismological Institute of Montenegro
Pel	Peláez JA, Chourak M, Tadili BA, Brahim LA, Hamdache M, López Casado C, Martínez Solares JM (2007) A catalog of main Moroccan earthquakes from 1045 to 2005. Seismol Res Letters 78(6): 614-621
Pou	Papaioannou, ChA (2001) A model for the shallow and intermediate depth seismic sources in the Eastern Mediterranean region. Boll Geof Teor Appl 42(1-2): 57-73 / + Data file until 2008
PP	Papazachos BC, Papaioannou ChA (1999) Lithospheric boundaries and plate motions in the Cyprus area. Tectonophysics 308(1-2): 193-204; doi: 10.1016/S0040-1951(99)00075-X
RCMTS	Pondrelli, S., S. Salimbeni, G. Ekström, A. Morelli, P. Gasperini and G. Vannucci, 2006, The Italian CMT dataset from 1977 to the present, Phys. Earth Planet. Int., doi:10.1016/j.pepi.2006.07.008,159/3-4, pp. 286-303. Pondrelli, S., G. Ekström, and A. Morelli, 2001, Seismotectonic re-evaluation of the 1976 Friuli, Italy, seismic sequence, J. Seismol., 5, 73-83.
RKB10	Roumelioti Z, Kiratzi A, Benetatos Ch (2010) The instability of the Mw and ML comparison for earthquakes in Greece for the period 1969 to 2007. J Seismol 14(2): 309-337; doi: 10.1007/s10950-009-9167-x
RKB11	Roumelioti Z, Kiratzi A, Benetatos Ch (2011) Time-domain moment tensors for shallow ($h \leq 40$ km) earthquakes in the broader Aegean Sea for the years 2006 and 2007: The database of the Aristotle University of Thessaloniki. J Geodynamics 51(2-3): 179-189; do
SDM	Sbeinati MR, Darawcheh R, Mouty M, (2005) The historical earthquakes of Syria: an analysis of large and moderate earthquakes from 1365 BC to 1900 AD. Ann Geophys 48:347-435
SED	http://www.seismo.ethz.ch/eq/latest/index?time=utc oder http://www.seismo.ethz.ch/de/earthquakes/switzerland/all-earthquakes/

She	Shebalin NV, Leydecker G, Mokrushina NG, Tatevossian RE, Erteleva OO, Vassiliev VYu (1998) Earthquake catalogue for central and southeastern Europe 342 BC - 1990 AD. European Commission, Report ETNU CT 93 - 0087, Brussels, Belgium
SisF10	BRGM-EDF-IRSN (2010), Base de données SisFrance des séismes historique en France. Bureau de recherche géologique et minière, Paris, France (www.sisfrance.net)
SKO	University Seismological Observatory, Skopje
SMM	Stich D, Martin R, Morales J (2010) Moment tensor inversion for Iberia-Maghreb earthquakes 2005-2008. Tectonophysics 483:390-398 doi:10.1016/j.tecto.2009.11.006
SMTS	http://www.seismo.ethz.ch/static/moment_tensor/homepage.html
SOF	Department of Seismology, Geophysical Institute, Bulgarian Academy of Sciences, Acad
Sul	Sulstarova E, Koçiu S, Muço B, Peçi V (2000) Catalogue of earthquakes in Albania with Ms≥4.5 for the period 58-2000. Internal Report, Seismological Institute, Tirana, Albania
TIR	Seismological Institute, Academy of Sciences of Albania, Rruga Don Bosko, Tirana, Albania (Datafiles from ISC)
Tot	Tóth L, Mónus P, Zsíros T, Kiszely M, Czifra T (2006) Data file of Hungarian earthquakes. GeoRisk Ltd, Budapest, Hungary /for 2000-2005/ (www.georisk.hu)
TR-GSHAP	Turkish GSHAP catalogue (2000) Turkish catalogue of significant earthquakes provided for GSHAP. Available at Swiss Seismological Service, Swiss Federal Institute of Technology, Zurich, Switzerland (www.seismo.ethz.ch/gshap/turkey/seisgshap.prn)
WG	Seismicity and seismotectonic implications in the southern Baltic Sea area, Terra Nova, 6, 149-157, 1994.
ZAMG	Lenhardt W (1996) Data file of Austrian earthquakes. Zentralanstalt für Meteorologie und Geodynamik, Hauptabteilung für Geophysik, Vienna, Austria /until 1995/
ZAMG09L	Lenhardt, W (2009) Data file of Austrian earthquakes. Zentralanstalt für Meteorologie und Geodynamik, Hauptabteilung für Geophysik, Vienna, Austria
Zi94	Zsíros T (1994) Data file of Hungarian earthquakes. Seismological Observatory, Geodetic and Geophysical Research Institute, Hungarian Academy of Sciences, Budapest, Hungary /for 1987-1994/
Ziv18	Živčić M (2018) Data file “Earthquake Catalogue of Slovenia” of the Seismology and Geology Office. Environmental Agency of the Republic of Slovenia, Ljubljana, Slovenia
ZivS	Živčić M (1993) Data file “Earthquake Catalogue of Slovenia” of the Seismology and Geology Office. Environmental Agency of the Republic of Slovenia, Ljubljana, Slovenia
Zsi	Zsíros T, Mónus P, Tóth L (1990) Hungarian earthquake catalogue (456-1986). Seismological Observatory, Geodetic and Geophysical Research Institute, Hungarian Academy of Sciences, Budapest, Hungary
Zsi99	Zsíros T (1999) Data file of Hungarian earthquakes. Seismological Observatory, Geodetic and Geophysical Research Institute, Hungarian Academy of Sciences, Budapest, Hungary /for 1995-1999/

2.2 SHEEC 1000 - 1899

The 1000-1899 part of the earthquake catalogue at the basis of ESHM13 is SHEEC (SHARE European Earthquake Catalogue) 1000-1899 (Stucchi et al., 2013; <https://www.emidius.eu/SHEEC/>; SHEEC 1000-1899 or SHEEC from now on). Instead of a collation of parameters from national catalogues as the 1900-present part, SHEEC 1000-1899 relies upon the homogenous assessment of locations and moment

magnitude, achieved through the processing of macroseismic intensity data (Macroseismic Data Points, MDPs from now on) with the same procedure throughout Europe. To take into account the knowledge provided by regional and national earthquake catalogues, SHEEC 1000-1899, considers for each earthquake parameters determined from both i) the homogeneous and repeatable processing of MDPs, and ii) the homogenization of those provided by selected regional catalogues.

As detailed in Stucchi et al. (2013) and Gomez Capera et al. (2015), earthquake parameters were derived from MDPs with the following methods, all based on the attenuation of macroseismic intensity as a function of earthquake magnitude and epi-/hypocentral distance:

1. Boxer 4.0 (Gasperini et al., 1999; 2010);
2. MEEP (Musson and Jiménez, 2008);
3. B&W (Bakun and Wentworth, 1997).

The three methods rely on attenuation models that depend on the regional variations in both the attenuation characteristics and the peculiarities of intensity assessment. For each method, the attenuation models were calibrated for five regions using, in each of them, the same set of calibrating events, i.e earthquakes of known instrumental magnitude and with reliable MDPs distributions (details are in Gomez Capera et al., 2015).

Parameters from 30 regional catalogues selected according to their reliability, with preference to publicly available ones, were also considered. From such catalogues, the epicentral location was adopted, and moment magnitude was calculated from epicentral intensity (I_0) with five regional I_0 -to- M_w empirical relations derived, for the sake of homogeneity, from the same datasets used for calibrating the MDPs methods. As an exception, if a catalogue provides M_w values, they were adopted without any modifications.

As for the final parameters, locations were selected from those calculated from MDPs or derived from regional catalogues according to a priority scheme. The M_w value and related uncertainty is i) the weighted mean of the determinations from MDPs and from the regional catalogue when they are both available, or either ii) obtained from MDPs methods or iii) from regional catalogues, when they are the only available ones.

Input data for each earthquake, in terms of MDPs sets and parameters from regional catalogues, were selected from the European Archive of Historical Earthquake Data (AHEAD; <http://www.emidius.eu/AHEAD/>; Locati et al., 2014; Rovida and Locati, 2015). Figure 7 shows the procedure followed in the compilation of SHEEC 1000-1899 and its relationship with AHEAD.

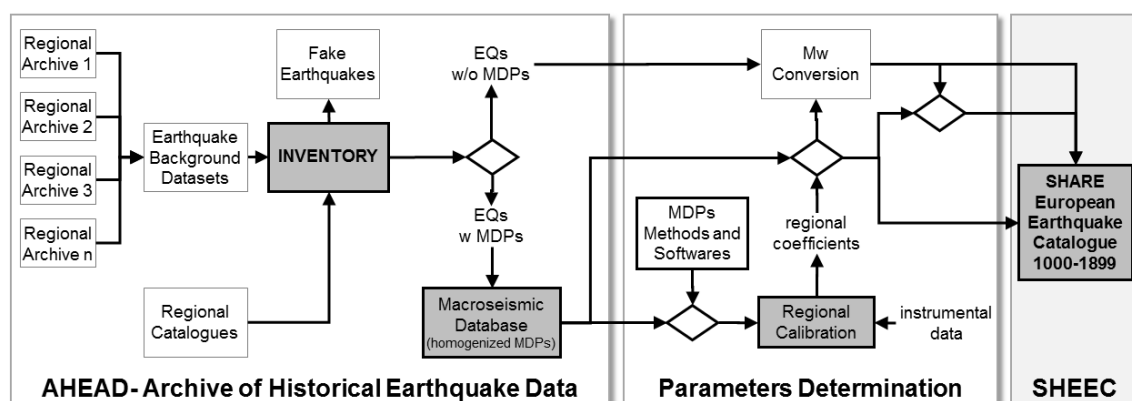


Figure 7: Workflow followed in the compilation of SHEEC 1000-1899 (from Stucchi et al., 2013).

AHEAD inventories and makes available the results of historical seismological research considering:

- Regional and national macroseismic databases,

- Regional historical seismological studies,
- Studies on individual earthquakes,
- The main current parametric catalogues.

AHEAD deals with the multiplicity of studies and datasets that may refer to the same earthquake, providing coinciding or conflicting information. In such cases datasets referring to the same earthquake are thoroughly examined and compared, and then clustered on a case-by-case basis. In the compilation of an earthquake catalogue, such a procedure is useful to deal with i) duplications of earthquakes; ii) fake events, and iii) earthquakes missing in one or more catalogues.

As a result, AHEAD provided a reliable list of 4,722 earthquakes with approximately $10 > 5$ and/or $M > 3.5$. For about 51% of such earthquakes, MDPs derived from regional databases or from the literature are available (42,358 MDPs as a whole), 40% of the earthquakes are supported by a seismological study not providing MDPs, while the remaining 9% is known only through an entry from a national or regional catalogue.

Taking into account the strategy followed for the compilation of SHEEC 1000-1899 summarized above, a future update of the catalogue should face the possible changes/updates in each of the three following aspects:

1. Updates in the input macroseismic datasets
2. Updates in the input regional catalogues
3. Updates in the regional calibration of the method(s) used for deriving earthquake parameters from MDPs.

There are no major innovations that could justify a revision of regional calibrations, as new datasets on recent earthquakes that can significantly improve the calibration datasets used for SHEEC 1000-1899 have not been published since then. The only exception is Italy, as detailed in the following Section dedicated to the update of the Italian catalogue.

Updates in the input macroseismic datasets and regional catalogue are manifold and are described in the following sub-sections.

2.2.1 Updates of the input macroseismic datasets

As a whole, SHEEC 1000-1899 relies on 128 historical macroseismic studies providing MDPs, and 51 regional catalogues, all archived in AHEAD. The content of AHEAD has not been updated since the end of the SHARE Project, and the release of SHEEC 1000-1899 in 2012. This means that recent datasets published after 2011 are not taken into account, as well as a few studies published before.

In this period, among the regional macroseismic repositories (“regional nodes”) contributing data to AHEAD, only the Italian Archive of Historical Earthquake Data (ASMI, <https://emidius.mi.ingv.it/ASMI/>) and the French database SisFrance (BRGM-EDF-IRSN/SisFrance, 2016; www.sisfrance.org) were updated, as described in the following.

Italian Archive of Historical Earthquake Data ASMI

The Italian Archive of Historical Earthquake Data ASMI (Archivio Storico Macrosismico Italiano; <https://emidius.mi.ingv.it/ASMI/>) provides access to data on more than 5000 Italian earthquakes in the period 461 b.C to 2014, deriving from more than 300 seismological studies and catalogues. As in AHEAD, ASMI presents different kinds of studies for the same earthquake, giving a wide perspective on the multiplicity of the available information. ASMI provided data for the compilation of the Parametric Catalogue of Italian Earthquakes CPTI15 (Rovida et al., 2016) and its associated macroseismic database DBMI15 (Locati et al., 2016), both available at <https://emidius.mi.ingv.it/CPTI15-DBMI15/>. Although existing since many years as a working platform, ASMI was made fully accessible through a dedicated web portal and related webservice in 2017. ASMI is continuously updated, as soon as new studies are

published. For the period of interest (1000-1899), ASMI contains 2653 earthquakes derived from 168 studies (for a total of more than 15,000 records). In the area of validity of ASMI (the area covered by the Italian territory and sea, plus a buffer of about 50 km, see Figure 8) SHEEC 1000-1899 lists 1853 earthquakes derived from 107 studies. The records in AHEAD, related to the 1853 earthquakes are 6888. Out of the studies considered in ASMI, 38 are new with respect to those in AHEAD and contribute a total of 1167 new records. It is worth noting that such records refer to 25 newly recognized fake earthquakes, and several earthquakes that are not in the Italian portion of SHEEC 1000-1899.

SisFrance

Two versions of the French database SisFrance (www.sisfrance.org) were released in 2014 and 2016 (BRGM-EDF-IRSN/SisFrance, 2014; 2016) after the completion of SHEEC 1000-1899. The latest version, SisFrance 2016, contains 5704 earthquakes as a whole. All earthquakes have at least one MDP, and for 1760 of them also epicentral coordinates and epicentral intensity are provided.

For the period 1000-1899, SisFrance 2016 lists 3009 earthquakes, while the 2010 version considered in SHEEC 1000-1899, contains 2855 events. The common earthquakes are 2839, with 16 earthquakes of SisFrance 2010 that are no longer in SisFrance 2016, 14 of which are considered as fakes. SisFrance 2016 contains 170 earthquakes that were not in SisFrance 2010, only 6 of them have $I_0 > 5$, and 5 additional ones have maximum intensity > 5 .

In SHEEC MDPs distributions from SisFrance 2010 were parameterized for 583 earthquakes, that are all listed also in SisFrance 2016, except for one earthquake that is now considered fake.

A detailed comparison of the MDPs distributions of the 582 common earthquakes has not yet been performed, however, considering just the variations in the number of MDPs and maximum intensity, 113 MDPs distributions result as updated in SisFrance 2016.

In addition, SisFrance 2016 contains 203 earthquakes in common with SisFrance 2010 that are within the thresholds of SHEEC 1000-1899 but were not selected as the reference dataset for SHEEC. Of these 203, 85 earthquakes show a number of MDPs higher than the dataset selected in SHEEC, implying that the replacement of the selected datasets with the new SisFrance ones should be considered in the update of SHEEC.

Single studies

A thorough, though possibly incomplete, survey of the recent historical seismological literature resulted in a list of 14 historical macroseismic studies published between 2012 and 2018 and dealing with a total of about 150 earthquakes (Table 3). Of such earthquakes, 47 (with a total of more than 1400 MDPs) are in the time-span and intensity threshold of SHEEC 1000-1899, and some are new with respect to it. In addition, the new studies contain information about fake earthquakes that may cancel records of SHEEC.

Table 3: Historical seismological studies providing MDPs published after SHEEC 1000-1899

REFERENCE	GEO COVERAGE	TOTAL EQ	INPUT EQ.	INPUT MDPS	NOTES
ALBINI & ROVIDA, 2018	Croatia, Montenegro	24	8	22	4 fakes
ALBINI & ROVIDA, 2016	Croatia, Montenegro	1	1	37	
ALBINI ET AL., 2017	Greece	5	5	144	
ALBINI, 2015	Croatia, Montenegro	1	1	37	
ALEXANDRE & ALEXANDRE, 2012	Eastern Europe	54			41 fakes
ALEXANDRE & ALEXANDRE, 2018	Eastern Europe	19	2	38	1 fake
BAPTISTA ET AL., 2014	Portugal	1	1	32	
HAMMERL & LENHARDT, 2013	Lower Austria	18	12	722	
HERAK ET AL., 2017	Croatia	13	7	38	
HERAK ET AL., 2018	Croatia	5	4	108	
KNUTS ET AL., 2015	Luxembourg	1	1	21	
KNUTS ET AL., 2016	Belgium, Germany	1	1	75	
RIBEIRO ET AL., 2015	Portugal	1	1	88	
SCHWARZ-ZANETTI ET AL., 2017	Switzerland	3	3	55	

2.2.2 Updates of the input regional catalogues

In the following, we describe the catalogues that became available after the release of SHEEC 1000-1899. According to the principles of SHEEC, we exclusively refer to published catalogues (i.e. those made publicly available through a scientific publication or a website). The new catalogues have been compared with SHEEC 1000-1899 in terms of both the number of earthquakes and their parameters.

Italy – CPTI15

In 2016 a new version of the Italian national catalogue CPTI15 (Italian Parametric Earthquake Catalogue) was released (Rovida et al., 2016; <http://emidius.mi.ingv.it/CPTI15-DBMI15/>). As its previous versions, CPTI15 is compiled according to the same procedures later adopted by SHEEC 1000-1899, based on ASMI for the collection and comparison of the input datasets and on DBMI15 (Locati et al., 2016) as a macroseismic database. Relying on the content of ASMI, CPTI15 has an informative background more recent than SHEEC, as a consequence of the already mentioned differences between ASMI and AHEAD. Such diversity reflects in the content and the parameters of the two catalogues.

For the time period 1000-1899, the Italian part (i.e. in the area shown in Figure 8) of SHEEC 1000-1899 lists 1857 earthquakes, compared to the 1765 earthquakes in the 1000-1899 part of CPTI15. The earthquakes in both CPTI15 and SHEEC are 1436. Earthquakes that are in SHEEC and not in CPTI15 are 417, out of which 383 are below the threshold of CPTI15 (maximum intensity ≥ 5 and $M_w \geq 4.0$, versus epicentral intensity > 5 and $M_w > 3.5$ of SHEEC), 21 are fake according to the new study selected for CPTI15, and 8 are not included in CPTI15 because their informative background is not robust enough. Conversely, 329 earthquakes in CPTI15 are not in SHEEC. Out of these, 220 earthquakes were unknown at the time of the compilation of SHEEC, and 75 are below its thresholds. In addition, 15 earthquakes were below the thresholds of SHEEC, while the new selected study brings them above it, 2 were

considered as fakes and 17, being not parametrizable, were not included in SHEEC. In addition, 4 earthquakes in SHEEC were recognized as duplications while compiling CPTI15.

The 1436 earthquakes that are in both catalogues rely upon the same study in 799 cases, while 637 are based on a different, more recent one. Such studies are 39, and supply 5307 MDPs for 486 earthquakes. As a whole, CPTI15 considers 27 studies new with respect to SHEEC that provide 1249 MDPs to 329 earthquakes. Of the 637 mentioned earthquakes, 416 were supported in SHEEC only by an entry from a parametric catalogue, whereas the new studies supply 2679 new MDPs for 316 of them.

In addition to the changes in the input datasets, the parameterization of MDPs in CPTI15 is slightly different from SHEEC 1000-1899. Although both catalogues make use of the Boxer method (Gasperini et al., 1999; 2000), for CPTI15 it was recalibrated with an updated and robust dataset of instrumental magnitudes and intensity data. On the other hand, for earthquakes in the Italian area, two regional calibrations of Boxer were applied in SHEEC 1000-1899, i) for earthquakes in the Western Alps (“WAP”; see Gomez Capera et al., 2015), and ii) for the Apennine region (“APD”). The first calibration was specifically derived during the compilation of SHEEC, while the second was realized for, and adopted by, the CPTI04 catalogue in 2004 (Working Group CPTI, 2004).

The combination of the different input data and calibrations obviously results in differences in the parameters of the earthquakes that are in both CPTI15 and SHEEC 1000-1899.

Figure 8 shows the differences in locations of the 1359 that are in both catalogues and have an epicentral location.

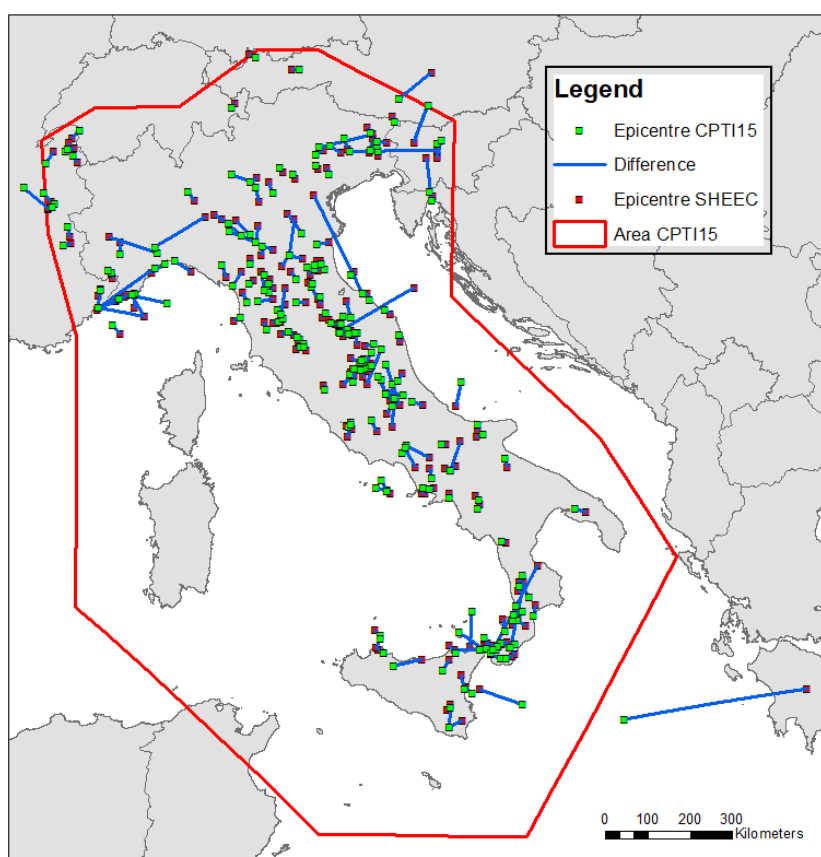


Figure 8: Location differences ≥ 10 km between SHEEC 1000-1899 and CPTI15. The area of validity of CPTI15 is also shown.

Differences in locations ≥ 10 km are 219 and are mostly the consequence of the change of the input dataset. Differences in the location of earthquakes with the same input macroseismic data are due to different choices in the parametrization strategy. For example, in SHEEC the parameters of offshore earthquakes were derived with B&W instead of Boxer, and in few cases the solution proposed by the

regional catalogue was preferred. In addition, a different conversion into numerical values of unconventional intensities, such as “felt”, “damage”, etc., results in different epicentral locations.

The magnitude differences between CPTI15 and SHEEC 1000-1899 (Figure 9) are within the average uncertainty of the CPTI15 values (± 0.41 Mw units) for the 73% of the 1334 common events with a Mw determination. However, 5% of the earthquakes has differences ≥ 1 Mw units, and as high as 2.3 Mw units. As a general trend, magnitudes in SHEEC 1000-1899, especially in the range 4.5 to 5.5 are higher than in CPTI15, and the highest differences are observed in the same range.

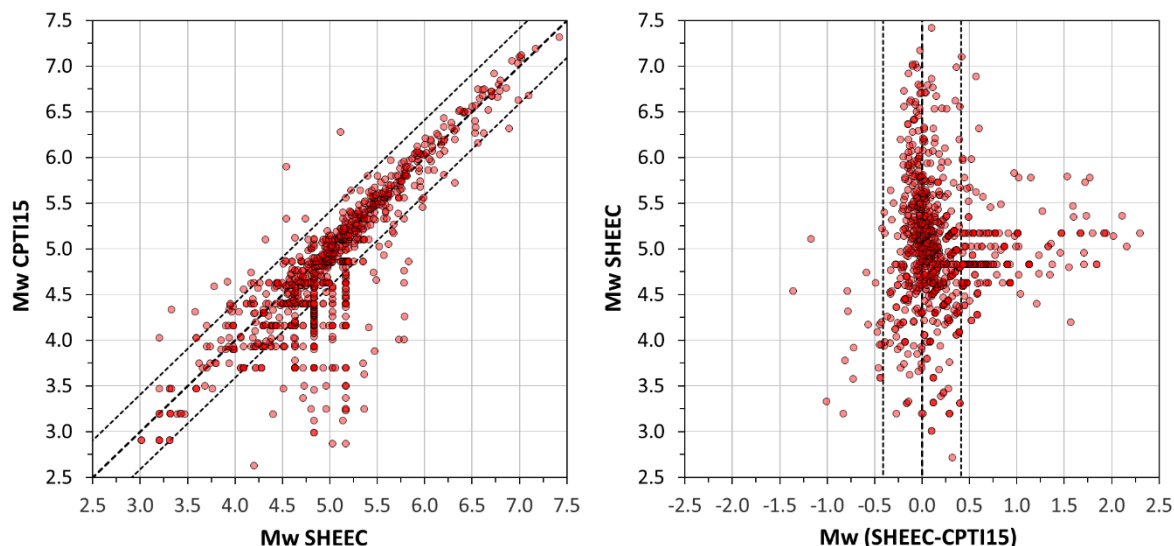


Figure 9: Comparison of the Mw values in SHEEC 1000-1899 and CPTI15

To investigate the reasons behind the identified differences, we first analysed the values resulting from the parameterization of MDPs, separately for the APD and WAP regional calibrations (Figure 10). The earthquakes with MDPs in both CPTI15 and SHEEC 1000-1899 are 918, 788 of them are parametrized in SHEEC according to the APD calibration, and 130 according to the WAP calibration. On average, Mw from the APD calibration show the already observed trend, characterized by the lowering of Mw between 4.5 and 5.5. On the contrary, Mw derived with the WAP calibration are generally lower than those obtained with the new CPTI15 calibration. For the APD region, 93% of the earthquakes have a Mw difference within the average Mw uncertainty in CPTI15, for the WAP region the percentage is 62%, while for both regions together it is the 88%. Most (68%) of the differences ≥ 1 Mw units, resulting from the APD calibration and particularly evident for earthquakes with a decreased Mw in CPTI15, are due to a different parametrization strategy used in CPTI15 for earthquakes in the Etna, Ischia island and Campi Flegrei volcanic areas, that was not applied in SHEEC 1000-1899.

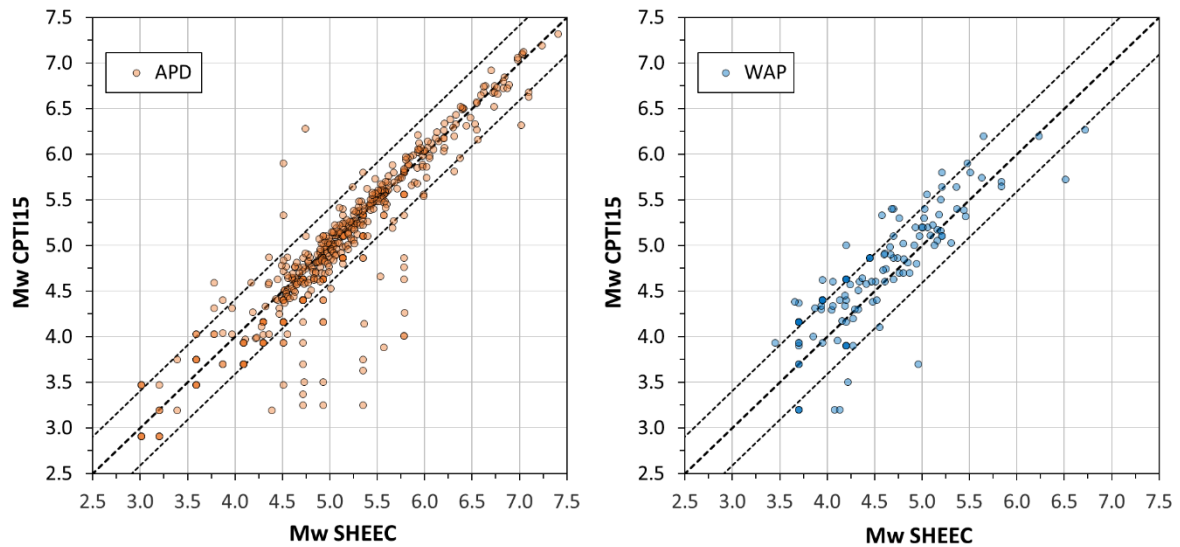


Figure 10: Comparison of the Mw values from MDPs in SHEEC 1000-1899 and CPTI15, according to the APD (left) and WAP (right) calibrations.

To remove from the analysis the effect of the change in the input macroseismic dataset, we finally compare only the 695 earthquakes that are supported by the same MDP dataset in both CPTI15 and SHEEC 1000-1899, and whose magnitudes are calculated with Boxer (Figure 11). The resulting general trends are similar to those observed above, with all the 634 earthquakes bar one in the APD region and the 70% of the 61 in the WAP region that have a Mw difference within the average Mw uncertainty in CPTI15. For the APD calibration, the percentage of decreased Mw in CPTI15 versus increased ones are 74% and 26%, respectively. The opposite is observed for the WAP region, where 85% of the magnitudes are higher in CPTI15 than in SHEEC, and 15% are lower.

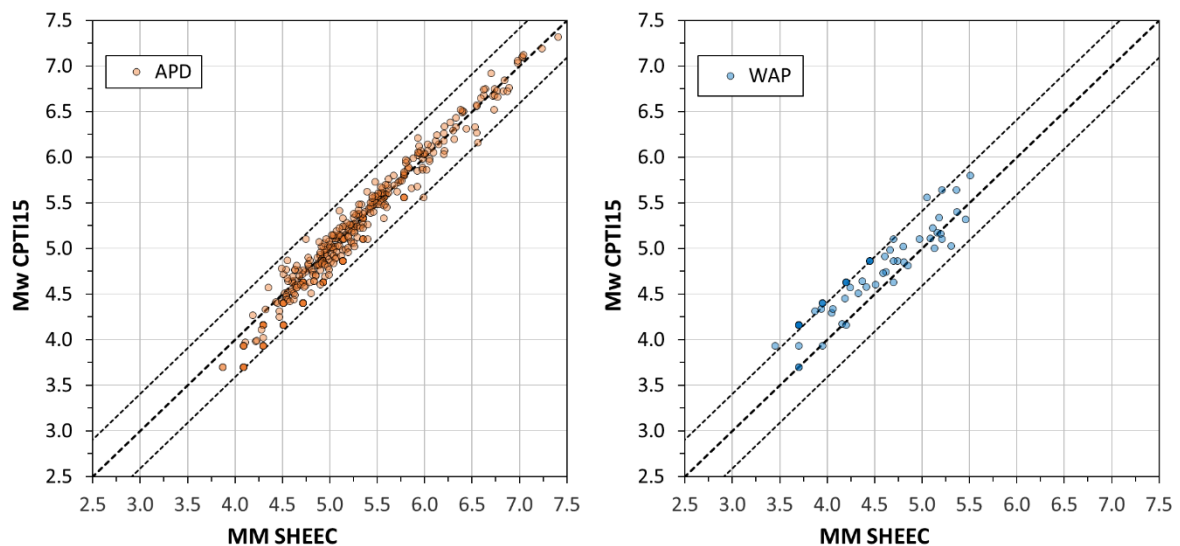


Figure 11: Comparison of the Mw values from the same MDP distributions in SHEEC 1000-1899 and CPTI15, according to the APD (left) and WAP (right) calibrations.

The new parametrization of CPTI15 also includes an updated I0-to-MW empirical conversion relation, derived from the same dataset used for the calibration of Boxer. Consequently, the new relation is based on a larger set of calibration earthquakes than the WAP and APD ones and results more robust, especially for low magnitudes (Figure 12).

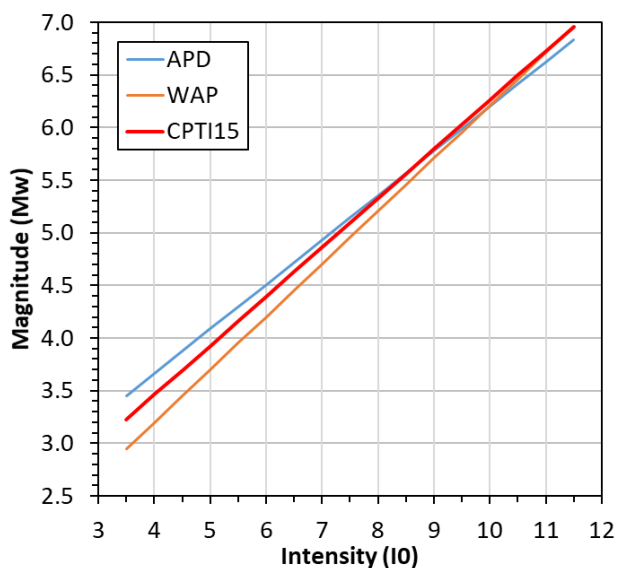


Figure 12: Comparison of the epicentral intensity to Mw empirical relations for the APD and WAP calibrations, with the new CPT115 one.

The final Mw in SHEEC 1000-1899 results from the combination of the determination from MDPs and from regional catalogues. For the Italian area, the selected regional catalogue was the 2004 version of CPTI (CPTI04), the reference catalogue for Italy at the time. Figure 13 compares the Mw values of CPTI04 with those from CPT115 for the 934 earthquakes whose magnitudes in SHEEC took into account also CPTI04. The figure shows significant variations in the magnitudes of the two catalogues, especially for Mw(CPTI04) between 4.6 and 5.3.

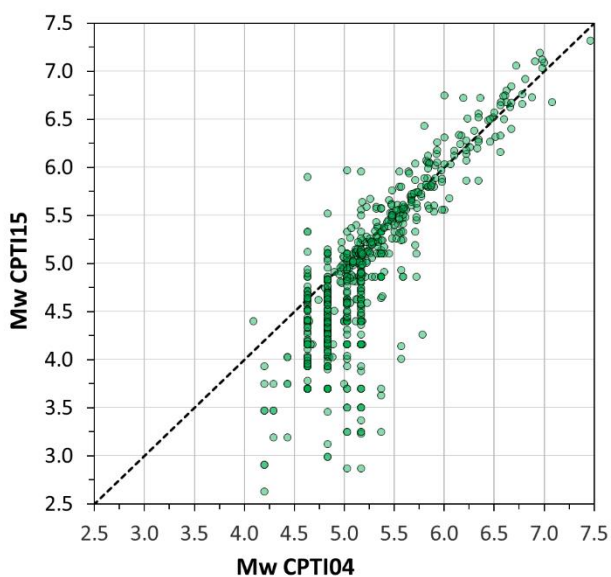


Figure 13: Comparison of the Mw values in CPTI04 and CPT115 for the earthquakes that consider CPTI04 as a reference catalogue.

The differences in the magnitudes explained above are summarized in Figure 14, which compares the SHEEC 1000-1899 “default” Mw, together with its two components (from macroseismic data and from CPTI04), with the Mw according to CPT115.

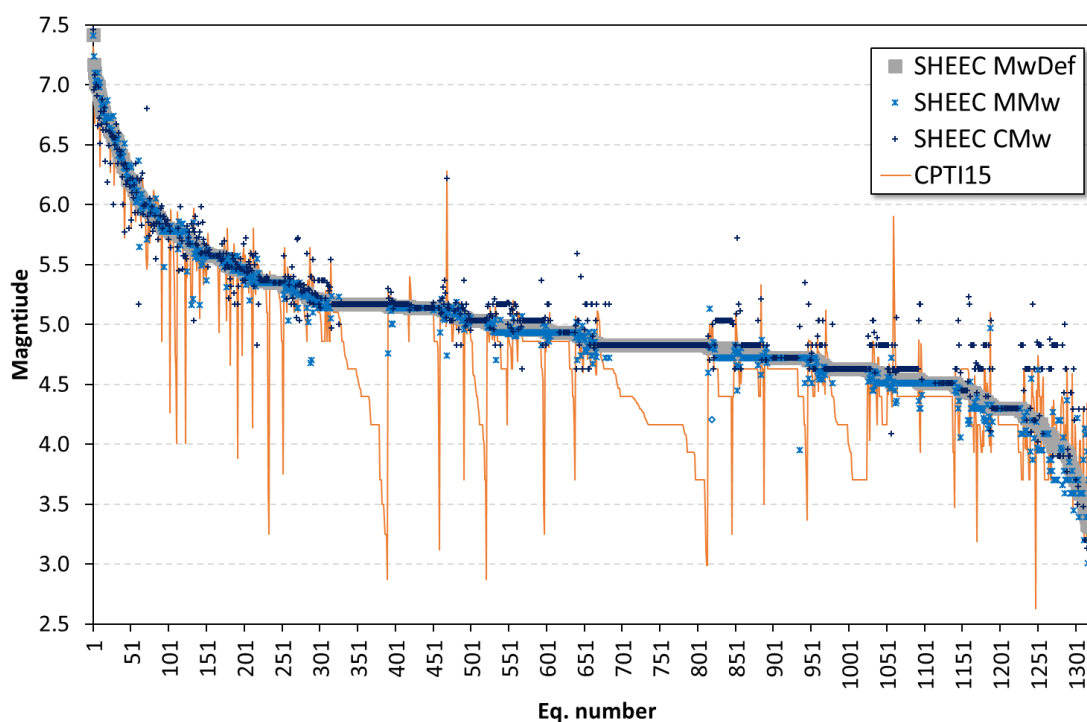


Figure 14: Comparison of SHEEC 1000-1899 “default” Mw and of its two components, from macroseismic data (MMw) and from the regional catalogue CPTI04 (CMw), with the Mw of CPTI15.

France – FCAT-17

The earthquake catalogue for the French “metropolitan” area named FCAT-17 was published in 2018 (Manchuel et al., 2018). The catalogue collates two parts, instrumental (1965-2009) and macroseismic (463-1964). The instrumental part coincides with the recent Si-Hex instrumental catalogue (Cara et al., 2015), whereas the macroseismic part consists of the location provided by SisFrance, version 2014, and the parametrization of SisFrance MDPs in terms of Mw and depth, only. Macroseismic magnitudes and depths are assessed through a set of specifically derived Intensity Prediction Equations – IPE (Baumont et al., 2018) calibrated and applied with a complex logic-tree approach (Traversa et al., 2018) that takes into account the peculiarities of SisFrance intensity data and the epistemic uncertainty related to both macroseismic data and the IPE selection. The whole catalogue contains about 41'658 earthquakes located within 40 km or 20 km to the French borders, respectively for historical and instrumental events.

For the macroseismic part of the catalogue, only the 27% of the earthquakes have both Mw and depth jointly assessed, and for 73% of them depth is assigned a-priori according to a 9-zones seismological and geological regionalization. For the same part, uncertainties in both Mw and depth are assessed, and a quality index is provided.

The 1000-1899 portion of FCAT-17 is compared with SHEEC 1000-1899, for the 663 common events.

Location is different in the two catalogues in 280 cases, of which 149 have distances ≥ 10 km (Figure 15). Such differences are mostly due to the different way epicentres are determined in the two catalogues. With respect to the location provided in SHEEC 1000-1899, 55% of the differences regards epicentres estimated from MDPs, the remaining from the reference regional catalogue, i.e. 8% from the adopted French regional catalogue FPEC V.1.1 (Baumont and Scotti, 2011; see below), and 37% from regional catalogues of neighbouring countries.

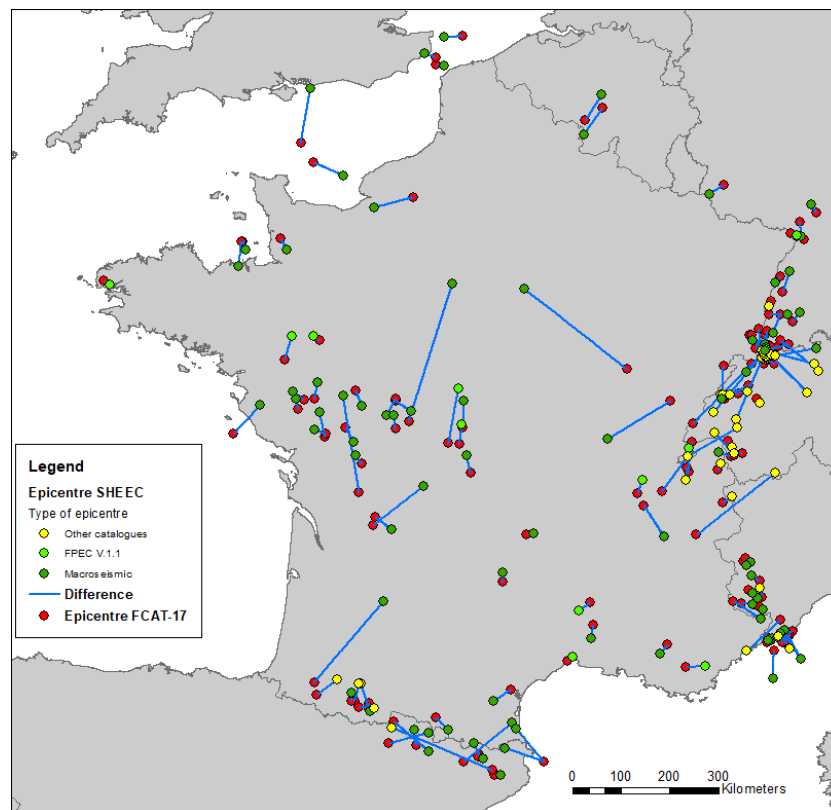


Figure 15: Location differences ≥ 10 km between SHEEC 1000-1899 and FCAT-17.

The 648 common earthquakes with a M_w determination in SHEEC present significant differences in the magnitude estimated by the two catalogues (Figure 16), most evident in intermediate-to-low magnitudes, with 36% of the differences outside the average uncertainty of the SHEEC 1000-1899 estimates (± 0.45 M_w units), and almost 10% of the differences that are ≥ 1 M_w units, up to a difference of 3.1 M_w units. As a general trend, FCAT-17 tends to underestimate SHEEC magnitudes, as these latter are higher than in FCAT-17 in 59% of the cases.

As for the component of the SHEEC 1000-1899 final magnitudes assessed from MDPs with Boxer (621 earthquakes), magnitude differences exceed the average uncertainty in SHEEC in 38% of the cases, and 8% of the earthquakes have differences ≥ 1 M_w units and as high as 2.02 M_w units. For 43% of the earthquakes, the M_w estimate in SHEEC is higher than FCAT-17's one.

FCAT-17 is also compared with the regional catalogue considered for France, that is the macroseismic catalogue FPEC v.1.1 (Baumont and Scotti, 2011), based on an approach similar to the one adopted by FCAT-17 applied to data in the 2009 version of SisFrance, and with a different set of IPEs and logic-tree.

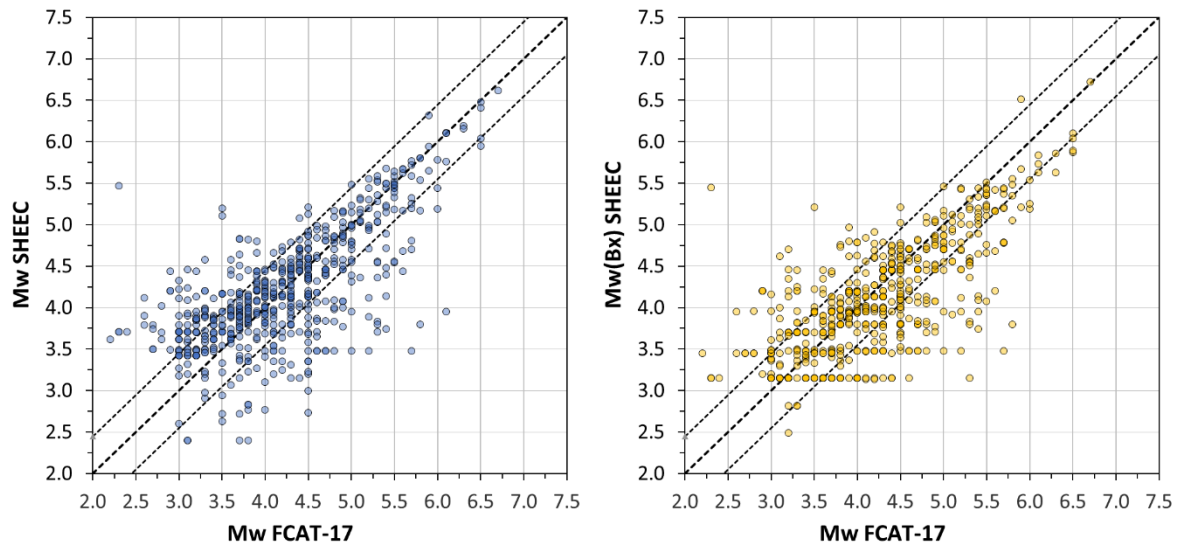


Figure 16: Magnitude comparison of FCAT-17 and SHEEC 1000-1899 for all the magnitudes (left), and for Mw calculated with Boxer in SHEEC (right).

The comparison, limited to the time-period of interest 1000-1899, deals with 479 earthquakes and shows significant differences in magnitudes (Figure 17), with the 38% of the differences exceeding ± 0.4 Mw units. FCAT17 magnitudes are lower than those in FPEC V.1.1 in the 72% of the cases. Being adopted from SisFrance in both catalogues, locations are very similar, with only 24 different ones (12 with distances ≥ 10 km), possibly resulting from SisFrance updates.

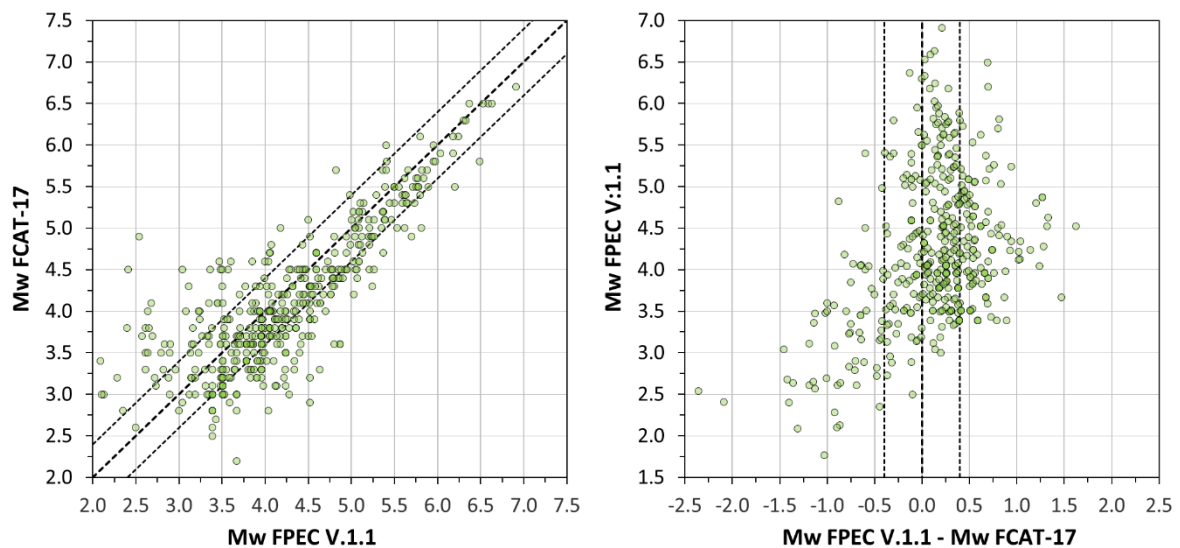


Figure 17: Magnitude comparison of FPEC V:1.1 and FCAT-17 and SHEEC 1000-1899.

Depths assessed for the 479 earthquakes in both FCAT-17 and FPEC V.1.1 show almost no correlation (Figure 18), evidencing the low reliability of the assessment of depth from macroseismic data.

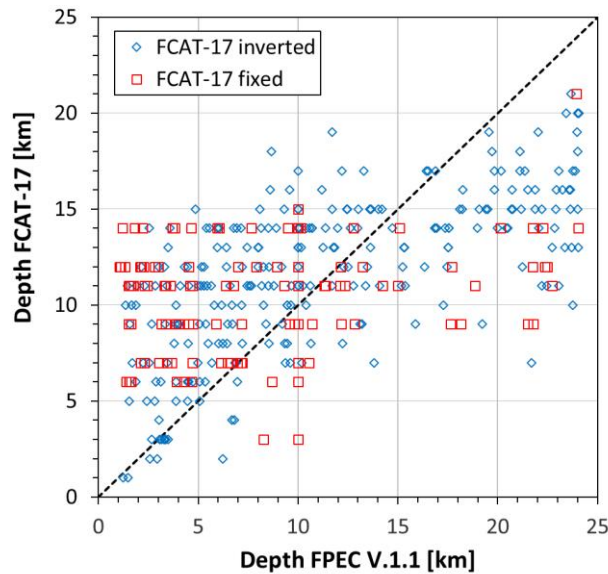


Figure 18: Depth comparison of FPEC V:1.1 and FCAT-17 and SHEEC 1000-1899.

Figure 19 summarizes the comparison of SHEEC 1000-1899 Mw assessments (final, macroseismic and from the selected regional catalogue FPEC V.1.1) with the value proposed by the new FCAT-17.

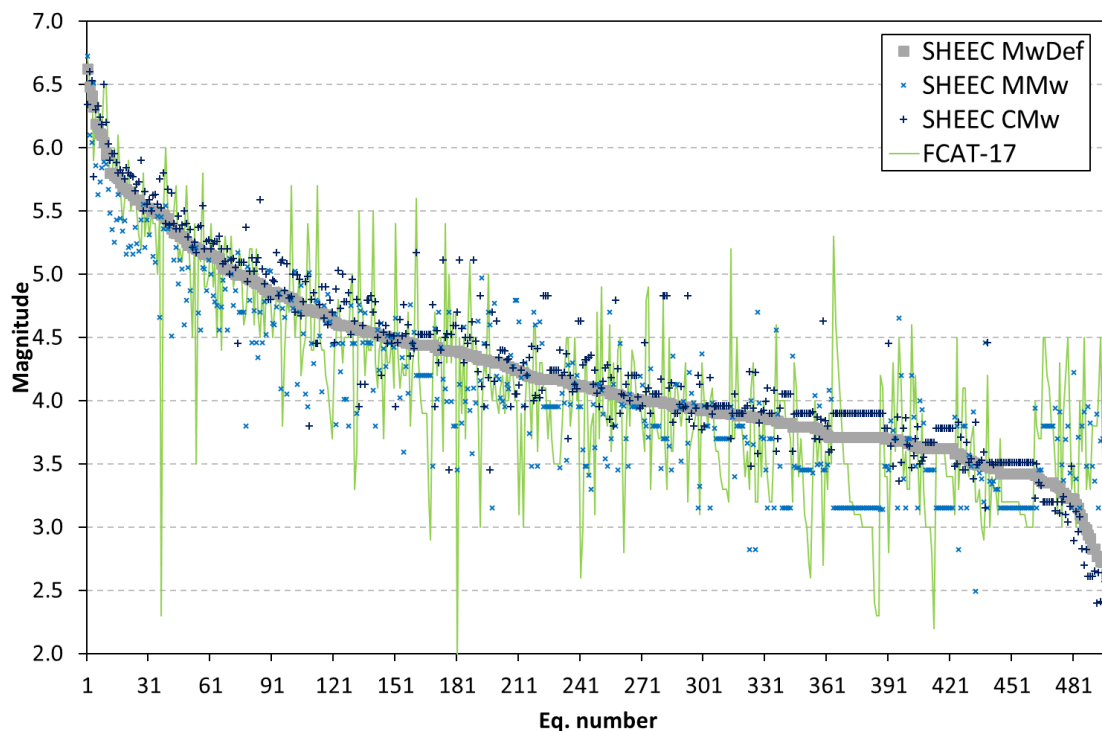


Figure 19: Comparison of SHEEC 1000-1899 “default” Mw and of its two components, from macroseismic data (MMw) and from the regional catalogue FPEC V.1.1 (CMw), with the Mw of FCAT-17.

Turkey

The most recent PSHA of Turkey (Sesetyan et al., 2018; Demircioglu et al., 2018; Akkar et al., 2018) made use of an earthquake catalogue derived, for the 1000-1899 time-window, from SHEEC and its extension east of 32° longitude (SHARE-CET; Sesetyan et al., 2012). In particular, the catalogue used in the Turkish hazard model complemented SHEEC/SHARE-CET with entries from the Global Historical Earthquake Catalogue (GHEC; Albini et al., 2014) for earthquakes with $M \geq 7$, and from the catalogue

compiled and used in the frame of the Earthquake Model of the Middle-East Project (Zare et al., 2014), especially for earthquakes to the east and to the south of Turkey.

3 Faults

3.1 Summary of fault data published after the end of project SHARE

This section illustrates the main compilations of active and seismogenic faults in the Euro-Mediterranean region. Only the compilations covering significantly large regions are considered, relying on the work of the compilers and contributors of each compilation for summarizing the knowledge derived from the literature and the used original data. We will resort to work on single faults only in case of troublesome situations, e.g. area of overlap between two regional compilations.

This overview starts with the European Database of Seismogenic Faults (EDSF; Basili et al., 2013; Figure 21) compiled during the EU-FP7 Project SHARE and carries on with other similar datasets completed independently during and after that project.

Two main categories of seismogenic faults are considered: 1) crustal faults; and 2) subduction zones (Figure 20).

In EDSF and other compilations, crustal faults are represented with a down-dip planar geometry, whereas subduction zones are represented by a complex 3D geometry of the slab. In some cases, crustal faults are represented only by the trace of the fault upper edge and the fault plane need to be extruded from the dip and depth values.

The minimum set of basic fault parameters required for constructing a seismogenic source model refer to Geometry (Location: Lat, Lon, Depth; Size: Length, Width; Orientation: Strike, Dip) and Behavior (Rake and Slip Rate). These are indispensable elements for devising and applying a fault recurrence model to be expressed by a Magnitude-Frequency Distribution (MFD). Not all fault compilations provide this characterization in full and strategies need to be devised to fill in the missing information.

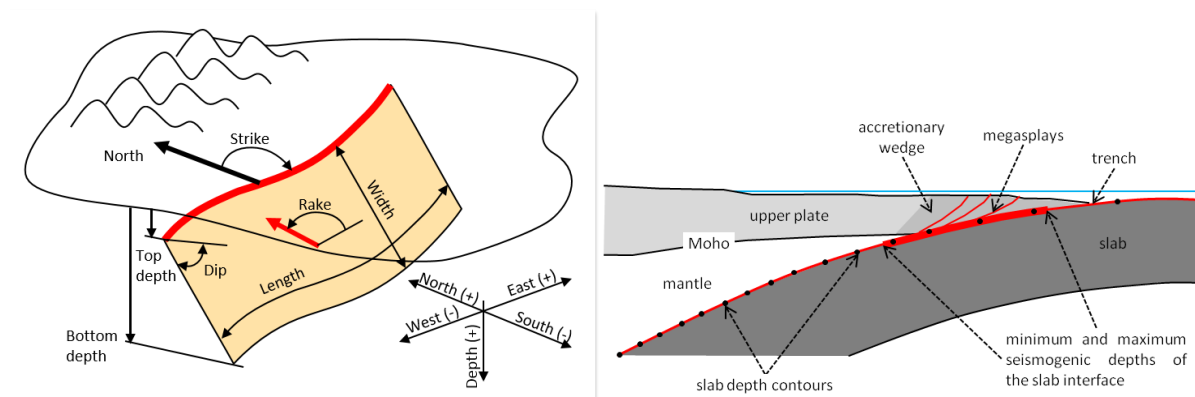


Figure 20: Generalized scheme representing a crustal seismogenic fault (left) and a subduction (right).

Crustal faults

Concerning crustal faults, we identified ten different regional datasets (Table 4) in addition to the EDSF 2013 (Figure 21). These datasets vary in date of latest update, geographical extent, level of fault characterization, accessibility and reusability, and more importantly data formats. DISS, GREDASS, and QAFI are accessible through dedicated websites. The faults in the Lower Rhine Graben in addition to what was incorporated in EDSF, were then published by Vanneste et al. (2013) and a later review of the slip rates is available from Gold et al. (2018). These for datasets (Figure 22) can be easily incorporated into the fault source model for ESHM20.

Table 4: Collection of datasets about crustal faults.

TITLE	REFERENCE	URL	COVERAGE	LICENSE	ACCESS
EDSF 2013	Basili et al. (2013); Giardini et al. (2013)	http://diss.rm.ingv.it/share-edsf/	Europe and Mediterranean	CC BY-SA 4.0	OGC WFS WMS, file download
QAFI 3	IGME (2015)	http://info.igme.es/qafi/	Iberia	CC BY-SA 4.0	file download
DISS 3.2.1	DISSWG (2018)	http://diss.rm.ingv.it/diss/	Central Mediterranean	CC BY-SA 4.0	OGC WFS WMS, file download
GREDASS 2.0.0	Caputo & Pavlides (2013)	http://gredass.unife.it/	Aegean	Attribution only	file download
LRGM	Vanneste et al. (2013)	--	Lower Rhine Graben	Attribution only	from ROB
AFCD	Emre et al. (2018); Demircioğlu et al. (2017)	http://www.mta.gov.tr/eng/maps/active-fault-1250000	Anatolia	Attribution only	--
EMME FAULT SOURCES	Danciu et al. (2018)	http://www.efehr.org/en/Documentation/specific-hazard-models/middle-east/active-faults/	Middle East	Attribution only	file download
NOAFAULTS	Ganas et al. (2013)	--	Greece	freeware	file download
INFP	Diaconescu et al. (2018)	http://faults.inf.p.ro/	Northern Black Sea	Attribution only	--
BDFA	Jomard et al. (2017)	https://www.nat-hazards-earth-syst-sci.net/17/1573/2017/	France	CC BY	file download
SLOVENIAN FAULT SOURCE MODEL	Atanackov et al. (2017)	--	Slovenia	Confidential, with permission to use	--
GULF OF CADIZ FAULT MODEL	Original work made in the framework of SERA JRA3	--	Gulf of Cadiz	--	--



Figure 21: Map view of the EDSF crustal faults covering the Euro-Mediterranean region (Basili et al., 2013).

A compilation of faults for Slovenia has recently been made by Atanackov et al. (2017). The GIS and attribute files were kindly provided to us for the scopes of the project.

The hazard map of Turkey was updated after SHARE in 2014 in the framework of the Earthquake Model of the Middle East (EMME) Project (Erdik et al., 2012), which used an updated version of the fault sources (Danciu et al., 2018). In the meanwhile, The Active Fault Map of Turkey as updated in 2013 by the Mineral Research and Exploration Institute of Turkey (Emre et al., 2013; Emre et al., 2018) and formed the basic input for the development of the fault source model in the updated seismic hazard maps. This new database includes mainly on-shore faults in the Turkish territory. For the project purposes it has been complemented with off-shore faults as well as faults in neighboring countries, the information of which was taken from relevant literature. The project report also included a comparison of the faults in both projects (Figure 23). The characterization of these fault sources in all projects follows the same standards as EDSF. However, the last version of these fault sources seems not to be publicly available, and we should perform a recompilation of the fault source model for Turkey.

The mapping of active faults in Romania, was recently published by Diaconescu et al. (2018), this is a very recent project and the characterization does not yet fully comply with the requirements of ESHM20.

The active fault model for France (Jomard et al., 2017) is targeted at surface faulting in metropolitan areas and the provided information cannot be used straightforwardly in ground-shaking hazard at continental scale.

The NOAFAULTS for Greece by Ganas et al. (2013) overlaps with GREDASS but the parameterization is more focused on the ground-surface expression of the faults rather than the seismogenic depth.

For the Gulf of Cadiz, a working group led by ITS is currently revising offshore crustal faults.

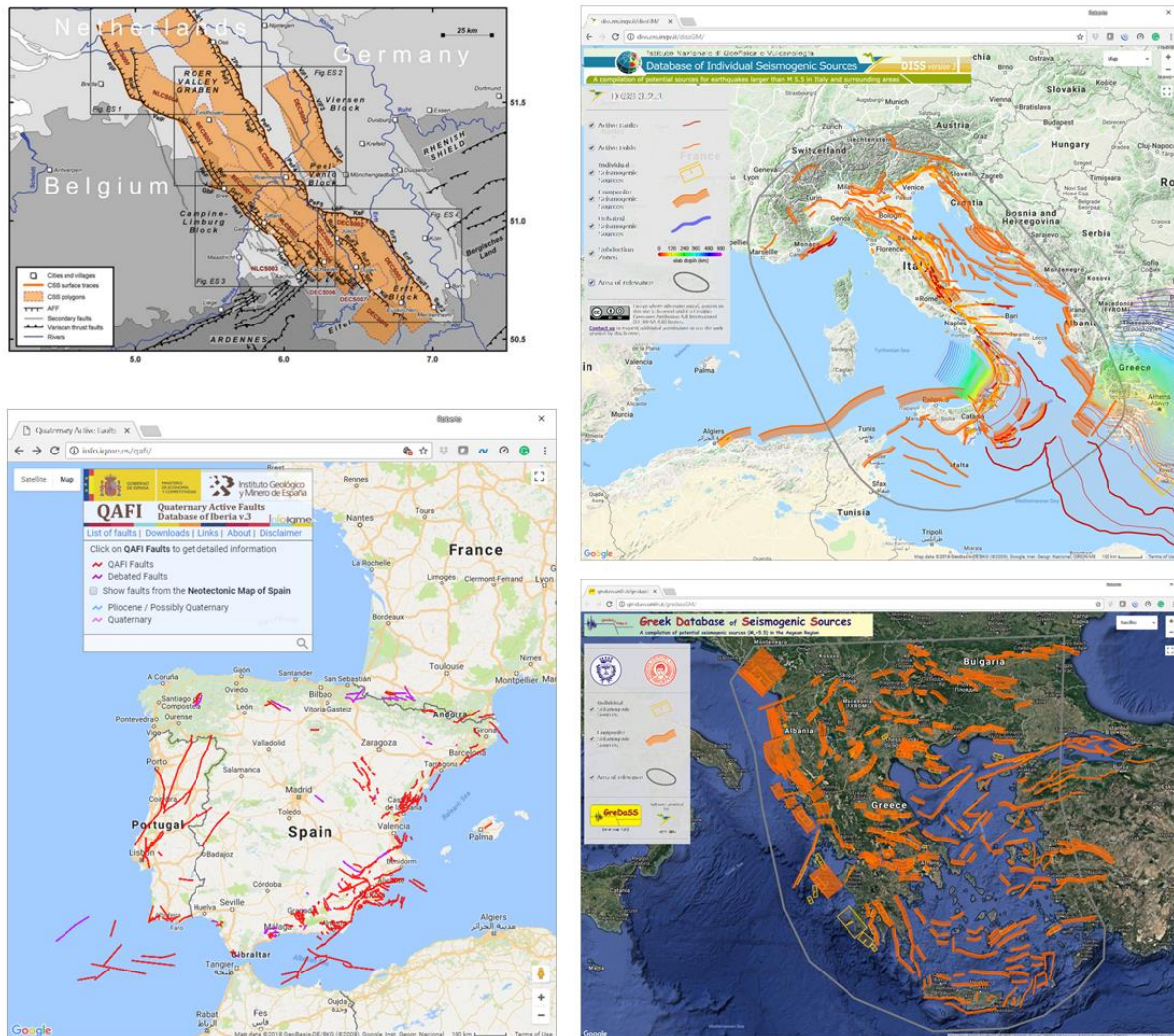


Figure 22: Map view of selected fault datasets that are freely available online: (upper left) composite seismogenic sources (CSS) in the Lower Rhine Graben (Vanneste et al., 2013); (lower left) Quaternary Active Faults Database of Iberia v.3 covering the Iberia region (Garcia-Mayordomo et al., 2012); (upper right) Database of Individual Seismogenic Sources (DISS v.3.2.1) covering the central Mediterranean region (DISS Working Group, 2018); (lower right) Greek Database of Seismogenic Sources (GreDaSS v.2.0.0) covering the Aegean region (Caputo and Pavlides, 2013).

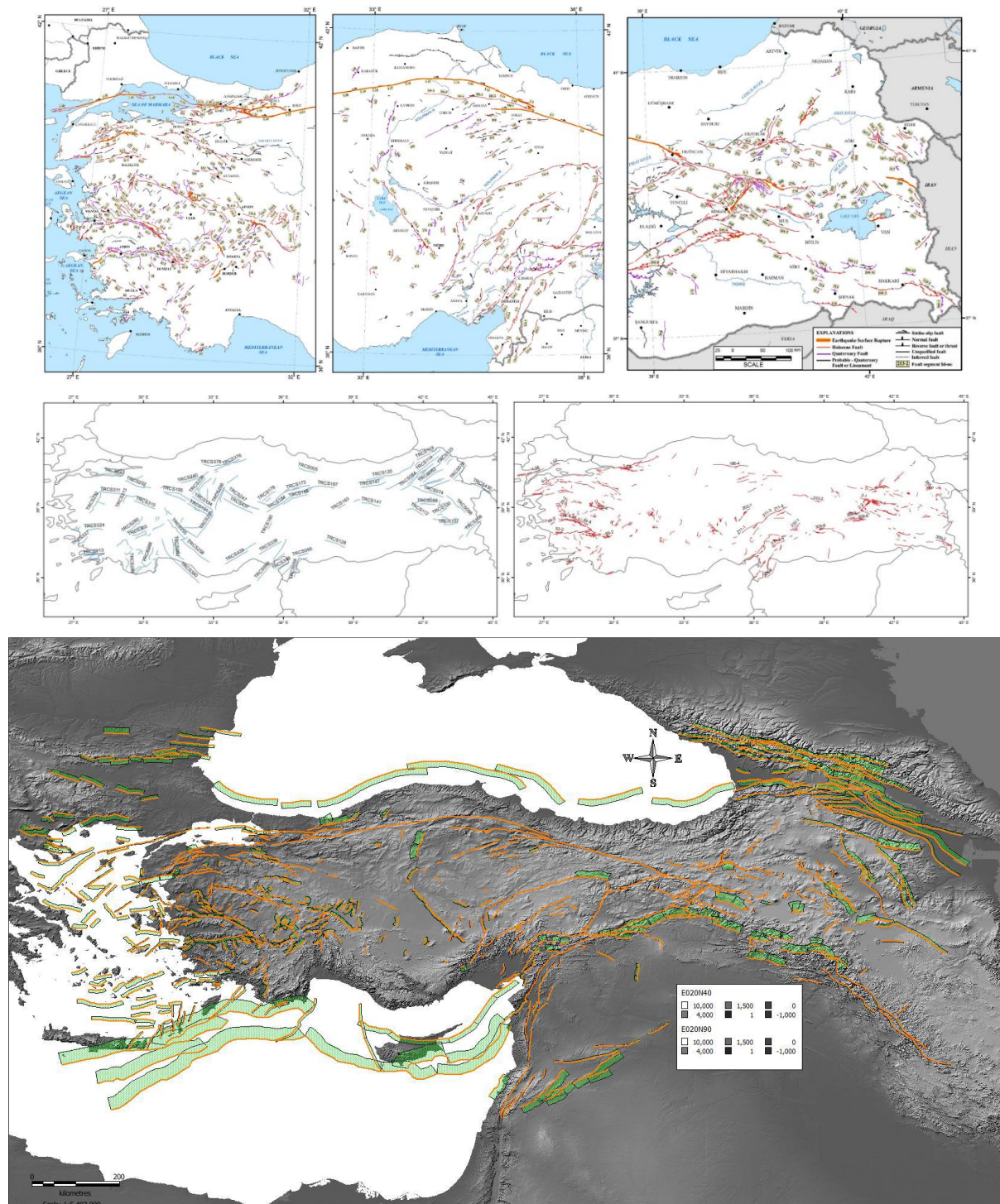


Figure 23: (Top) Map of active faults in Anatolia (Emre et al., 2013, 2018). (Middle) Map of faults included in EDSF 2013 but not in the Turkish Hazard Project database (left) and map of faults included in the MTA Active Fault Database, but not in EDSF 2013. (Bottom) Map of the fault source model used in the Turkey Hazard Project (Demircioğlu et al., 2018).

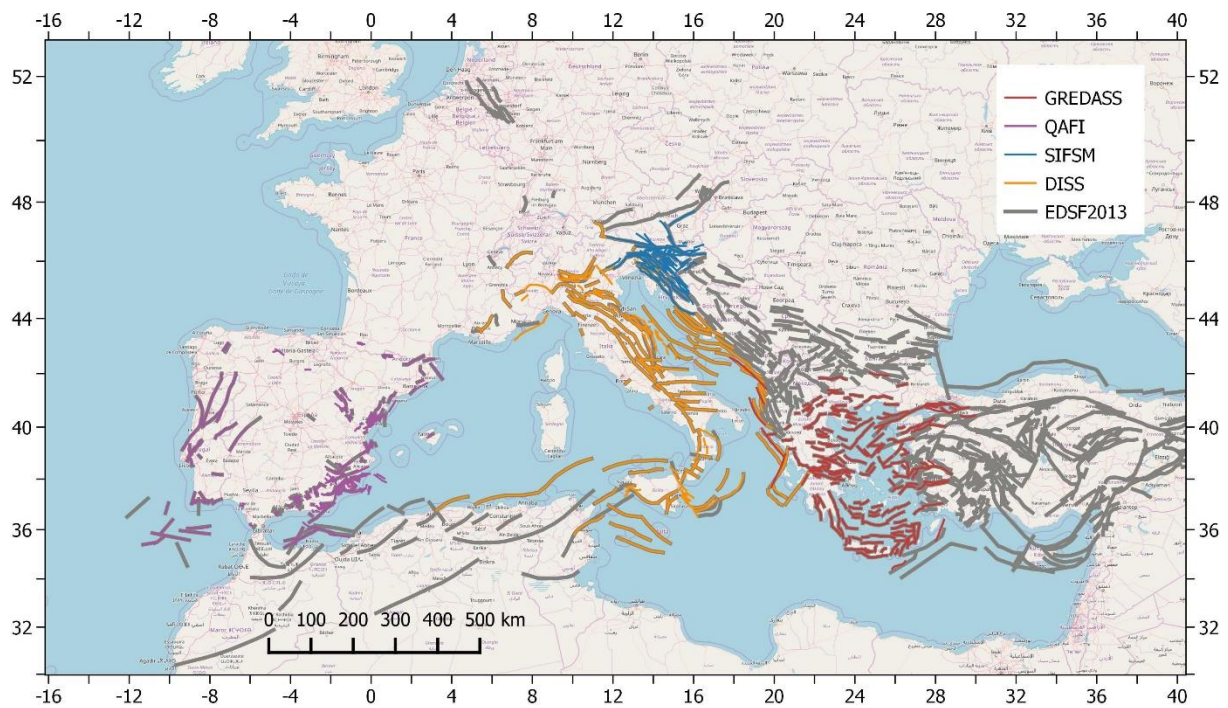


Figure 24: Map of collated fault datasets (see Table 4) compared with EDSF. Datasets that still needs to be evaluated, such as those of Turkey, Gulf of Cadiz, Romania, and France are not shown.

Figure 24 shows a map of the fault datasets that have already been collated and their parameter verified for use in ESHM20. Below is a list of issues emerged from the pre-processing actions performed onto these selected regional datasets or from information obtained from the authors.

DISS, EDSF, and GreDaSS

- These datasets share the same data structure and thus need no further processing.

QAFI

- Redrawing the top trace by interpolation because the mapping is inhomogeneous, sometimes it is too detailed and other it is coarse.
- Verify depth datum (ground surface or mean geoid/spheroid).
- Fill in missing values or remove uncomplete records.
- Check fault intersections at depth.

Slovenian Fault Source Model

- Verify depth datum (ground surface or mean geoid/spheroid).
- Check fault intersections at depth.

Lower Rhine Graben

- Verify slip rates provided by Gold et al. (2018) as a possible update of the slip rates provided by Vanneste et al. (2013).

Turkey Fault Source Model

- Geographic features and their parameters as used in the Demircioğlu et al. (2018) hazard model should be the same as EDSF and thus need no further processing. However, the fault source model is not yet freely available.

For the remaining datasets, the following actions are necessary:

- complete dataset collation, also by contacting the relevant authors;
- remove duplicates and deprecated records from EDSF 2013;

- harmonize overlaps;
- develop moment rate model.

Subduction sources

Concerning subduction sources, we identified several datasets (Table 5) in addition to the EDSF 2013 (Figure 25). Similarly to crustal faults, these datasets vary in date of latest update, geographical extent, level of characterization, accessibility and reusability, and data formats. Four of them are post-2013 and contain either slab geometry or activity parameters or both. Two pre-2013 datasets that contains useful data for the subduction characterization, and an initiative to reconstructing the Cadiz slab interface by a working group led by ITS.

Table 5: Collection of datasets about subduction zones.

TITLE	REFERENCE	URL	COVERAGE	LICENSE	ACCESS
EDSF 2013	Basili et al. (2013); Giardini et al. (2013)	http://diss.rm.ingv.it/share-edsf/	Central-Eastern Mediterranean	CC BY-SA 4.0	OGC WFS WMS, file download
DISS 3.2.1	DISSWG (2018)	http://diss.rm.ingv.it/diss/	Central-Eastern Mediterranean	CC BY-SA 4.0	OGC WFS WMS, file download
CAM	Maesano et al. (2017)	https://www.nature.com/articles/s41598-017-09074-8	Central Mediterranean	CC BY 4.0	file download
SLAB 2.0	Hayes (2018); Hayes et al. (2018)	https://doi.org/10.5066/F7PV6JNV	World	Public Domain	WMS, file download
GEM-FE SICP 2.0	Berryman et al. (2015)	--	World	CC BY 3.0	file download
SUBMAP 4.2	Heuret & Lallemand (2005)	http://submap.gm.univ-montp2.fr/index.php	World	Attribution only	file download
PB2002	Bird et al. (2003)	http://peterbird.name/publications/2003_PB2002/2003_PB2002.htm	World	Attribution only	file download
GULF OF CADIZ FAULT MODEL	Original work made in the framework of SERA JRA3	--	Gulf of Cadiz	--	--

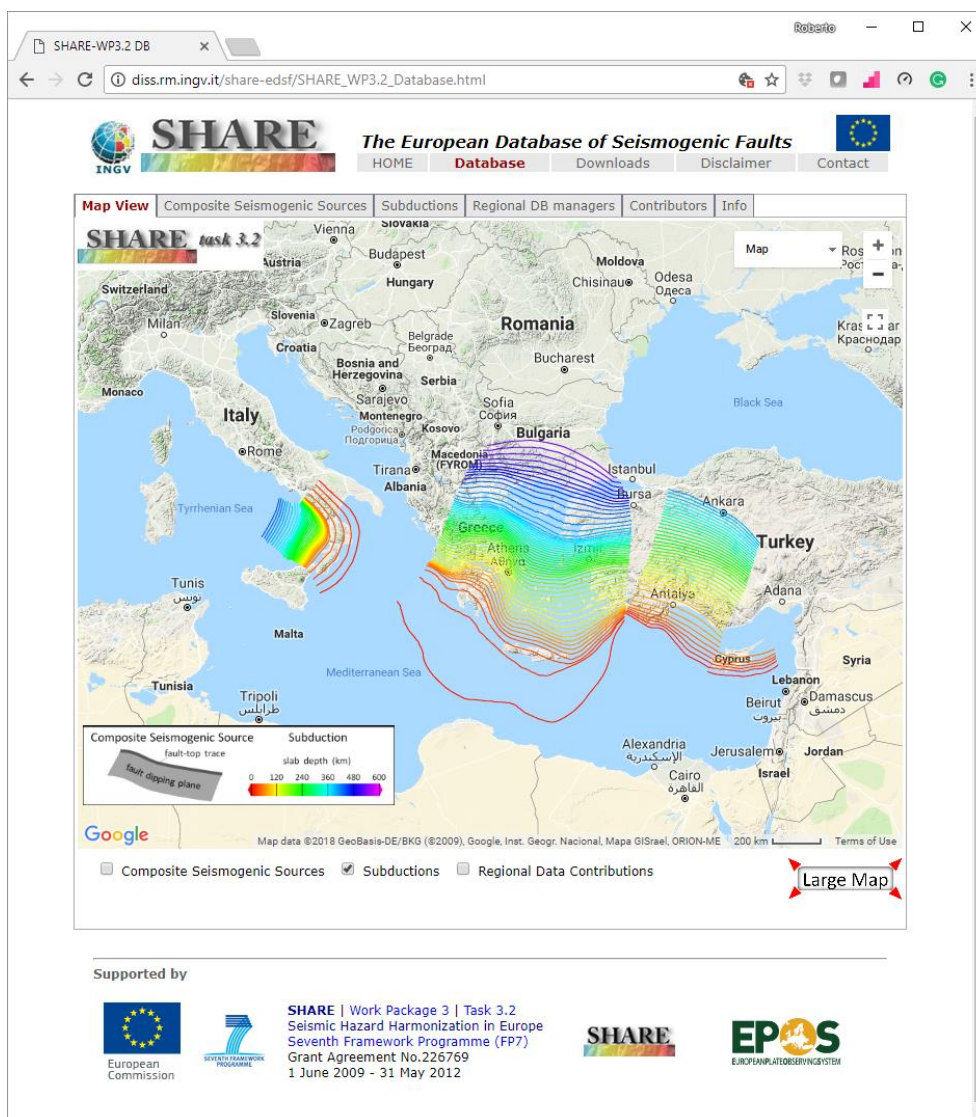


Figure 25: Map view of the EDSF subduction zones in the eastern Mediterranean region (Basili et al., 2013).

The most recent slab geometrical reconstructions are those for the Calabrian Arc (Figure 26) by Maesano et al. (2017) and the global compilation (Figure 27) by Hayes et al. (2018). Figure 28 shows a pair-wise comparison between the models with the most updated reconstruction of the slab geometry.

The other datasets play an important role in completing the characterization of these slabs. For example, the SUBMAP 4.2 tools (Heuret & Lallemand, 2005) can help constrain convergence rates (Figure 29), seismogenic depths, and other properties. Further subduction characterization can also be derived by the global compilations of subduction sources such as that of Berryman et al (2015) or that for tsunami hazard assessment by Davies et al. (2018) and references therein.

Further actions needed to complete the subduction zones are listed below:

- verify the availability of a model for the Cadiz subduction
- decide on how to establish the upper and lower seismogenic depths of slab interfaces;
- build 3D grid for intraslab seismicity
- develop moment rate model for interface and intraslab.

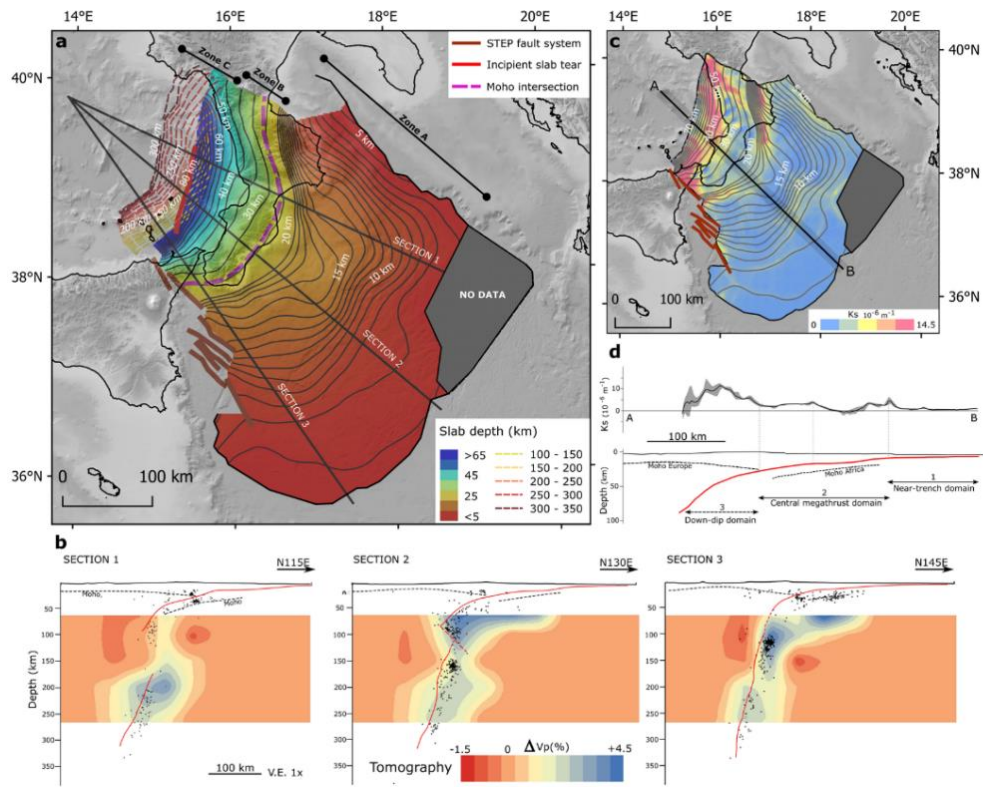


Figure 26: Slab model of the Calabrian Arc (Maesano et al., 2017).

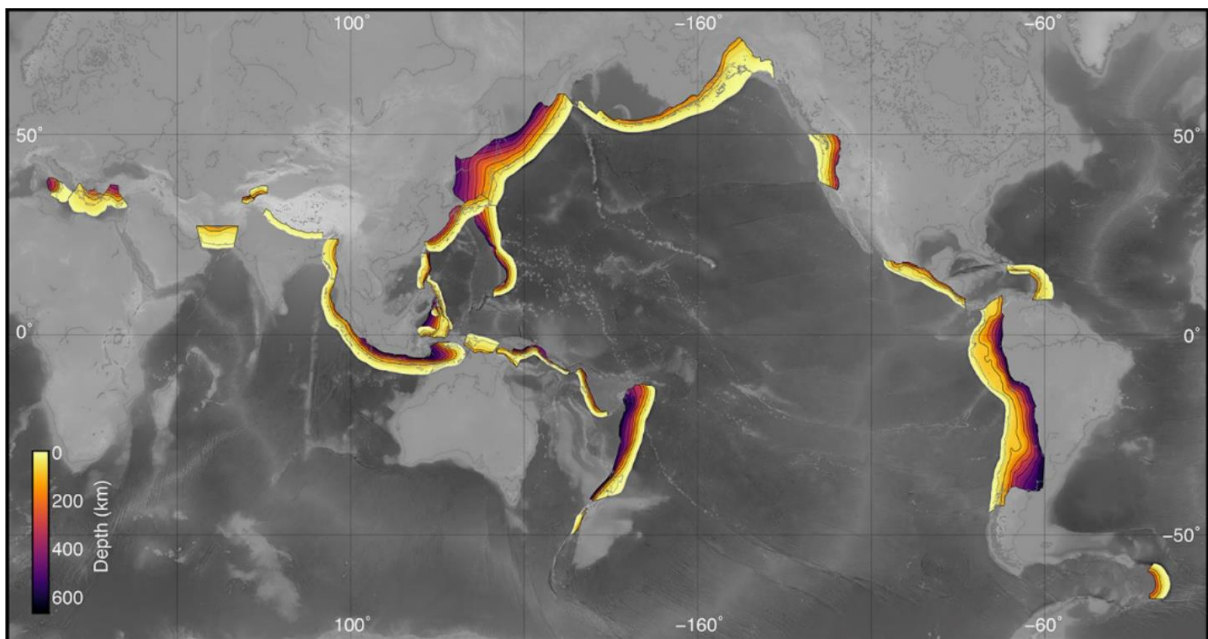


Figure 27: Slab 2 models (Hayes et al., 2018).

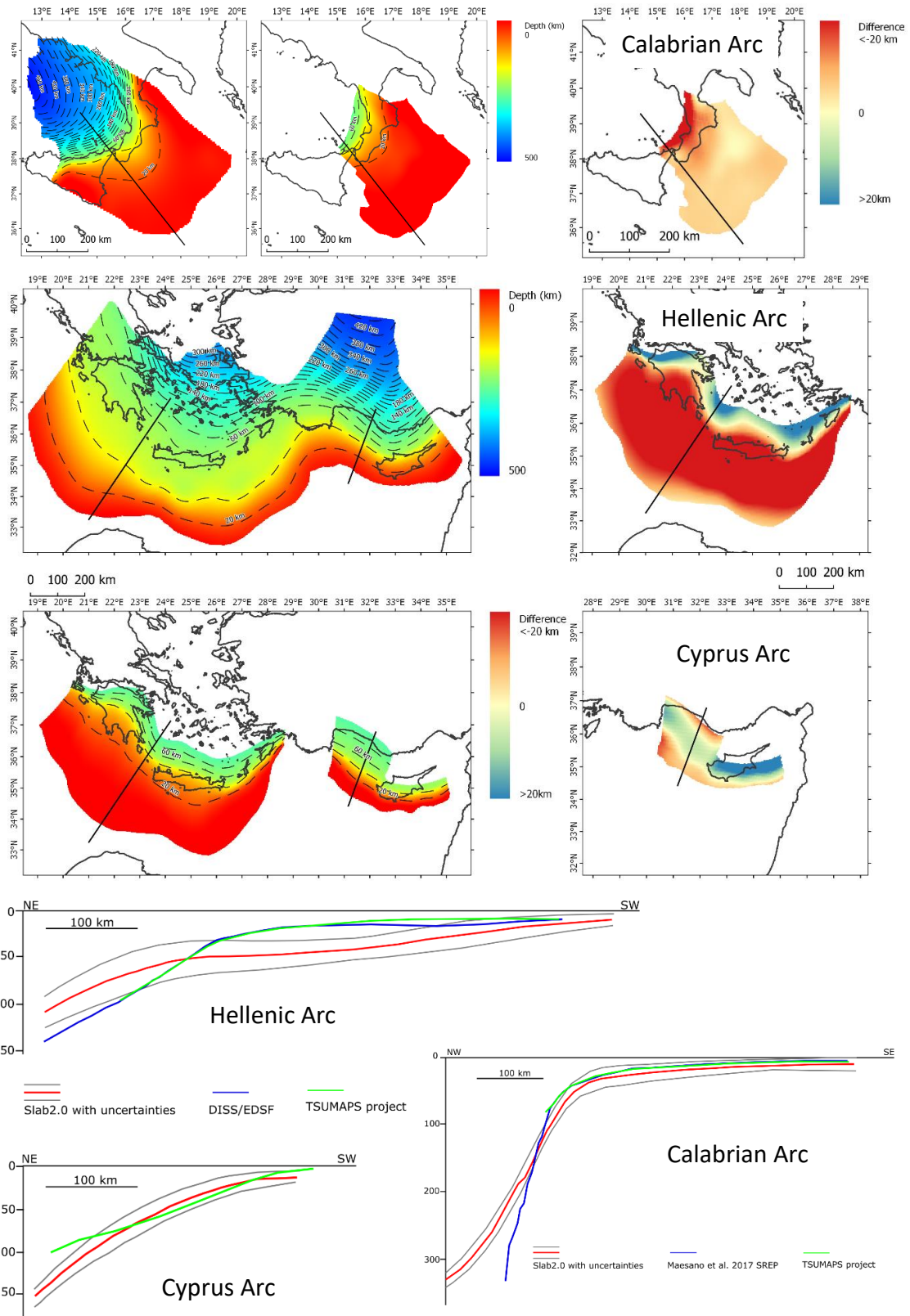
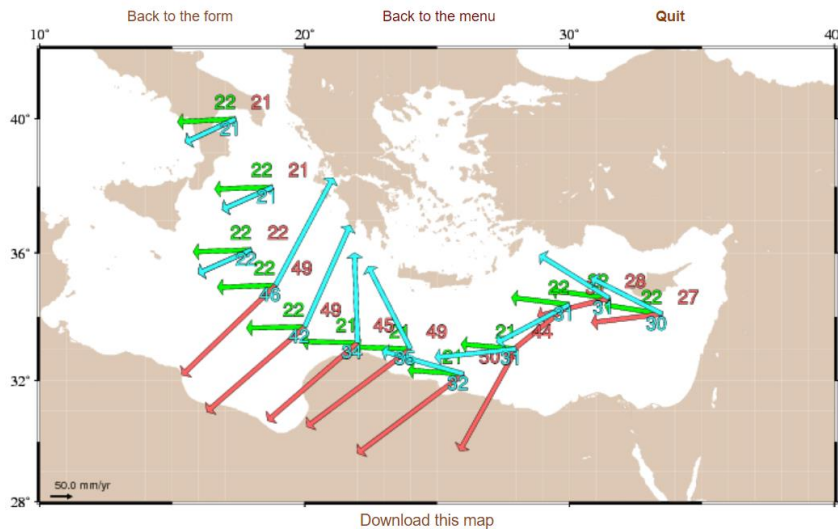


Figure 28: Comparison of the slab geometry between Slab 2 (Hayes, 2018) and the models for the Hellenic Arc from EDSF (Basili et al., 2013) and Cyprus Arc updated by the TSUMAPS-NEAM Team (2017) from EDSF and the Calabrian Arc from Maesano et al., (2017).



4.2



--in the HS3 absolute reference frame--
trench absolute motion (in mm/yr)
upper plate absolute motion (in mm/yr)
subduction plate absolute motion (in mm/yr)

Figure 29: Example of a map of Mediterranean subduction zones generated using the SUBMAP 4.2 tools (Heuret & Lallemand, 2005).

3.2 Description of the fault source data model

This Chapter illustrates how the fault source data models for both crustal faults and subduction zones.

The geometry of fault sources is geographically represented in 3D by depth contours. The only difference between crustal faults and slabs is that the first have down-dip planar geometry, and thence the contours are all parallel to each other, whereas the second have complex geometry of any shape. Each depth contour is defined by a variable number of nodes, whose location is given by a pair of geographic coordinates, i.e., longitude and latitude, with reference to the WGS84 geodetic datum (EPSG 4326; <http://www.epsg-registry.org/>). A set of attributes is associated to each geographic feature, whose main objective is to constrain a magnitude-frequency distribution (MFD) for each fault source. To this end, the geologic information contained in the fault datasets illustrated in the previous section can be used to estimate two key parameters: 1) the seismic moment rate that constrain the integral of the MFD, and 2) a proxy for the moment magnitude upper bound of the MFD. All other information needed for the full definition of the MFD must be derived from seismicity data and therefore will not be described here. These two parameters are independent from the functional form, or model, adopted for the MFD.

The seismic moment rate \dot{M}_s of a seismogenic fault can be derived from the geologic moment rate \dot{M}_g as follows:

$$\dot{M}_s = \chi \dot{M}_g = \chi \mu L W \dot{D} \quad (1)$$

where μ is the shear modulus, L and W are fault length and width (Figure 20), respectively, \dot{D} is slip rate, and χ is a coefficient that determines how much geologic rate is converted into seismic rate. This coefficient is often referred to as seismic efficiency (Kagan and Jackson, 2013). The moment rate also

find use in MFD models based on the combination of faults and smoothed seismicity (e.g., Hiemer et al., 2014).

Although the seismicity rate model can be entirely described by seismic moment quantities, many practical applications require that earthquake size be provided in terms of moment magnitude. Conversion between seismic moment and moment magnitude in such cases will be given by

$$m = \frac{\log_{10} M}{1.5} - 6.07 \quad (2)$$

where m is moment magnitude and M is seismic moment in Nm as in Kanamori and Brodsky (2001).

The earthquake magnitude upper bound of a seismogenic fault can be estimated from the size of the largest earthquake rupture that it can host, based on empirical relationships between rupture dimensions and moment magnitude observed in past earthquakes. This approach alone cannot predict the occurrence of larger earthquake magnitudes arising from rupture spanning across multiple faults, therefore such estimates must be considered as a proxy for the upper bound, i.e. the upper bound cannot be smaller than that value.

Abundant literature exists on these relationships, hereinafter referred to as fault scaling laws (FSL). The generalized functional form between moment magnitude (M_w) and rupture dimensions (L , W , A , D) is

$$M_w = a + b \times \log_{10}(X) \quad (3)$$

where X is the rupture dimension under consideration (e.g., L or W in km, A in km^2 , D in m) and the coefficients a and b are empirically determined.

We here propose to adopt the FSL developed by Leonard (2014) for crustal ruptures and by Strasser et al (2010) for subduction ruptures.

Major features of the Leonard (2014) scaling laws are:

- two tectonic settings: interplate and stable continental region (SCR);
- two faulting mechanisms: dip slip (normal and reverse together) and strike slip;
- relations are consistent with one another depending on length/width ratio and displacement/area ratio;
- fitted relations can either be linear, or bilinear, or trilinear;
- relations provided for seismic moment and moment magnitude vs. length (L), width (W), area (A), and displacement (D);
- a comparison between these relations and previously published relations is given.

Major features of the Strasser et al. (2010) scaling laws are:

- two tectonic settings: subduction interface and intraslab;
- fitted relations are linear;
- relations provided for moment magnitude vs. length (L), width (W), and area (A);
- relations for the various dimensions are independent from one another;
- a comparison between these relations and previously published relations is given.

The best estimates of the coefficients a and b of the above two FSLs are listed in Table 6 and Table 7, along with other relevant information.

Table 6. Coefficients and range of application of the fault scaling laws from Leonard (2014) adopted for crustal ruptures.

SETTING	DIMENSION	B	A	S(A)*	RANGE**
INT DS	A	1	4	3.73-4.33	>0
INT DS	L	1.667	4.24	3.81-4.73	>5.4
INT DS	W	2.5	3.63	3.61-3.73	>5.4
INT SS	A	1	3.99	3.73-4.25	>0
INT SS	L	1.667	4.17	3.77-4.55	3.4-45.0
INT SS	L	1	5.27	-	>45
INT SS	W	2.5	3.88	3.82-3.95	3.4-19.0
SCR DS	A	1	4.19	4.08-4.28	>0
SCR DS	L	1.667	4.32	4.12-4.51	>2.5
SCR DS	W	2.5	4.14	4.08-4.17	>2.5
SCR SS	A	1	4.18	4.07-4.25	>0
SCR SS	L	1.667	4.25	4.07-4.43	1.6-70
SCR SS	L	1	5.44	-	>60
SCR SS	W	2.5	4.22	4.17-4.23	1.6-20

INT: interplate, SCR: stable continental region, DS: dip slip (normal and reverse), SS: strike-slip, A: area, L: length, W: width.

* S(A) is the one standard deviation range of A.

** The units for the range of application are km for L and W, km² for A.

Table 7. Coefficients and range of application of the fault scaling laws from Strasser et al. (2010) adopted for subduction ruptures.

SETTING	DIMENSION	A	S.E.(A)	B	S.E.(B)	σ
INF	L	4.868	0.141	1.392	0.069	0.277
INF	W	4.41	0.277	1.805	0.151	0.392
INF	A	4.441	0.179	0.846	0.046	0.286
INS	L	4.725	0.274	1.445	0.164	0.234
INS	W	3.407	0.317	2.511	0.217	0.178
INS	A	4.054	0.288	0.981	0.093	0.193

INF: interface, INS: intraslab, A: area, L: length, W: width.

S.E.: standard error of the coefficient; σ : is the standard deviation of the relation.

In addition to the problem of having ruptures spanning multiple faults, it must be considered that the coefficients of these FSLs bear significant statistical uncertainty within each FSL, depending on the scattering of the used dataset and represented by the standard deviations of their coefficients reported in Table 6 and Table 7, and between different FSLs, depending on the fitting model adopted. Figure 30 and **Error! Reference source not found.** show the between-FSL deviations in predicting the moment magnitude from earthquake rupture dimensions for different tectonic settings and faulting types for the selection of FSLs proposed here, whose coefficients are reported in Table 6 and Table 7.

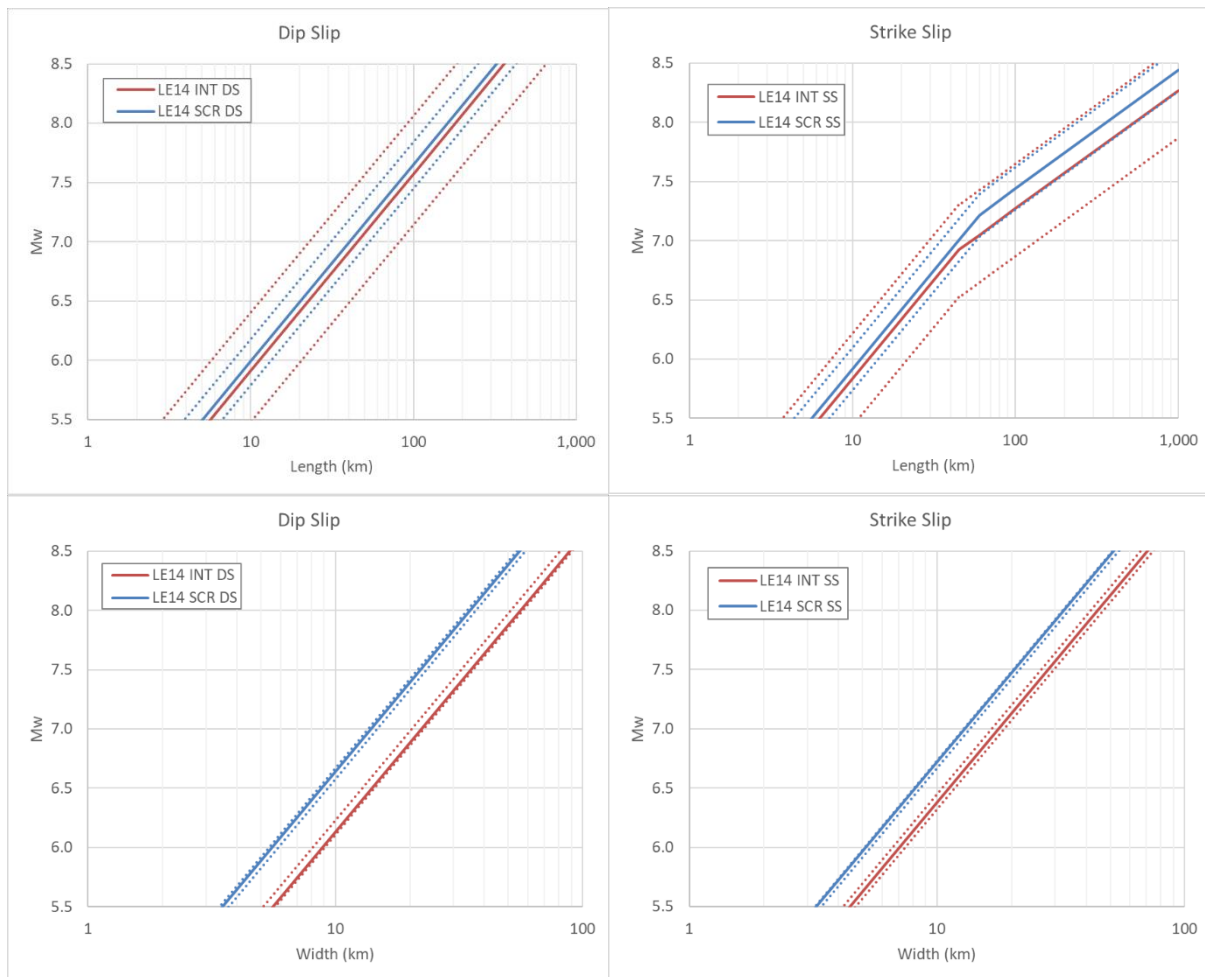


Figure 30: Comparison of relations by Leonard (2014; LE14) for interplate (INT) and stable continental regions (SCR) in predicting moment magnitude (M_w) from either rupture length (L ; top) or width (W ; bottom) in the case of dip-slip (DS; left) and strike-slip (SS; right) faulting earthquakes. Same-color dotted lines are obtained with the one standard deviation of coefficient a , while b is fixed (see Table 6).

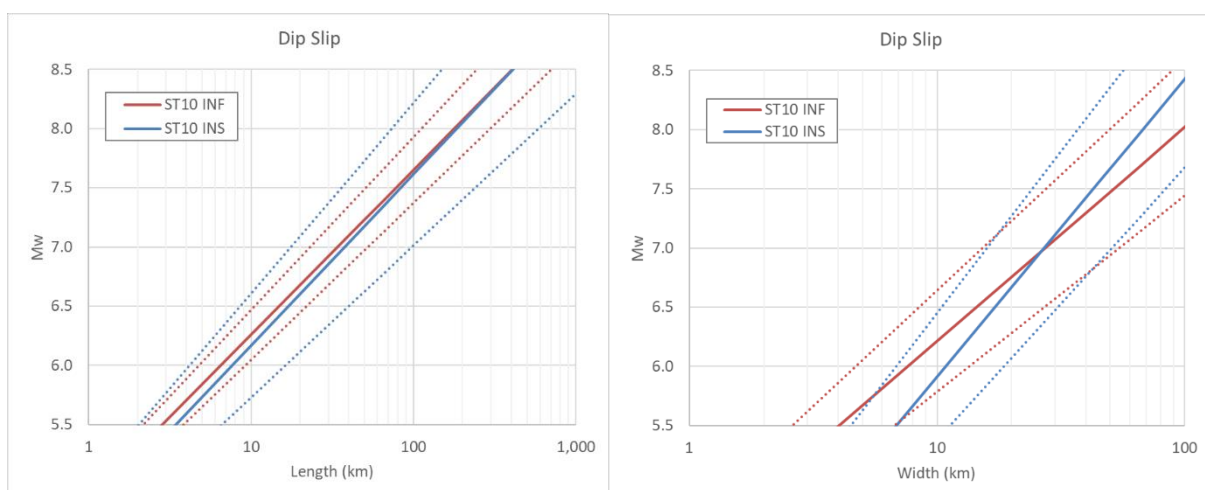


Figure 31: Comparison of relations by Strasser et al. (2010; ST10) for interface (INF) and intraslab (INS) in predicting moment magnitude (M_w) from either rupture length (L ; left) or width (W ; right) in the case of dip-slip (reverse only) faulting earthquakes. Same-color dotted lines are obtained with the one standard deviation of coefficient a and b . (see Table 7).

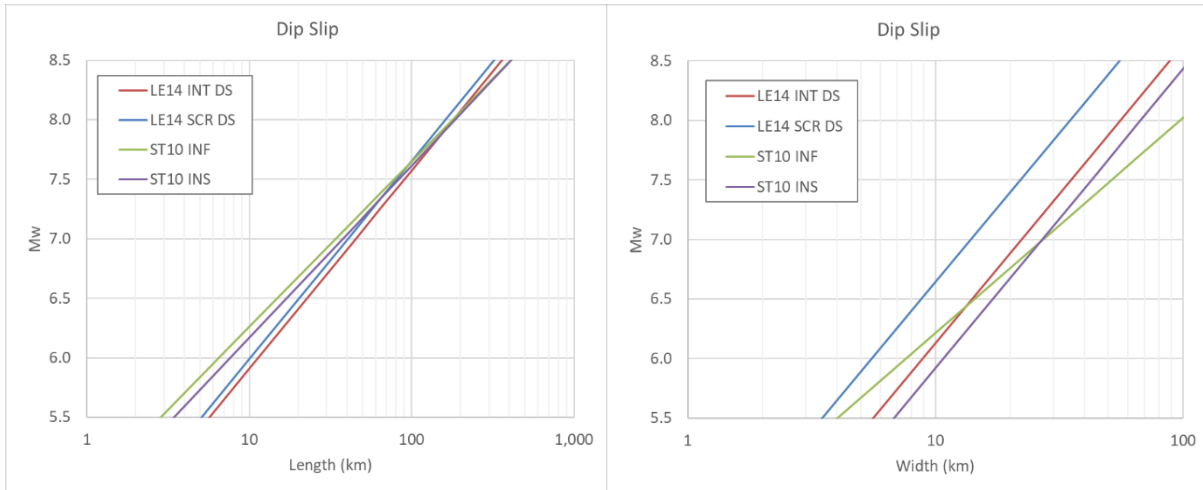


Figure 32: Comparison of relations by Leonard (2014; LE14) and those by Strasser et al. (2010; ST10) for dip-slip faulting earthquakes in different tectonic settings, interplate (INT), stable continental regions (SCR), subduction interface (INF), and subduction intraslab (INS) in predicting moment magnitude (M_w) from either rupture length (L ; left) or width (W ; right) in the case of dip-slip (reverse only) faulting earthquakes.

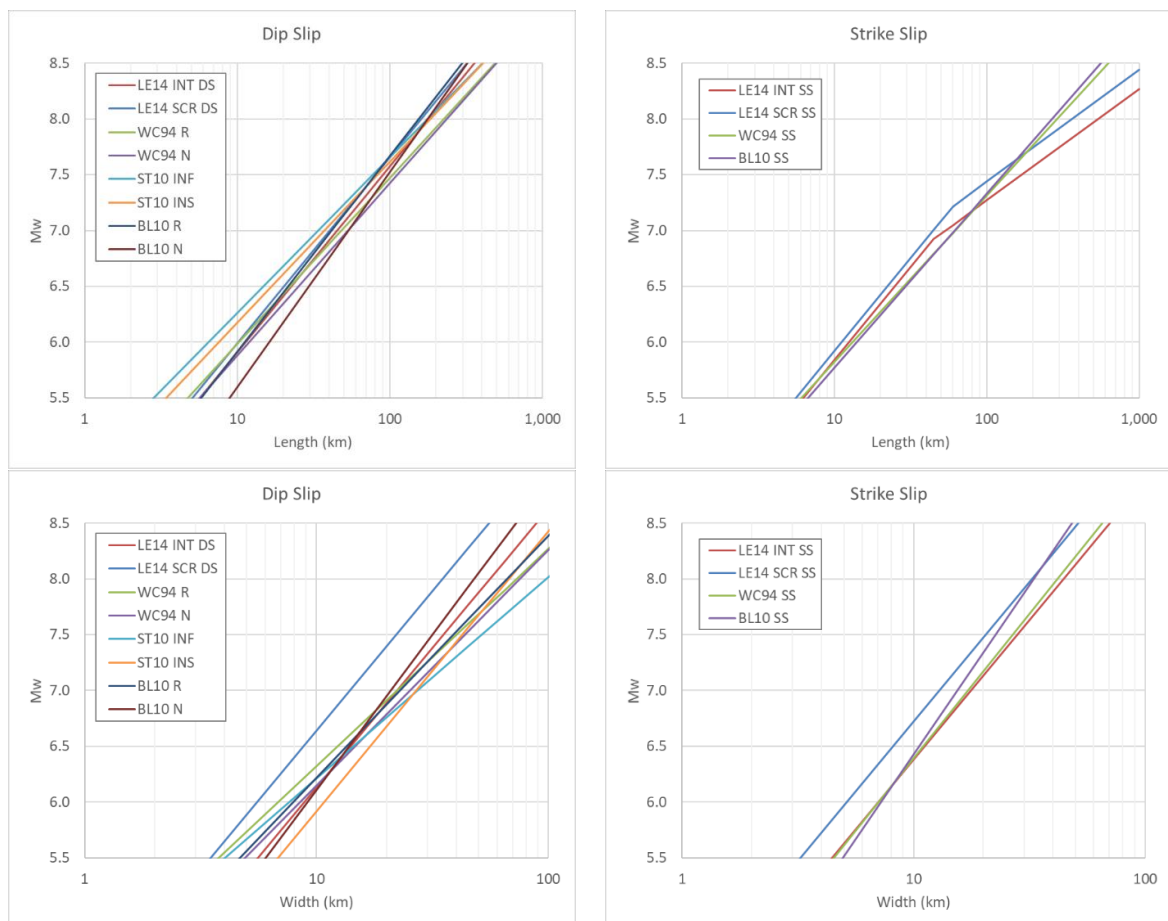


Figure 33: Comparison of relations by Leonard (2014; LE14) and Strasser et al. (2010; ST10) in predicting moment magnitude (M_w) from either rupture length (L ; top) or width (W ; bottom) in the case of dip-slip (DS; left) and strike-slip (SS; right) faulting earthquakes with other common relations such as those by Wells and Coppersmith (1994; WC94) and Blaser et al. (2010; BL10).

In particular, Figure 30 shows that for crustal faults of any given rupture dimension the moment magnitude prediction in SCR is higher than in interplate regions. Note also that the relation for strike-

slip faulting based on rupture length is bilinear, indicating that the increase in magnitude for increasing length is lower for longer faults. Figure 31 shows the importance of distinguishing between interface and intraslab earthquakes, especially if the moment magnitude has to be estimated from the rupture width, which has a proxy in the thickness of the subduction slab. Figure 32 shows the different moment magnitude predictions between crustal ruptures and subduction ruptures.

Figure 33 shows a more general comparison between the relations proposed here and other common relations for both crustal and subduction earthquake ruptures. Note that one of the most important differences among all relations occur for the bilinear relation by Leonard (2014) for strike-slip faulting based on rupture length in interplate setting and for dip-slip faulting based on rupture width in SCR.

The parameters derived from the approach above illustrated are incorporated in the data model represented by the attributes described in Table 8 and Table 9 for crustal fault sources and subduction sources, respectively.

Table 8: Attributes for crustal faults.

FIELD	VARIABLE	UNITS	DESCRIPTION
IDFS	String	n.a.	Identifier of the fault source within EFSM20
IDDS	String	n.a.	Identifier of the data source - link to table of datasets.
IDSOURCE	String	n.a.	Identifier given in the original source
PREFERRED	Logical	n.a.	True or false (T/F), to identify faults to be used or ignored.
FAULTTYPE	String	n.a.	One-letter code: R = reverse, N = normal, T = transcurrent.
STRIKEMIN	Float	degrees	Minimum value of the fault orientation, in the range 0-360° increasing clockwise from north following the right-hand rule.
STRIKEAVG	Float	degrees	Average value of the fault orientation, in the range 0-360° increasing clockwise from north following the right-hand rule.
STRIKEMAX	Float	degrees	Maximum value of the fault orientation, in the range 0-360° increasing clockwise from north following the right-hand rule.
DIPMIN	Float	degrees	Minimum value of the dip angle, between 0-90° increasing downward from the horizontal.
DIPAVG	Float	degrees	Average value of the dip angle, between 0-90° increasing downward from the horizontal.
DIPMAX	Float	degrees	Maximum value of the dip angle, between 0-90° increasing downward from the horizontal.
RAKEMIN	Float	degrees	Minimum value of the hanging-wall sense of movement in the range -180/+180°, positive counterclockwise from the horizontal.
RAKEAVG	Float	degrees	Average value of the hanging-wall sense of movement in the range -180/+180°, positive counterclockwise from the horizontal.
RAKEMAX	Float	degrees	Maximum value of the hanging-wall sense of movement in the range -180/+180°, positive counterclockwise from the horizontal.
MINDEPTH	Float	km	Value of the minimum depth of the fault, or depth of the upper edge, positive downward from sea level.
MAXDEPTH	Float	km	Value of the maximum depth of the fault, or depth of the upper edge, positive downward from sea level.
TOTALLENGTH	Float	km	Length of the fault measured along the trace of the upper edge.

END2ENDLENGTH	Float	km	Length of the fault corresponding to the shortest distance between the farthest endpoints on the trace of the upper edge.
WIDTHMIN	Float	km	Minimum value of the fault width, measured along the maximum slope direction, as calculated from depth and dip.
WIDTHAVG	Float	km	Average value of the fault width, measured along the maximum slope direction, as calculated from depth and dip.
WIDTHMAX	Float	km	Maximum value of the fault width, measured along the maximum slope direction, as calculated from depth and dip.
AREAMIN	Float	km ²	Minimum value of the fault area obtained by multiplying total length by width.
AREAAVG	Float	km ²	Average value of the fault area obtained by multiplying total length by width.
AREAMAX	Float	km ²	Maximum value of the fault area obtained by multiplying total length by width.
SRMIN	Float	mm/yr	Minimum value of the slip rate in mm/yr. Minimum value of slip as a function of time.
SRMAX	Float	mm/yr	Maximum value of the slip rate in mm/yr.
SRMEAN	Float	mm/yr	Aritmetic mean value of the slip rate in mm/yr.
SRGMEAN	Float	mm/yr	Geometric mean value of the slip rate in mm/yr.
FSLTECTO	String	n.a.	Three-letter code: INT = interplate; SCR = stable continental region.
FSLSLIP	String	n.a.	Two-letter code: DS = dip slip; SS = strike slip.
FSLDIM	String	n.a.	One-letter code indicating which rupture dimension is used to estimate the maximum magnitude: L = length, W = width, A = area, D = displacement.
FSLSIZE	Float	km/km ² /m	Value of the used dimension (km for L and W; km ² for A, m for D)
MWMAXORIGINAL	Float	scalar	Maximum earthquake magnitude assigned in the original source (NaN=-9.9), see field IDDS.
MWMAXFSLAVG	Float	scalar	Average value of the earthquake moment magnitude of the maximum rupture size that fits the fault dimension based on a fault scaling law.
MWMAXFSLMIN	Float	scalar	Minimum value of the earthquake moment magnitude of the maximum rupture size that fits the fault dimension based on a fault scaling law.
MWMAXFSLMAX	Float	scalar	Maximum value of the earthquake moment magnitude of the maximum rupture size that fits the fault dimension based on a fault scaling law.
MWMAXBUF	Float	scalar	Earthquake moment magnitude from the earthquake catalog within a buffer of a given radius.
MWMAXFORAR	Float	scalar	Earthquake moment magnitude to be used for the MFD.
MWMAXFORTRU	Float	scalar	Earthquake moment magnitude to be used for the truncated MFD model.
MWMAXFORTGR	Float	scalar	Earthquake moment magnitude to be used for the tapered MFD model.
MU	Float	GPa	Average shear modulus or rigidity.
MORMIN	Float	Nm	Minimum value of the tectonic moment rate of the fault.
MORMAX	Float	Nm	Maximum value of the tectonic moment rate of the fault.
MORAMEAN	Float	Nm	Arithmetic mean of the tectonic moment rate of the fault.
MORGMEAN	Float	Nm	Geometric mean of the tectonic moment rate of the fault.

Table 9: Attributes for subduction zones.

FIELD	VARIABLE	UNITS	DESCRIPTION
IDFS	String	n.a.	Identifier of the fault source within EFSM20
IDDS	String	n.a.	Identifier of the data source - link to table of datasets.
IDSOURCE	String	n.a.	Identifier given in the original source
PREFERRED	Logical	n.a.	True or false (T/F), to identify faults to be used or ignored.
MINDEPTH	Float	km	Depth of the sub-element upper edge from sea level.
MAXDEPTH	Float	km	Depth of the sub-element lower edge from sea level.
CRUSTTHICKMIN	Float	km	Minimum value of the lower plate crustal thickness.
CRUSTTHICKMAX	Float	km	Maximum value of the lower plate crustal thickness.
STRIKEMIN	Integer	degrees	Minimum value of the fault orientation, in the range 0-360° increasing clockwise from north following the right-hand rule.
STRIKEMAX	Integer	degrees	Maximum value of the fault orientation, in the range 0-360° increasing clockwise from north following the right-hand rule.
DIPMIN	Integer	degrees	Value of the minimum dip angle (between 0 and $\pi/2$) from the horizontal.
DIPMAX	Integer	degrees	Value of the maximum dip angle (between 0 and $\pi/2$) from the horizontal.
RAKEMIN	Integer	degrees	Minimum value of the upper-plate sense of movement in the range -180/+180°, positive counterclockwise from the horizontal.
RAKEMAX	Integer	degrees	Maximum value of the upper-plate sense of movement in the range -180/+180°, positive counterclockwise from the horizontal.
CONVRATEMIN	Float	mm/year	Minimum value of slip as a function of time.
CONVRATEMAX	Float	mm/year	Maximum value of slip as a function of time.
EFFICIENCYMIN	Float	Scalar	Minimum value of the seismic efficiency, a factor between 0-1 that indicates how much convergence rate can be converted into seismic activity.
EFFICIENCYMAX	Float	Scalar	Maximum value of the seismic efficiency, a factor between 0-1 that indicates how much convergence rate can be converted into seismic activity.
EFFICIENCYAVG	Float	Scalar	Average value of the seismic efficiency, a factor between 0-1 that indicates how much convergence rate can be converted into seismic activity.
MAXMWIFOBS	Float	Scalar	Value of the maximum observed magnitude of slab interface earthquakes in the moment magnitude scale (Mw).
MAXMWISOBS	Float	Scalar	Value of the maximum observed magnitude of intraslab earthquakes in the moment magnitude scale (Mw).
MAXMWIFFSLAVG	Float	Scalar	Average value of the earthquake moment magnitude of the maximum rupture size that fits the interface dimension based on a fault scaling law.
MAXMWIFFSLMIN	Float	Scalar	Minimum value of the earthquake moment magnitude of the maximum rupture size that fits the interface dimension based on a fault scaling law.

MAXMWIFFSLMAX	Float	Scalar	Maximum value of the earthquake moment magnitude of the maximum rupture size that fits the interface dimension based on a fault scaling law.
MAXMWISFSLAVG	Float	Scalar	Average value of the earthquake moment magnitude of the maximum rupture size that fits the intraslab dimension based on a fault scaling law.
MAXMWISFSLMIN	Float	Scalar	Minimum value of the earthquake moment magnitude of the maximum rupture size that fits the intraslab dimension based on a fault scaling law.
MAXMWISFSLMAX	Float	Scalar	Maximum value of the earthquake moment magnitude of the maximum rupture size that fits the intraslab dimension based on a fault scaling law.
MU	Float	GPa	Average shear modulus or rigidity.
MORMIN	Float	Nm	Minimum value of the tectonic moment rate of the fault.
MORMAX	Float	Nm	Maximum value of the tectonic moment rate of the fault.
MORAMEAN	Float	Nm	Arithmetic mean of the tectonic moment rate of the fault.
MORGMEAN	Float	Nm	Geometric mean of the tectonic moment rate of the fault.

4 Strain rates

4.1 Summary of strain rate data published after the end of project SHARE

This section presents a survey of the strain-rate related works published since the end of the SHARE project. The strain rate model by Carafa et al. (2015; Figure 34) was one of the outcomes of SHARE WP3 and in its preliminary version (Deliverable D3.5) was used as a form of validation of the activity rates provided by the fault source model. Although this model could not be used as an input for ESHM13 at the time, it represents today the main reference for strain and earthquake rates at the scale of the entire area for ESHM20 update. This is a dynamic model based on the stress equilibrium equation constrained by geodetic data and provides the distribution of the velocity field, strain rate, of major fault slip rates, and seismicity rates.

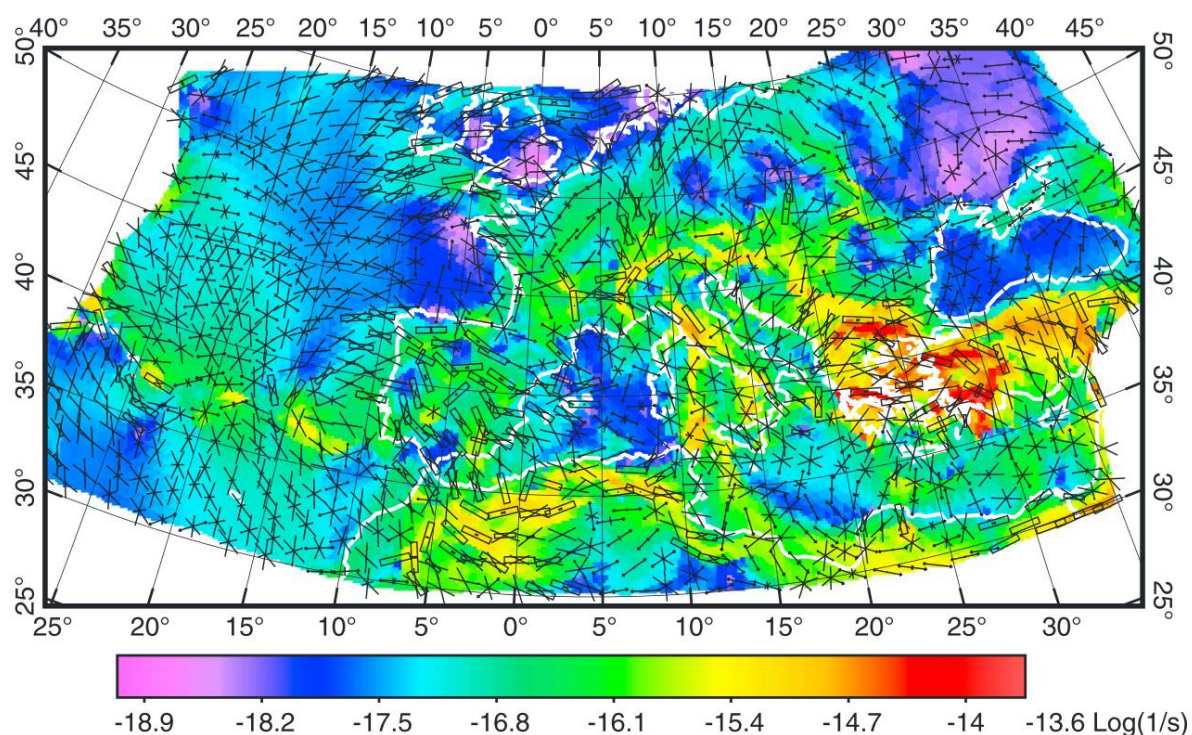


Figure 34: Scalar strain rates and orientations of conjugate microfaults from Carafa et al. (2015).

Other models of this kind vary in geographical extent, temporal scope, type of output, accessibility and reusability, and data formats.

The model from Neres et al. (2016), uses the same approach as Carafa et al. (2015), but its geographic coverage is focused on the Africa-Iberia plate boundary (Figure 35). Another similar example for the region of the Dinarides is provided by Carafa and Kastelic (2014).

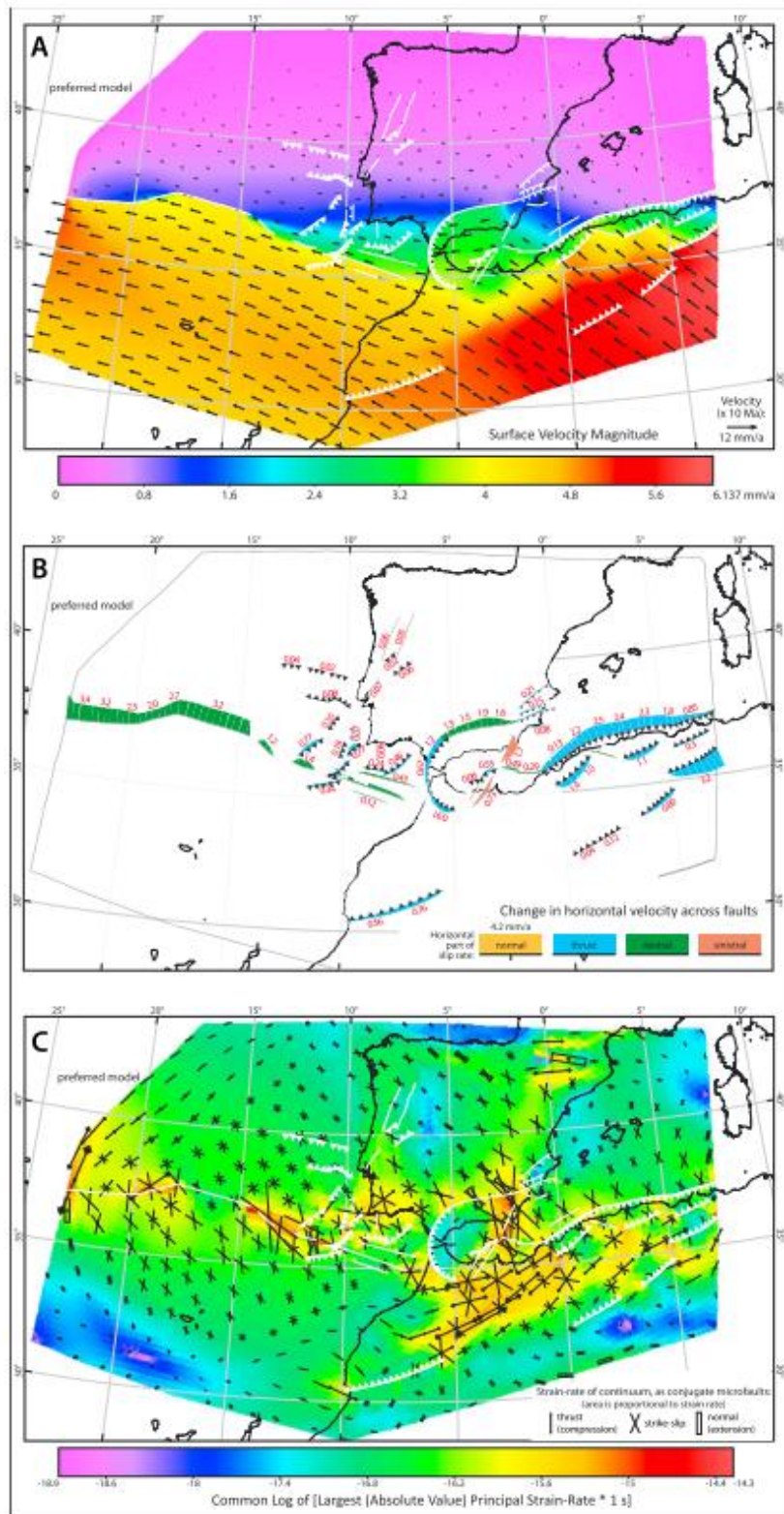


Figure 35: (a) Long-term horizontal velocity field. (b) Predicted long-term fault heave rates. (c) Scalar strain rates and orientation of conjugate microfaults, with area proportional to strain rates. From Neres et al. (2016).

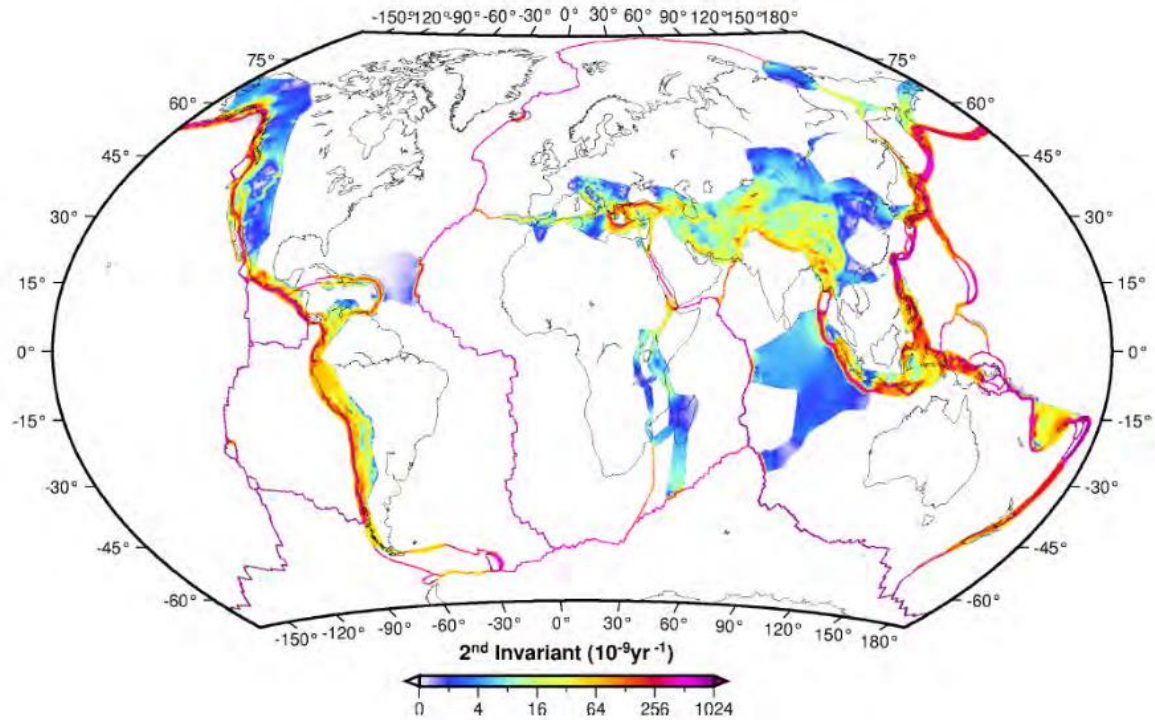


Figure 36: Contours of the second invariant of the strain rate tensor from Kreemer et al. (2014).

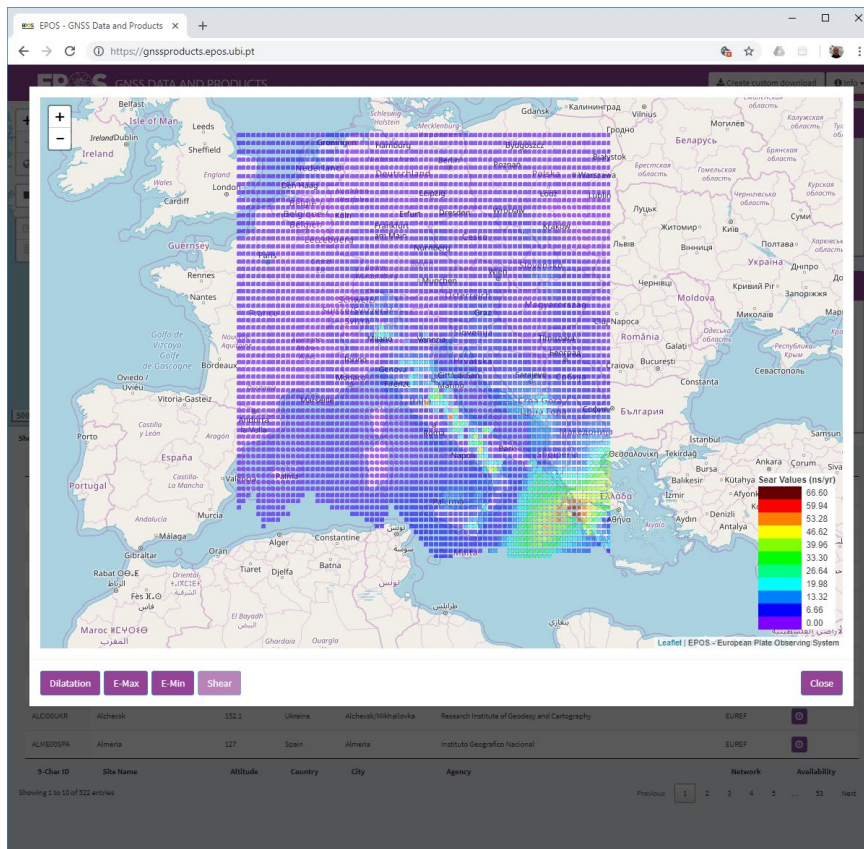


Figure 37: Strain map from the EPOS-GNSS Data and Products portal (<https://gnssproducts.epos.ubi.pt/>).

Another class of models are those based on the inversion of geodetic data, such as that by Kreemer et al. (2014) at the global scale, or that by Métois et al. (2015) for the peri-Adriatic region. Another such model at the scale of Europe could be represented by the data product provided by the EPOS-GNSS community (Figure 37) but its coverage and maturity seem not adequate for ESHM20 for the time being.

Yet another class of models is GEAR1 (Bird et al., 2015), it is based on seismic catalogs, global plate-boundary models, and GPS geodetic velocities, and provide uniform global coverage of earthquake rates (Figure 38).

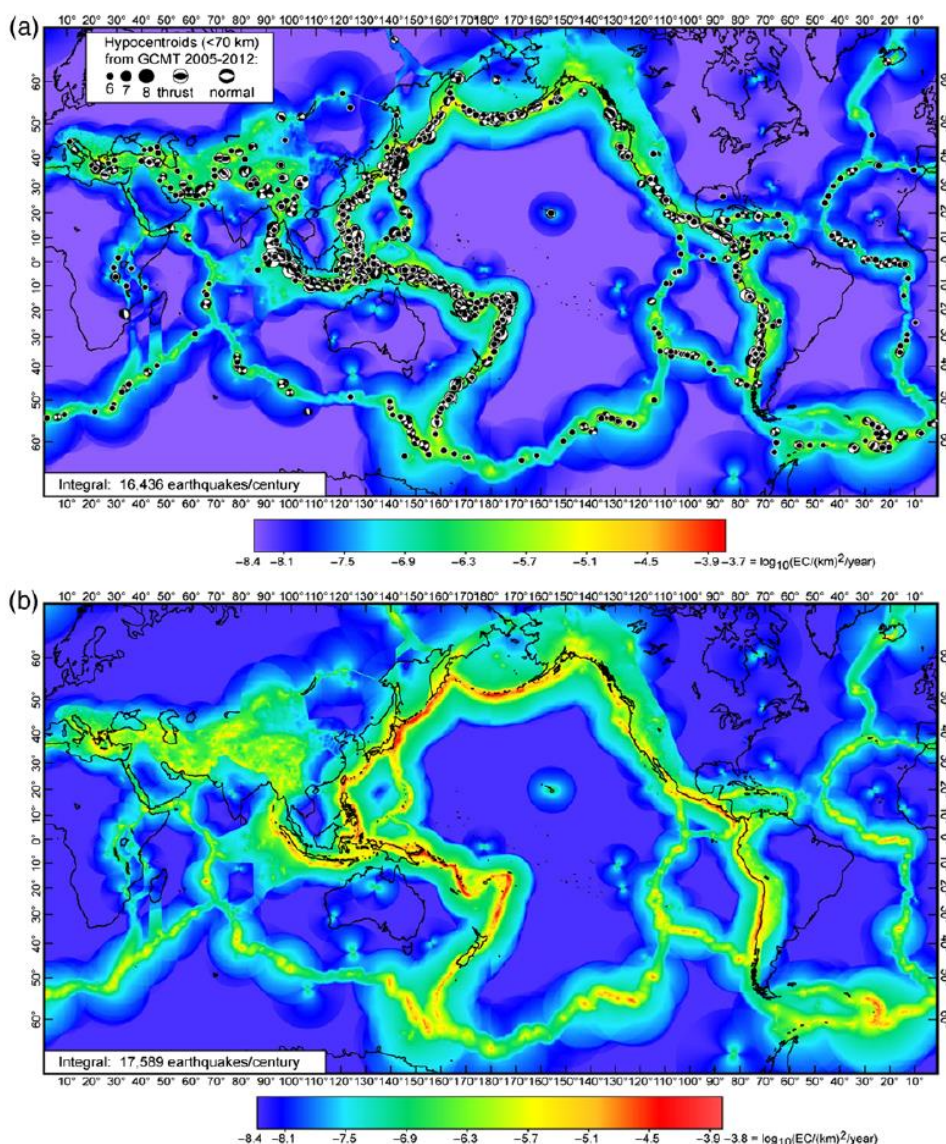


Figure 38: GEAR1 (Bird et al., 2015) preferred hybrid forecasts for threshold magnitude $m \geq 5.767+$, both with and without overlay of test earthquakes. (a) Preferred hybrid forecast H for years 2005+ compared with 1694 shallow test earthquakes from the Global Centroid Moment Tensor (CMT) catalog years 2005–2012. (b) Global earthquake activity rate model 1 (GEAR1) forecast for years 2014 and after.

The main issues with all these models are summarized below.

Only the Carafa et al. (2015) model is at the the same scale as the target area of ESHM20.

Global models could be used to validate the overall coherence of the seismicity rate model in comparison of other area of the world.

Regional or local models can be useful for validating specific aspect of the ESHM20 seismicity model. However, there is a large variety of such models in the literature (only a couple of examples are presented here) and the comparison with all them may even become misleading. However, these smaller scale models can be very useful to validate problematic area where other input data are considered too scarce or not fully representative of the seismicity rate.

Decisions need to be made on how to use any of these models for ESHM20. The most straightforward way is to select the models that provide seismicity rates at the temporal scale and units of interest and calculate the deviations with respect to the prediction coming from the ESHM20. One intrinsic difficulty in doing so is the separation between crustal seismicity and subduction seismicity. Geodetic data usually yield a picture of the compound strain in subduction zones, and a deep understanding of how the model was put together is necessary to guiding the comparison with the ESHM20 seismicity model appropriately. This analysis should thus be expanded and deepened when the preliminary results of the seismicity rate model will be available, presumably by mid-2019.

5 Conclusive remarks

As a contribution to WP25 - JRA3 “Updating and extending the European Seismic Hazard Model”, this document provides details on the updating of the most relevant datasets for elaborating a seismogenic source model in the ongoing efforts toward ESHM20. The data collection starts with the datasets released at the end of project SHARE and carries on until today. Although EPOS is doing any effort to supply all these data through webservices and promote the use of standards, there are still several local and regional advancements that do not, or cannot, follow the same standard everywhere. An additional effort was thus required in critically analyzing the available datasets, and various strategies were sought to harmonize them into a derived data product ready for use in the calculation of seismic hazard. Notwithstanding, a few open questions remain in each dataset, and further updates and refinements of these datasets are expected and envisaged before the actual calculation of the hazard begins in spring 2019. The present realizations of these datasets can be used in the meanwhile to start testing the procedures and identify possible weaknesses or gaps.

Apart from new data that can simply be appended to the existing files, more complex updates and harmonization should be discussed in meetings and agreed upon with the representatives of the other Tasks of WP25 to direct the efforts being made toward the most effective improvements of the final products. Importantly, the structure of the logic tree should be considered to evaluate the possible alternatives while having in mind the potential impact they can have without prejudice onto the results.

Regarding seismicity, two major issues must be addressed. As already envisaged, the EMEC hierarchy rules should be further discussed and feedback be sought from project partners and the wider community. In addition, the consistency between the instrumental part of the catalogue (1900-2014) and the historical part, i.e. based on macroseismic data, (1000-1899) should be addressed before the actual hazard calculations starts. Regarding faults, in addition to completing the regional datasets to the maximum extent possible, the harmonization in the overlapping areas will be critical. In addition, decisions must be made on how the subduction zones are modelled and what models, or combination of models, should be used among those available. The use of strain rates from geodesy implies several treatments of the available data, such as the selection of the models that provide seismicity rates at the temporal scale and units of interest and the difficult separation between crustal and subduction seismicity.

All the datasets describe here, including relevant publications, will be shared within the WP working group in a private repository (dropbox). It is important to understand, however, that most if not all the original datasets are released under different user licenses and therefore they cannot be redistributed to the public as they are. Only the derived data, i.e. data products for which there has been significant intellectual elaboration can. In the long term, these derived data products and elaborations will be distributed through EFEHR and EPOS services, as well as the SERA VAs where applicable, to ensure the integrity of the results and the repeatability of the hazard calculations.

6 References

Akkar S., Kale O., Yakut A., Ceken U. (2018). Ground-motion characterization for the probabilistic seismic hazard assessment in Turkey. *Bull Earthq Engineering*, 16, 8, 3439–3463. doi: 10.1007/s10518-017-0101-2

Albini P. (2015). The Great 1667 Dalmatia Earthquake. An in-depth case study. Springer briefs in earth sciences, The Netherlands, 111 pp. “Extra Materials” at <https://extras.springer.com/2015/978-3-319-16207-2>

Albini P., Musson R.M.W., Rovida A., Locati M., Gomez Capera A.A., Viganò D. (2014). The Global Earthquake History. *Earthq Spectra* 30, 2, 607–624.

Albini P., Rovida A. (2016). From written records to parameters: the case of the 6 April 1667 (Dalmatia) earthquake. *Geoscience Letters* 3:30, doi: 10.1186/s40562-016-0063-2

Albini P., Rovida A. (2018). Earthquakes in southern Dalmatia and coastal Montenegro before the large 6 April 1667 event. *J Seismol*, 22, 751-754, doi: 10.1007/s10950-018-9730-4.

Albini P., Rovida A., Scotti O., Lyon-Caen H. (2017). Large 18th-19th centuries earthquakes in Western Gulf of Corinth with reappraised size and location. *Bull Seismol Soc Am*, 107, 4, 1663–1687, doi: 10.1785/0120160181.

Alexandre P., Alexandre D. (2012). Les séismes en Europe orientale au Moyen Âge. *Ciel et Terre* 128, 6, 162-175

Alexandre P., Alexandre D. (2018). Les séismes en Europe orientale au Moyen Âge (suite): Les tremblement de terre du 5 Juin 1443 et du 29 Août 1471 - Les séismes en Prusse et en Dalmatie. *Ciel et Terre* 134, 1, 2-20.

Atanackov, J., Jamšek Rupnik, P., Celarc, B., Jež, J., Novak, M., Milanič, B., Markelj, A.: Seizmotektonska parametrizacija aktivnih prelomov Slovenije: 4. Del [Kartografsko gradivo in tolmač]. Naročnik: Agencija RS za okolje; Geološki zavod Slovenije, Ljubljana 2017.

Bakun W.H., Wentworth C.M. (1997). Estimating earthquake location and magnitude from seismic intensity data. *Bull Seismol Soc Am*, 87, 1502-1521.

Baptista M.A., Miranda J.M., Batlló J. (2014). The 1531 Lisbon Earthquake: A Tsunami in the Tagus Estuary? *Bull Seismol Soc Am*, 104, 5, 2149-2161. doi: 10.1785/0120130316.

Basili, R., Kastelic, V., Demircioglu, M.B., Garcia Moreno, D., Nemser, E.S., Petricca, P., Sboras, S.P., Besana-Ostman, G.M., Cabral, J., Camelbeeck, T., Caputo, R., Danciu, L., Domac, H., Fonseca, J., García-Mayordomo, J., Giardini, D., Glavatovic, B., Gulen, L., Ince, Y., Pavlides, S., Sesetyan, K., Tarabusi, G., Tiberti, M.M., Utkucu, M., Valensise, G., Vanneste, K., Vilanova, S., Wössner, J. (2013). The European Database of Seismogenic Faults (EDSF) compiled in the framework of the Project SHARE. <http://diss.rm.ingv.it/share-edsf/>, doi: 10.6092/INGV.IT-SHARE-EDSF.

Baumont D., Manchuel K., Traversa P., Durouchoux C., Nayman E., Ameri G. (2018). Intensity predictive attenuation models calibrated in Mw for metropolitan France. *Bull Earthquake Eng* 16, 6, 2285–2310, doi: 10.1007/s10518-018-0344-6.

Baumont D., Scotti O. (2011). The French Parametric Earthquake Catalogue (FPEC) based on the best events of the Sisfrance macroseismic database - Version 1.1 - IRSN/DEI/2011-012.

Bird J.F. and Bommer J.J. (2004). Earthquake losses due to ground failure. *Engineering Geology* 75, 147-179.

Bird, P. (2003). An updated digital model of plate boundaries, Geochemistry, Geophysics, Geosystems, 4(3), n/a-n/a, doi: 10.1029/2001gc000252.

Bird, P., D. D. Jackson, Y. Y. Kagan, C. Kreemer, and R. S. Stein (2015). GEAR1: A Global Earthquake Activity Rate Model Constructed from Geodetic Strain Rates and Smoothed Seismicity. *Bulletin of the Seismological Society of America*, 105(5):2538. <http://dx.doi.org/10.1785/0120150058>

Blaser, L., Krüger, F., Ohrnberger, M., Scherbaum, F., 2010. Scaling relations of earthquake source parameter estimates with special focus on subduction environment. *Bulletin of the Seismological Society of America* 100, 2914-2926, doi: 10.1785/0120100111.

BRGM-EDF-IRSN/SisFrance, 2016. Histoire et caractéristiques des séismes ressentis en France. <http://www.sisfrance.net/>.

Budnitz, R. J., Apostolakis, G., Boore, D. M., Cluff, L. S., Coppersmith, K. J., Cornell, C. A., and Morris, P. A. (1997). Recommendations for probabilistic seismic hazard analysis: guidance on uncertainty and the use of experts, US Nuclear Regulatory Commission, Washington, D.C., NUREG/CR-6372, Volume 2.

Caputo, R. and Pavlides, S. (2013). The Greek Database of Seismogenic Sources (GreDaSS), version 2.0.0: A compilation of potential seismogenic sources ($M_w > 5.5$) in the Aegean Region. <http://gredass.unife.it/>, doi: 10.15160/unife/gredass/0200.

Carafa, M. M. C. and Kastelic, V. (2014) Earthquake rates inferred from active faults and geodynamics: the case of the External Dinarides. *Bollettino di Geofisica Teorica ed Applicata*, 55(1), 69-83. DOI 10.4430/bgta0112.

Carafa, M. M. C., and P. Bird (2016), Improving deformation models by discounting transient signals in geodetic data: 2. Geodetic data, stress directions, and long-term strain rates in Italy, *J. Geophys. Res. Solid Earth*, 121, 5557–5575, doi: 10.1002/2016JB013038.

Carafa, M. M. C., S. Barba, and P. Bird (2015), Neotectonics and long-term seismicity in Europe and the Mediterranean region, *J. Geophys. Res. Solid Earth*, 120, 5311–5342, doi:10.1002/2014JB011751.

Carafa, M.M.C., and S. Barba (2013). The stress field in Europe: optimal orientations with confidence limits, *Geophysical Journal International*, 193(2), 531-548, doi:10.1093/gji/ggt024.

Cornell C.A. (1968). Engineering seismic risk analysis. *Bull. Seismol. Soc. Am.*, 58, 1583-1606.

Danciu, L., Şeşetyan, K., Demircioglu, M., Gülen, L., Zare, M., Basili, R., Elias, A., Adamia, S., Tsereteli, N., Yalçın, H., Utkucu, M., Khan, M.A., Sayab, M., Hessami, K., Rovida, A.N., Stucchi, M., Burg, J.-P., Karakhanian, A., Babayan, H., Avanesyan, M., Mammadli, T., Al-Qaryouti, M., Kalafat, D., Varazanashvili, O., Erdik, M., Giardini, D. (2018). The 2014 Earthquake Model of the Middle East: seismogenic sources. *Bulletin of Earthquake Engineering*, 16(8), 3465-3496, doi: 10.1007/s10518-017-0096-8.

Davies, G., Griffin, J., Løvholt, F., Glimsdal, S., Harbitz, C., Thio, H.K., Lorito, S., Basili, R., Selva, J., Geist, E., Baptista, M.A. (2018). A global probabilistic tsunami hazard assessment from earthquake sources. *Geological Society, London, Special Publications* 456, 219-244, doi: 10.1144/sp456.5.

Demircioglu M.B., Sesetyan K., Duman T.Y., Çan T., Tekin S., Semih Ergintav (2018). A probabilistic seismic hazard assessment for the Turkish territory: part II—fault source and background seismicity model. *Bull Earthq Engineering*, 16, 8, 3399–3438. doi: 10.1007/s10518-017-0130-x.

Demircioğlu, M.B., Şeşetyan, K., Duman, T.Y., Çan T., Tekin S., Ergintav S. (2017). A probabilistic seismic hazard assessment for the Turkish territory: part II—fault source and background seismicity model. *Bull. Earthquake Eng.* <https://doi.org/10.1007/s10518-017-0130-x>.

Diaconescu M., A. Craiu, D. Toma-Danila, G.M. Craiu (2018). Main active faults from the Eastern part of Romania (Dobrogea and Black Sea). Part I: longitudinal faults system. *Romanian Reports in Physics*, in press, <http://www.rpp.infim.ro/IP/A308.pdf>

DISS Working Group (2018). Database of Individual Seismogenic Sources (DISS), Version 3.2.1: A compilation of potential sources for earthquakes larger than $M 5.5$ in Italy and surrounding areas.

<http://diss.rm.ingv.it/diss/>, © INGV 2018 - Istituto Nazionale di Geofisica e Vulcanologia - All rights reserved; DOI:10.6092/INGV.IT-DISS3.2.1.

Dziewonski, A.M., T.A. Chou, and J.H. Woodhouse (1981). Determination of earthquake source parameters from waveform data for studies of global and regional seismicity, *Journal of Geophysical Research*, 86(B4), 2825, doi:10.1029/JB086iB04p02825.

Ekström, G., M. Nettles, and A.M. Dziewoński (2012). The global CMT project 2004–2010: Centroid-moment tensors for 13,017 earthquakes, *Physics of the Earth and Planetary Interiors*, 200–201, 1–9, doi:10.1016/j.pepi.2012.04.002.

Emre Ö., Duman T.Y., Özalp S., Elmacı H., Olgun Ş., Şaroğlu F. (2013) Active fault map of Turkey with an explanatory text 1:1,250,000 scale. General Directorate of Mineral Research and Exploration, Special Publication Series 30.

Emre Ö., Duman T.Y., Özalp S., Şaroğlu F., Olgun Ş., Elmacı H., Çan T. (2018). Active fault database of Turkey. *Bull. Earthquake Eng.* <https://doi.org/10.1007/s10518-016-0041-2>

Erdik M, Sesetyan K, Demircioglu MB, Tuzun C, Giardini D, Gulen L et al. (2012) Assessment of seismic hazard in the Middle East and Caucasus: EMME (Earthquake Model of Middle East) project. In: *Proceedings of 15th world conference on earthquake engineering*

Fäh, D., Giardini, D., Kästli, P., Deichmann, N., Gisler, M., Schwarz, Zanetti, G., Alvarez-Rubio, S., Sellami, S., Edwards, B., Bethman, F., Woessner, J, Gassner-Stamm, G., Fritsche, S., Eberhard, D. (2011). ECOS-09 Earthquake Catalogue of Switzerland Release (2011) Report and Database. Public catalogue 17.4.2011, Swiss Seismological Service ETH Zurich, Report SED/RISK/R/001/20110417.

Ganas A., Oikonomou A.I., and Tsimi C. (2013). NOFAULTS: a digital database for active faults in Greece. *Bulletin of the Geological Society of Greece*, vol. XLVII and *Proceedings of the 13th International Congress*, Chania, Sept. 2013.

García-Mayordomo, J., J.M. Insua-Arévalo, J.J. Martínez-Díaz, A. Jiménez-Díaz, R. Martín-Banda, S. Martín-Alfageme, J.A. Álvarez-Gómez, M. Rodríguez-Peces, R. Pérez-López, M.A. Rodríguez-Pascua, E. Masana, H. Perea, F. Martín-González, J. Giner-Robles, E.S. Nemser, J. Cabral (2012). The Quaternary Active Faults Database of Iberia (QAFI v.2.0). *Journal of Iberian Geology*, 38(1), 285–302, doi 10.5209/rev_JIGE.2012.v38.n1.39219.

Gasperini P., Bernardini F., Valensise G., Boschi E. (1999). Defining seismogenic sources from historical earthquake felt reports. *Bull Seism Soc Am*, 89, 94–110.

Gasperini P., Vannucci G., Tripone D., Boschi E. (2010). The Location and Sizing of Historical Earthquakes Using the Attenuation of Macroseismic Intensity with Distance. *Bull Seismol Soc Am*, 100, 2035–2066.

Giardini D., J. Woessner, L. Danciu, H. Crowley, F. Cotton, G. Grunthal, R. Pinho, G. Valensise, S. Akkar, R. Arvidsson, R. Basili, T. Cameelbeck, A. Campos-Costa, J. Douglas, M.B. Demircioglu, M. Erdik, J. Fonseca, B. Glavatovic, C. Lindholm, K. Makropoulos, F. Meletti, R. Musson, K. Pitilakis, K. Sesetyan, D. Stromeyer, M. Stucchi, A. Rovida (2013). Seismic Hazard Harmonization in Europe (SHARE): Online Data Resource, doi: 10.12686/SED-00000001-SHARE.

Gold R. D., A. Friedrich, S. Kübler, M. Salamon (2017). Apparent Late Quaternary Fault-Slip Rate Increase in the Southern Lower Rhine Graben, Central Europe. *Bulletin of the Seismological Society of America*; 107 (2): 563–580. doi: <https://doi.org/10.1785/0120160197>.

Gomez Capera A.A., Rovida A., Gasperini P., Stucchi M., Viganò D. (2015). The determination of earthquake location and magnitude from macroseismic data in Europe. *Bull Earthq Eng*, 13, 5, 1249–1280, doi: 10.1007/s10518-014-9672-3

Grünthal G. and R. Wahlström (2012). The European-Mediterranean Earthquake Catalogue (EMEC) for the last millennium. *Journal of Seismology*, 16, 535–570, doi 10.1007/s10950-012-9302-y.

Grünthal G., Stromeyer, D., Wahlström, R. (2009b), Harmonization check of MW within the central, northern and northwestern European earthquake catalogue (CENEC), *Journal of Seismology* 13(4), 613-632.

Grünthal G., Wahlström R., Stromeyer, D. (2009a), The unified catalogue of earthquakes in central, northern and northwestern Europe (CENEC) – updated and expanded to the last millennium, *Journal of Seismology*, 13(4), 514-541.

Grünthal, G., Wahlström, R. and Stromeyer D. (2013). The SHARE European Earthquake Catalogue (SHEEC) for the time period 1900-2006 and its comparison to the European-Mediterranean Earthquake Catalogue (EMEC). *Journal of Seismology*, 17, 1339-1344, doi 10.1007/s10950-013-9379-y

Hammerl Ch., Lenhardt W.A. (2013). Erdbeben in Niederösterreich von 1000 bis 2009 n. Chr. *Abhandlungen Der Geologischen Bundesanstalt*, Band 67, 297 pp, Wien.

Hanks, T.C., Bakun, W.H., 2008. M-logA Observations for Recent Large Earthquakes. *Bulletin of the Seismological Society of America* 98, 490-494, doi: 10.1785/0120070174.

Hayes G.P., G.L. Moore, D.E. Portner, M. Hearne, H. Flamme, M. Furtney, G.M. Smoczyk (2018). Slab2, a comprehensive subduction zone geometry model. *Science*, 10.1126/science.aat4723.

Hayes, G., 2018, Slab2 - A Comprehensive Subduction Zone Geometry Model: U.S. Geological Survey data release, <https://doi.org/10.5066/F7PV6JNV>.

Herak D., Sović I., Cević I., Živčić M., Dasović I., Herak M. (2017). Historical Seismicity of the Rijeka Region (Northwest External Dinarides, Croatia) - Part I: Earthquakes of 1750, 1838, and 1904 in the Bakar Epicentral Area. *Seismol Res Lett* 88, 3, 904-915. doi: 10.1785/0220170014.

Herak M., Živčić M., Sović I., Cević I., Dasović I., Stipčević J., Herak D. (2018). Historical Seismicity of the Rijeka Region (Northwest External Dinarides, Croatia) - Part II: The Klana Earthquakes of 1870. *Seismol Res Lett*, doi: 10.1785/0220180064.

Heuret A. and S., Lallemand (2005). Plate motions, slab dynamics and back-arc deformation. *Physics of the Earth and Planetary Interiors* 149, 31-51.

Hiemer, S., J. Woessner, R. Basili, L. Danciu, D. Giardini, and S. Wiemer (2014), A smoothed stochastic earthquake rate model considering seismicity and fault moment release for Europe, *Geophys. J. Int.*, 198, 1159-1172, doi:10.1093/gji/ggu186.

Ichinose, G.A., 2006. Moment Tensor and Rupture Model for the 1949 Olympia, Washington, Earthquake and Scaling Relations for Cascadia and Global Intraslab Earthquakes. *Bulletin of the Seismological Society of America* 96, 1029-1037, doi: 10.1785/0120050132.

Jomard, H., Cushing, E. M., Palumbo, L., Baize, S., David, C., and Chartier, T. (2017). Transposing an active fault database into a seismic hazard fault model for nuclear facilities – Part 1: Building a database of potentially active faults (BDFa) for metropolitan France, *Nat. Hazards Earth Syst. Sci.*, 17, 1573-1584, <https://doi.org/10.5194/nhess-17-1573-2017>.

Knuts E., Alexandre P., Camelbeeck T. (2015). Le séisme luxembourgeois du 13 avril 1733: nouvelles recherches. *Ciel et terre* 131, 5, 130-137.

Knuts E., Camelbeeck T., Alexandre P. (2016). The 3 December 1828 moderate earthquake at the border between Belgium and Germany. *J Seismol*, 20, 419-437, doi: 10.1007/s10950-015-9535-7

Kreemer, C., G. E. Klein, Z.-K. Shen, M. Wang, L. Estey, S. Wier, F. Boler (2014), Global Geodetic Strain Rate Model, GEM Technical Report 2014---07 V1.0.0, 129 pp., GEM Foundation, Pavia, Italy, doi: 10.13117/GEM.GEGD.TR2014.07.

Leonard, M., 2010. Earthquake Fault Scaling: Self-Consistent Relating of Rupture Length, Width, Average Displacement, and Moment Release. *Bulletin of the Seismological Society of America* 100, 1971-1988, doi: 10.1785/0120090189.

Leonard, M., 2014. Self-Consistent Earthquake Fault-Scaling Relations: Update and Extension to Stable Continental Strike-Slip Faults. *Bulletin of the Seismological Society of America*, doi: 10.1785/0120140087.

Locati M., Camassi R., Rovida A., Ercolani E., Bernardini F., Castelli V., Caracciolo C.H., Tertulliani A., Rossi A., Azzaro R., D'Amico S., Conte S., Rocchetti E. (2016). DBMI15, the 2015 version of the Italian Macroseismic Database. Istituto Nazionale di Geofisica e Vulcanologia. doi: 10.6092/INGV.IT-DBMI15

Locati M., Rovida A., Albini P., Stucchi M. (2014). The AHEAD portal: a gateway to European historical earthquake data. *Seismol. Res. Lett.* 85, 3, 727-734.

Manchuel K., Traversa P., Baumont D., Cara M., Nayman E., Durouchoux C. (2018). The French seismic CATalogue (FCAT-17). *Bull Earthquake Eng*, 16, 6, 2227-2251, doi: 10.1007/s10518-017-0236-1.

Métois, M., N. D'Agostino, A. Avallone, N. Chamot-Rooke, A. Rabaute, L. Duni, N. Kuka, R. Koci, and I. Georgiev (2015), Insights on continental collisional processes from GPS data: Dynamics of the peri-Adriatic belts, *J. Geophys. Res. Solid Earth*, 120, 8701–8719, doi: 10.1002/2015JB012023.

Murotani, S., Miyake, H., Koketsu, K., 2008. Scaling of characterized slip models for plate-boundary earthquakes. *Earth Planets Space* 60, 987-991, doi.

Murotani, S., Satake, K., Fujii, Y., 2013. Scaling relations of seismic moment, rupture area, average slip, and asperity size for $M \sim 9$ subduction-zone earthquakes. *Geophysical Research Letters* 40, 5070-5074, doi: 10.1002/grl.50976.

Musson R.M.W., Jimenéz M.J. (2008). Macroseismic estimation of earthquake parameters. NA4 deliverable D3, NERIES Project.

Neres, M., M. M. C. Carafa, R. M. S. Fernandes, L. Matias, J. C. Duarte, S. Barba, and P. Terrinha (2016), Lithospheric deformation in the Africa-Iberia plate boundary: Improved neotectonic modeling testing a basaldriven Alboran plate, *J. Geophys. Res. Solid Earth*, 121, 6566–6596, doi:10.1002/2016JB013012.

Papazachos, B.C., Comninakis, P.E., Scordilis, E.M., Karakaisis, G.F., Papazachos, C.B. (2009). A catalogue of earthquakes in Greece and surrounding area for the period 1901-2008 Publication of the Geophysics Laboratory, University of Thessaloniki http://geophysics.geo.auth.gr/the_seisnet/WEBSITE_2005/station_index_en.html

Pondrelli S. and Salimbeni S. (2015). Regional Moment Tensor Review: An Example from the European Mediterranean Region. In *Encyclopedia of Earthquake Engineering* (pp. 1-15), http://link.springer.com/referenceworkentry/10.1007/978-3-642-36197-5_301-1, Springer Berlin Heidelberg.

Ribeiro J.R., Ribeiro A.I., Correia A.P. (2015). Solving the Mystery: The 21 October 1880 Portuguese Earthquake. *Seismol Res Lett* 86, 3, 991-998, doi: 10.1785/0220140178.

Romanowicz, B., Ruff, L.J., 2002. On moment-length scaling of large strike slip earthquakes and the strength of faults. *Geophysical Research Letters* 29, 45-41-45-44, doi: 10.1029/2001GL014479.

Rovida A., Locati M. (2015). Archive of Historical Earthquake Data for the European-Mediterranean Area. In: A. Ansal (ed.), *Perspectives on European Earthquake Engineering and Seismology, Geotechnical, Geological and Earthquake Engineering* 39, doi 10.1007/978-3-319-16964-4_14

Rovida A., Locati M., Camassi R., Lolli B., Gasperini P. (eds), (2016). CPTI15, the 2015 version of the Parametric Catalogue of Italian Earthquakes. Istituto Nazionale di Geofisica e Vulcanologia. doi: 10.6092/INGV.IT-CPTI15

Schwarz-Zanetti G., Fäh D., Gache S., Kästli P., Loizeau J., Masciadri V., Zenhäusern G. (2017). Two large earthquakes in western Switzerland in the sixteenth century: 1524 in Ardon (VS) and 1584 in Aigle (VD). *J Seismol*, 22, 439-455, doi: 10.1007/s10950-017-9715-8.

Sesetyan K., Demircioglu M.B., Duman T.Y., Çan T., Tekin S., Azak T.E., Zülfikar Fercan Ö (2018). A probabilistic seismic hazard assessment for the Turkish territory—part I: the area source model. *Bull Earthq Engineering*, 16, 8, 3367–3397. doi: 10.1007/s10518-016-0005-6.

Sesetyan K., Demircioglu M.B., Rovida A., Albinì P., Stucchi M. (2013). SHARE-CET, the SHARE earthquake catalogue for Central and Eastern Turkey complementing the SHARE European Earthquake Catalogue (SHEEC). <https://www.emidius.eu/SHEEC/>.

Skarlatoudis, A.A., Somerville, P.G., Thio, H.K., 2016. Source-Scaling Relations of Interface Subduction Earthquakes for Strong Ground Motion and Tsunami Simulation. *Bulletin of the Seismological Society of America* 106, 1652-1662, doi: 10.1785/0120150320.

Strasser, F.O., Arango, M.C., Bommer, J.J., 2010. Scaling of the source dimensions of interface and intraslab subduction-zone earthquakes with moment magnitude. *Seismological Research Letters* 81, 941-950, doi: 10.1785/gssrl.81.6.941.

Stucchi M., A. Rovida, A.A. Gomez Capera, P. Alexandre, T. Camelbeeck, M.B. Demircioglu, P. Gasperini, V. Kouskouna, R.M.W. Musson, M. Radulian, K. Sesetyan, S. Vilanova, D. Baumont, H. Bungum, D. Faeh, W. Lenhardt, K. Makropoulos, J.M. Martinez Solares, O. Scotti, M. Zivcic, P. Albinì, J. Batllo, C. Papaioannou, R. Tatevossian, M. Locati, C. Meletti, D. Viganò, D. Giardini (2012). The SHARE European Earthquake Catalogue (SHEEC) 1000-1899. *Journal of Seismology*, doi 10.1007/s10950-012-9335-2.

Traversa P., Baumont D., Manchuel K., Nayman E., Durouchoux C. (2018). Exploration tree approach to estimate historical earthquakes Mw and depth, test cases from the French past seismicity. *Bull Earthquake Eng*, 16, 6, 2169-2193, doi: 10.1007/s10518-017-0178-7

TSUMAPS-NEAM Team (2017). TSUMAPS-NEAM, PHASE I – STAGE 4: Preliminary Implementation Plan (Workflow). Technical report available at http://www.tsumaps-neam.eu/wp-content/uploads/2018/09/Doc_P1_S4_Prel_Impl_Plan.pdf.

Vannucci, G., Gasperini, P., 2004. The new release of the database of Earthquake Mechanisms of the Mediterranean Area (EMMAVersion 2). *Ann. Geophys.* 47(1) (Suppl. 1), 307–334.

Wells, D.L., Coppersmith, K.J., 1994. New empirical relationships among magnitude, rupture length, rupture width, rupture area, and surface displacement. *Bull. Seismol. Soc. Am.* 84, 974-1002, doi.

Woessner J., Danciu L., Giardini D., Crowley H., Cotton F., Grünthal G., Valensise G., Arvidsson R., Basili R., Demircioglu M., Hiemer S., Meletti C., Musson R.W., Rovida A., Sesetyan K., Stucchi M., and the SHARE consortium. (2015). The 2013 European Seismic Hazard Model - Key Components and Results. *Bulletin of Earthquake Engineering*, 13, 3553-3596, doi: 10.1007/s10518-015-9795-1.

Working Group CPTI (2004). *Catalogo Parametrico dei Terremoti Italiani, versione 2004 (CPTI04)*. INGV, Bologna. <http://emidius.mi.ingv.it/CPTI/>

Zare M., Amini H., Yazdi P., Sesetyan K., Demircioglu M.B., Kalafat D., Erdik M., Giardini D., Khan M.A., Tsereteli N. (2014). Recent developments of the Middle East catalog. *J Seismol*, 18, 749–772. doi: 10.1007/s10950-014-9444-1.

Contact

Project lead	ETH Zürich
Project coordinator	Prof. Dr. Domenico Giardini
Project manager	Dr. Kauzar Saleh
Project office	ETH Department of Earth Sciences Sonneggstrasse 5, NO H62, CH-8092 Zürich sera_office@erdw.ethz.ch +41 44 632 9690
Project website	www.sera-eu.org

Liability claim

The European Commission is not responsible for any use that may be made of the information contained in this document. Also, responsibility for the information and views expressed in this document lies entirely with the author(s).